Development of Performance-Related Specifications for Asphalt Mixtures in Ontario

by

Saeid Salehi Ashani

A thesis

presented to the University of Waterloo

in fulfillment of the

thesis requirement for the degree of

Doctor of Philosophy

in

Civil Engineering

Waterloo, Ontario, Canada, 2021

Examining Committee Membership

The following served on the Examining Committee for this thesis. The decision of the

Examining Committee is by majority vote.

External Examiner

Professor Ahmed Shalaby   Civil Engineering, University of Manitoba

Supervisor

Professor Susan Tighe   Civil and Environmental Engineering, University of Waterloo

Supervisor

Professor Shunde Yin   Civil and Environmental Engineering, University of Waterloo

Internal Member

Professor Hassan Baaj   Civil and Environmental Engineering, University of Waterloo

Internal Member

Professor Sina Varamini   Civil and Environmental Engineering, University of Waterloo

Internal-external Member

Professor Kaan Inal   Mechanical & Mechatronics Engineering, University of Waterloo

AUTHOR'S DECLARATION

I hereby declare that I am the sole author of this thesis. This is a true copy of the thesis, including any required final revisions, as accepted by my examiners. I understand that my thesis may be made electronically available to the public.

Statement of Contributions

This thesis is comprised of eight chapters: Chapter 4, entitled "Characterization of Five Plant-Produced Asphalt Mixtures" is authored by me and was reviewed by my supervisors. Chapter 5, entitled "The Evaluation of DC(T) and SCB Tests Using Five Plant-Produced Asphalt Mixtures" is authored by me and was reviewed by supervisors. Chapter 6, entitled "The Evaluation of I-FIT Test Using Five Plant-Produced Asphalt Mixtures" is authored by me and was reviewed by my supervisors. Chapter 7, entitled "Investigation of Sixteen Asphalt Mixtures to Recommend Preliminary Specifications for I-FIT, DC(T) and HWT Tests" is authored by me and the Ministry of Transportation Ontario, and was reviewed by my supervisors.

Abstract

Superpave mix design relying on volumetric specifications is not completely able to predict the long-term performance of asphalt pavements. Therefore, implementation of suitable performance specifications is crucial to maintain sustainability in highway infrastructure. Overall, performance specifications can be divided into two categories: performance-based specifications (PBS) and performance-related specifications (PRS). PBS are Quality Assurance (QA) specifications that describe the desired level of fundamental engineering properties and can be used in performance prediction, while PRS are QA specifications that describe the desired levels of key materials and construction quality characteristics that have been found to correlate with fundamental engineering properties. The implementation of efficient and practical performance-related specifications can be used in asphalt mix design process and Quality Control/Quality Assurance (QC/QA) specifications.

In this research, tests such as Disc-Shaped Compact Tension (DC(T)) test, Semi-Circular Bend (SCB) test, Illinois Flexibility Index Test (I-FIT), IDEAL-CT test, complex modulus and cyclic tests, and Hamburg Wheel Tracking (HWT) test, which have shown promise to be considered as performance-related tests, were investigated through laboratory research on five plant-produced asphalt mixtures. The characterization of these asphalt mixtures by DC(T) and SCB tests revealed that no statistically significant difference could be found between fracture energies of DC(T) and SCB tests at three testing temperatures, namely -18°C, -24°C and -30°C for asphalt mixtures investigated. However, SCB test was not able to distinguish and rank low temperature cracking resistance of asphalt mixtures at -18°C and -30°C. This can be attributed to the behavior of asphalt mixtures when they are too ductile and too brittle, respectively, and the discrepancies existing with the geometry of DC(T) and SCB specimens, and CMOD rate. Furthermore, DC(T) test was not sensitive to the two methods of long-term aging (forced-draft oven aging at 85°C for 120 hours and forced-draft oven aging at 95°C for 72 hours) employed in this research. Moreover, the characterization of these asphalt mixtures by the I-FIT test revealed that forced-draft oven aging of I-FIT specimens at 95°C for 72 hours produced statistically similar Flexibility Index (FI) values as the specimens aged at

85°C for 120 hours. The results of FI values showed that asphalt mixtures containing hard PG asphalt binder (PG64-28 and PG70-28) were more sensitive to testing temperature variability compared to asphalt mixtures having softer PG asphalt binder.

Additionally, a survey was distributed to asphalt mixture laboratories in Ontario to investigate the capability of laboratories for carrying out the aforementioned performance tests. Overall, responses from forty-six laboratories revealed that several of them are capable of conducting I-FIT, IDEAL-CT, DC(T) and HWT tests.

Based on the analysis of the tests results from five plant-produced asphalt mixtures and the survey data, three performance tests, namely I-FIT, DC(T) and HWT tests were selected for further research. For this purpose, sixteen plant-produced asphalt mixtures with their corresponding field cores were investigated by conducting the tests selected. The statistical analysis conducted by t-test on sixteen mixtures determined that there was a significant difference between the average FI of PPLC (Plant-Produced Laboratory Compacted specimens) and their corresponding field cores with some exception. In addition, the CV of FI results for most of PPLC specimens and pavement field cores was less than 20% showing the low variability for I-FIT test for post-production mixtures and field cores. The statistical analysis conducted by t-test on sixteen mixes determined that there is not a significant difference between the average fracture energy of PPLC specimens and their corresponding field cores except for one mix in DC(T) test. Furthermore, the CV of fracture energy results for most of PPLC specimens and pavement field cores is less than 20% showing the low variability of DC(T) test.

Moreover, the analysis of the tests results provided preliminary specifications for I-FIT, DC(T) and HWT tests. According to the data analysis, a preliminary threshold FI value of 10 can be used for all mixtures except for SMA mixtures. A preliminary threshold FI value of 15 is suggested for SMA mixtures. Moreover, based on the data analysis in this study, a premilitary threshold DC(T) fracture energy value of 700 J/m^2 can be considered for traffic category E mixtures, and a preliminary threshold DC(T) fracture energy value of 600 J/m^2 can be considered for all other traffic categories. With regard to HWT test results, as a preliminary threshold criterion, mixes containing PG70-XX, must not reach a rut depth of more than 6.0

mm at 50°C after 20000 passes. In addition, mixes containing PG64-XX must not exhibit a rut depth of more than 12.5 mm at 50°C after 20000 passes. For mixes containing PG58-XX and PG52-XX, the rut depth should not exceed 12.5 mm at 44°C after 20000 passes.

These results provide, besides of a comprehensive evaluation of performance-related tests in Canadian asphalt mixtures, a basis for implementation of performance specifications for I-FIT, DC(T) and HWT tests in Ontario.

Acknowledgements

The work presented in this thesis would have not been completed without the direction of my supervisor, the guidance of my committee members, the help and support from the Ministry of Transportation Ontario (MTO) and the Civil and Environmental Engineering Department Staff at the University of Waterloo, and the encouragement from my friends and family.

I would like to express my sincere gratitude to my supervisors, Professor Tighe and Professor Yin, for their excellent guidance, support, encouragement, and providing me with their expertise through my PhD research.

I would also like to thank Professor Baaj, Professor Inal, Professor Varamini, and my external examiner, Professor Shalaby, who honored me by accepting to be a part of my committee. I benefitted greatly from their guidance and feedback.

Additionally, since this research was funded by MTO, I would like to acknowledge the help and support from MTO's staff.

Moreover, I would like to thank the Civil and Environmental Engineering Department staff, particularly Richard Morrison, Douglas Hirst, and Peter Volcic.

Furthermore, I would like to thank my CPATT colleagues for their help and support during my research.

Last, but certainly not least, I thank my parents and siblings for their support and encouragement throughout my educational endeavors.

Dedication

To my parents

Table of Contents

List of Figures

List of Tables

Chapter 1
Introduction

1.1 Background

In Canada, asphalt pavement has been relatively selected as the material of choice, compared to concrete pavement, due to lower cost, ease and speed of construction, maintenance, and rehabilitation. Generally, asphalt mix design is an essential part of asphalt pavement construction and rehabilitation since it significantly influences the in-service performance of asphalt pavements. The main purpose of asphalt mix design is to determine an economical and optimal portion of aggregate and asphalt binder content that will result in desirable properties such as durability, stability, workability, impermeability, flexibility, fatigue resistance and skid resistance (Asphalt Institute, 2001). Overall, an asphalt mixture must be designed, produced, placed, and compacted in the field such that it can provide two principal properties: durability and stability.

Asphalt mixture durability is defined as the characteristic that determines how asphalt pavement can preserve structural integrity while exposed to climate and traffic loading, thus resulting in maintaining the same satisfactory level of service throughout its service life (Bonaquist, 2014). On the other hand, the stability of an asphalt mixture refers to the resistance required to prevent permanent deformation (rutting) in asphalt pavements under traffic loading and high temperature (Asphalt Institute, 2001). Cracking and rutting are known as two of the main critical distresses on asphalt pavements. Cracking, the principal distress affecting the asphalt mixture durability, is defined as a type of distress in asphalt pavements that can occur in different modes such as bottom-up and top-down fatigue cracking, thermal (low temperature) cracking and reflective cracking which are caused by various factors and mechanisms (West, 2018). Not only can cracking affect the structural integrity of asphalt pavements, but also it can lead to water, moisture, and air infiltrate into the pavement structure. Consequently, water and moisture can give rise to other distresses such as moisture damage in the form of stripping and potholes, thus resulting in a reduction in serviceability. In addition,

air infiltration can accelerate aging of asphalt binder within an asphalt pavement structure that eventually will result in increasing brittleness, ravelling, and cracking.

Rutting is referred to as the permanent deformation occurring on the surface of asphalt pavements along with the wheel path of moving traffic due to the excessive densification and shear stress caused by traffic usually at high temperatures (Brown, et al., 2009). This permanent deformation can act as a potential source of hydroplaning, diminishing safety of driving due to the lack of traction between tires and pavement surface. Therefore, these distresses are the main cause of maintenance and rehabilitation activities which impose a high budgetary spending on highway agencies, which brings about economic issues. The importance of problems associated with cracking and rutting have generated increased attention from highway agencies across the world.

The Superpave mix design method developed by the Strategic Highway Research Program (SHRP) from 1987 to 1993 is currently the preferred asphalt mix design method compared to other preceding methods such as Hveem and Marshall. The significant objectives of SHRP were to develop and implement an asphalt mix design system, including performance-based asphalt binder specifications and performance-based asphalt mixture specifications. SHRP was successful with the implementation of the first objectives. However, the second objective, i.e., performance-based asphalt mixture specifications, was not implemented successfully due to the cost and other complexities. Hence, the Superpave mix design protocol did not provide a simple performance test to measure the stability and durability of asphalt mixtures as Hveem and Marshall methods had provided (Huber, 2017) and (Brown, et al., 2009). Therefore, the Ministry of Transportation of Ontario (MTO) and Departments of Transportation (DOTs) across the US have utilized only the SHRP mix design and asphalt binder specifications for the design and construction of asphalt pavements. Thus, the method is unable to predict and measure the expected asphalt pavement performance against distresses such as rutting, reflective cracking, fatigue cracking (top-down and bottom-up), low temperature cracking and moisture susceptibility. Furthermore, according to the Superpave mix design method, the proportioning of the aggregate and asphalt binder in a mix design is dependent on two components of the mix design: aggregate and asphalt binder

characteristics, as well as volumetric properties such as air voids, voids in the mineral aggregate (VMA) and voids filled with asphalt (VFA). However, distresses observed on asphalt pavements, such as premature cracking, have indicate that asphalt mixtures produced by the Superpave mix design method based on volumetric properties, are lean on asphalt content, thus resulting in low compaction in the field followed by premature cracking and durability problems (Newcomb & Zhou, 2018). The Superpave mix design is not sufficient to predict the potential behaviour of asphalt pavements in the field, and the aforementioned shortcomings have gradually become more complicated with the introduction of Reclaimed Asphalt Pavement (RAP), Recycled Asphalt Shingles (RAS), warm-mix asphalt additives, rejuvenators, polymers, and fibres into asphalt mixtures (West, 2018).

Alternatively, controlling the volumetric properties of asphalt mixtures placed and compacted as End Results Specification (ERS) is still considered the main component of Quality Control and Quality Assurance (QC/QA) specifications in Ontario, and MTO is using ERS as Quality Acceptance (QA) criteria to determine whether the as-built asphalt mixture corresponds to the as-designed asphalt mixture. However, various concerns have been raised with regard to the correlation between ERS and long-term performance of asphalt mixtures.

Highway agencies and research centres across the world such as those in Canada, the US, Australia, and New Zealand are investigating ways to develop and implement asphalt mixture performance tests to solve premature cracking and rutting issues, which are some of the most significant drawbacks currently related to the Superpave volumetric mix design method (Grobler, 2018).

To identify the most promising asphalt mixture performance tests, this research is intended to investigate various state-of-the-art performance tests that can be employed to evaluate cracking and rutting resistance of asphalt mixtures.

1.2 Research Hypothesis

As mentioned above, the volumetric properties of asphalt mixtures are not sufficient to predict the long-term performance of asphalt pavements, and performance testing not only can predict

the long-term performance of asphalt pavements, but it can also facilitate the use of new materials and technologies in the asphalt pavement industry. Consequently, the main research hypothesis of this project is the following: <u>The implementation of suitable and practical performance tests in the mix design procedure and QA/QC activities can help overcome the limitations of volumetric mix design to evaluate cracking and rutting resistance of asphalt mixtures and can be employed to enhance durability and stability of asphalt mixtures.</u>

1.3 Research Objectives

This research is directed at investigating and finding the most suitable performance tests to evaluate cracking and rutting resistance of asphalt mixtures. Therefore, the significant objectives of this study are as follows:

- To determine suitable and practical tests for crack and rutting resistance of asphalt mixtures in Ontario.
- To validate asphalt mixture design through analysis of various new tests on the crack and rutting resistance of asphalt mixtures.
- To provide a basis for implementation of performance specifications for crack and rutting resistance of asphalt mixtures in Ontario in the future.
- To complete End Results Specifications (ERS), used as Quality Acceptance (QA) criteria, with suitable performance tests.

1.4 Thesis Organization

This thesis is divided into eight chapters. Chapter 1 provides the introduction, research hypothesis, research objectives and lay out of the thesis. Chapter 2 comprises the literature review that summarizes asphalt mix design methods, main asphalt pavement distresses, and performance testing and specifications used across the world. Chapter 3 discusses the research methodology and procedure. Chapter 4 includes the results and discussions of six laboratory tests, including Disk-Shaped Compact Tension (DC(T)), Semi-Circular Bend (SCB), IDEAL-

CT, I-FIT, cyclic and Hamburg Wheel Tracking (HWT) tests, conducted on five plant-produced asphalt mixtures. Chapter 5 investigates DC(T) and SCB tests conducted on five plant-produced asphalt mixtures. Chapter 6 investigates I-FIT test conducted on five plant-produced asphalt mixtures. Chapter 7 investigates I-FIT, DC(T) and HWT tests conducted on sixteen plant-produced asphalt mixtures in order to recommend preliminary specifications for these tests. Chapter 8 comprises the conclusions of this research the recommendations, and future work.

Chapter 2
Literature Review

2.1 Asphalt Mix Design

Asphalt mix design has been developed and improved over the past seventy years in order to provide asphalt pavements with desirable properties during their service life. The main purpose of asphalt mix design is to determine economical and optimal portions of aggregate and asphalt binder content that will result in desirable properties such as durability, stability, workability, impermeability, flexibility, fatigue resistance and skid resistance. Overall, a RILEM technical committee work program divided the asphalt mix designs used across the world in six groups, including recipe, empirical testing, analytical computations, volumetric method, performance related testing and fundamental testing (Francken, 1998). As can be seen in Table 2.1, most countries in the world are practicing Marshall or Superpave mix design except for France where the French mix design method is being used. Overall, the Marshall mix design method is considered an empirical mix design, while Superpave and French mix designs are considered volumetric and performance-based mix designs, respectively.

Table 2.1 Asphalt Mix Design Methods Practiced in Some Countries (Grobler, Rebbechi, & Denneman, 2018).

Country/Province or State	Mix Design Method	Performance Tests
Ontario-Canada	Superpave	Moisture Sensitivity
Quebec-Canada	A modified version of Superpave	Moisture Sensitivity and Hamburg Wheel Tracking (HWT)
Alberta-Canada	Marshall	Hamburg Wheel Tracking (HWT)
U.S.A.	Superpave	Hamburg Wheel Tracking (HWT), Asphalt Pavement Analyzer (APA), Complex Modulus and Uniaxial Cyclic, Flexural Beam Fatigue, Disc-Shaped Compact Tension (DC(T)), Semi-Circular Bend (SCB), Texas Overlay (OT) and Superpave Shear Tester (SST)
France	French	Moisture Sensitivity, Wheel Tracking, Stiffness Modulus and Fatigue
Germany/Central Europe	Marshall	Moisture Sensitivity and Hamburg Wheel Tracking
United Kingdom	Marshall	Moisture Sensitivity, Resistant to Permanent Deformation, Modulus and Fatigue
South Africa	Marshall and Superpave	Moisture Sensitivity, Complex Modulus, Hamburg Wheel Tracking and Flexural Beam Fatigue
Australia and New Zealand	Marshall and Superpave	Moisture Sensitivity, Resilient Modulus, Hamburg Wheel Tracking and Flexural Beam Fatigue

2.1.1 French Mix Design

The French mix design as a performance-based mix design has four distinguishing characteristics (Figure 2.1): (1) the optimum asphalt binder is determined based on performance tests; (2) asphalt mixtures are optimized by performance tests; (3) asphalt mixtures are classified for each need, and (4) asphalt mixtures are related to their use on highways. Hence, according to a type of asphalt mixture, a level of design, including Level 0, Level 1, Level 2, Level 3, and Level 4 is assigned. The higher levels always include the requirements addressed in the lower levels. Level 0 represents asphalt mixtures being used in non-trafficked areas. In Level 1, asphalt mixtures must satisfy the requirements of air void percentages and the water resistance according to gyratory compactor and Duriez tests,

respectively. Asphalt mixtures in Level 2 must meet Level 1 tests requirements in addition to wheel tracking test specifications. In Level 3, asphalt mixtures must meet Level 1 and Level 2 tests requirements in addition to stiffness modulus specifications. In Level 4, asphalt mixtures must meet the requirements of gyratory compactor and water resistance tests from Level 1, wheel tracking test from Level 2, stiffness modulus from Level 3 in addition to fatigue test specifications (Delorme, Roche, & Wendling, 2007). Overall, in Level 1, gyratory compactor and water resistance tests are considered empirical tests, while in Level 2, wheel tracking test can be considered as a performance-related test. Furthermore, in Level 3 and Level 4, stiffness modulus and fatigue tests, respectively, can be considered as fundamental or performance-based tests. It is worth noting that the results of performance-based tests can be employed in asphalt pavement models to predict the asphalt pavement performance.
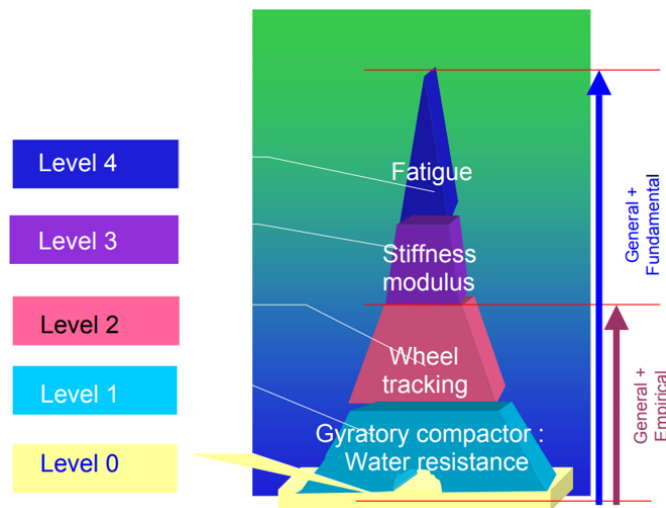
Figure 2.1 French Mix Design Levels (Delorme, 2007).

2.1.2 Hveem Mix Design Method

In 1927, Francis Hveem, a resident engineer in California employed a traditional method called paper stain test, invented by a Canadian engineer (Captain L.N. Edwards), to evaluate the appropriate amount of asphalt binder to be used in an asphalt mixture. Hveem had managed to develop a method to determine the optimum asphalt binder content using aggregate surface area by 1932. Then, Hveem started implementing a stability test as a recognition for

mechanical strength of the asphalt mixtures. In general, the philosophy of Hveem's method was that there must be enough asphalt binder in an asphalt mixture so that it can satisfy aggregate absorption and to provide a minimum film thickness on the surface of the aggregates. Hveem believed that an asphalt mixture can carry loads based on two conditions: aggregates must have a sliding resistance (measured by stabilometer) to resist shear stress, and meanwhile a minimum tensile strength (measured by cohesiometer) to resist tensile stress. Both stability and cohesion are governed by aggregate properties and asphalt film thickness existing on the aggregate surface. The amount of air voids, which were only taken in consideration until the 1980's and 1990's, did not play a role in Hveem's method. Unlike those created with Marshall's method, asphalt mixtures designed by Hveem's method did not generally show rutting problems; however, they did show potential for fatigue cracking.

2.1.3 Marshall Mix Design Method

Bruce Marshall, an engineer in the Mississippi's Department of Highways developed the Marshall mix design method in the late 1930s to early 1940s. Marshall essentially considered air voids and voids filled with asphalt to design asphalt mixtures and did not give importance to voids in the mineral aggregate. However, Norman McLeod in 1950's added voids in the mineral aggregate to Marshall method. Marshall mix design was the main mix design method supported by the Asphalt Institute (AI) in the US. The main problem with Marshall mix design in 1980's and late 1990's was excessive amount of rutting distress occurred on the surface of highways.

2.1.4 Superpave Mix Design Method

Subsequently, the Superpave mix design method was developed by the Strategic Highway Research Program (SHRP) from 1987 to 1993 to be an improved mix design method in comparison to its antecessors, i.e., the Hveem and Marshall methods. The significant objectives of SHRP were to develop and implement a mix design system, performance-based asphalt binder specifications and performance-based asphalt mixture specifications. SHRP was successful with the implementation of the first and the second of the objectives, however, the third objective, i.e., performance-based asphalt mixture specifications were not implemented

successfully due to cost and some complexities. Therefore, Departments of Transportation (DOTs) in the US and the Ministry of Transportation of Ontario (MTO) only utilized the mix design and asphalt binder specifications for construction of asphalt pavements. The lack of implementation of appropriate performance-based asphalt mixture specifications with the Superpave mix design has limited the ability to predict and measure the expected asphalt pavement performance and predicted distresses such as rutting, reflective cracking, fatigue cracking (top-down and bottom-up), low temperature cracking and moisture susceptibility. Moreover, according to the Superpave mix design method, proportioning of the aggregate and asphalt binder in a mix design is dependent on two components of the mix, i.e., the aggregate and asphalt binder's characteristics, as well as volumetric properties such as air voids, voids in the mineral aggregate (VMA) and voids filled with asphalt (VFA). However, asphalt mixes produced by the Superpave mix design, based on volumetric properties, are lean on asphalt content. Thus, it has been noted that they often fail prematurely due to cracking and durability problems (Newcomb, et al., 2018). Superpave mix design is not sufficient to predict the potential behavior of asphalt pavements in the field, and the shortcomings gradually began to become more complicated with the introduction of reclaimed asphalt pavement (RAP), recycled asphalt shingles (RAS), warm-mix asphalt additives, rejuvenators, polymers, and fibers into asphalt mixtures.

Overall, the primary focus of the Superpave method was to improve rutting resistance. Therefore, higher grade asphalt binders and higher quality aggregates were specified in asphalt mix designs for highways carrying low volume traffic, and many states began implementing rutting tests as an addendum to the mix design procedure for moderate and high traffic highways. Currently, even though the rutting problem has virtually resolved, most highway agencies are reporting that cracking in various forms have frequently emerged on highways. Overall, several factors can play a role to contribute to cracking, including issues with the mix designs, increased use of recycled materials and byproducts, issues with the quality of construction, and underlying pavement distresses during pavement rehabilitation. Since the current Superpave mix design has some shortcomings, many highway agencies are trying to

implement asphalt mixture performance tests in the mix design process to enhance the service life of asphalt pavements. (West, 2018)

Significant benefits of conducting performance tests include (Grobler, Rebbechi, & Denneman, 2018):

- Optimization of the performance of asphalt mixtures according to available materials, climate, and in-service requirements.
- Taking advantage of new technologies and introducing innovative materials that would have been close to impossible to use in volumetric mix designs.
- Utilizing local materials economically to achieve desirable level of performance.
- Understanding the risks associated with utilizing a specific asphalt mixture for a particular application.
- Coupling the asphalt mixture design with the structure of asphalt pavements to achieve the employment of quality materials and long-lasting pavement structures.

On the other hand, controlling the volumetric properties of asphalt mixtures laid down and compacted as End Results Specification (ERS) is still considered the main component of Quality Control and Quality Assurance (QC/QA) specifications in Ontario, and MTO is using ERS as Quality Acceptance (QA) criteria to define whether the as-built asphalt mixture is in accordance with the as-designed asphalt mixture. In general, the engineering properties of asphalt mixtures can be determined through performance testing in which a representative volume element (RVE) of an asphalt mixture is subjected to simulated stresses and strains to which the asphalt mixture is intended to encounter in the field. Not only can performance testing shed light on the ambiguities concerned with long-term performance of asphalt pavements, but also it can contribute to a new concept regarding mix design called balanced mix design (BMD) by which it is more likely to achieve an asphalt mixture that will not show premature cracking and rutting in place. Therefore, there is an urgent need to establish and implement reliable performance-related and performance-based specifications and acceptance criteria to produce more durable asphalt mixtures in Ontario.

Furthermore, the Superpave mix design method (AASHTO M323 and R35) currently is requiring strict criteria for air voids content (Va), void in the mineral aggregate (VMA) and

void filled with asphalt (VFA) to guarantee satisfactory performance of asphalt mixtures (Kandhal, Foo, & Mallick, 1998). However, distresses such as premature cracking have prompted many highway agencies to ponder, investigate and exercise modifications to the Superpave mix design method due to their specific climate, available materials, traffic, and their experience. In general, following modifications to Superpave mix design can be considered:

- Setting up a minimum asphalt content (Newcomb & Zhou, 2018).
- Lowering the number of gyrations (Christensen & Bonaquist, 2006).
- Regression to 3% air voids (Newcomb & Zhou, 2018).
- 5% Design air voids (Christensen & Bonaquist, 2006) and (Newcomb & Zhou, 2018).
- Increasing minimum VMA values by 0.5-1% (Christensen & Bonaquist, 2006).
- Setting up maximum VMA values (1.5-2% greater than minimum VMA) (Christensen & Bonaquist, 2006).
- Expanding the design air voids content to 3-5% instead of constant value of 4% air void (Christensen & Bonaquist, 2006).
- Implementing performance suitable tests to measure crack resistance (Newcomb & Zhou, 2018).
- Using Balanced Mix Design (BMD) (McCarthy, Callans, Quigley, & Scott, 2016).

Among the modifications proposed and practiced by various highway agencies and research centres, implementing performance tests to measure cracking and rutting resistance of asphalt mixtures could be the first step that could be taken since the lack of suitable performance tests has not verified the crucial importance of altering the volumetric criteria to improve the performance of asphalt mixtures. The second step could be investigating the applicability of the BMD method in which two or more performance tests are incorporated to assess rutting and cracking resistance of asphalt mixtures.

Recently, highway agencies and research centres in some countries such as Canada, the US and Australia have started investigating various performance tests to find the most suitable tests to evaluate cracking and rutting resistance of asphalt mixtures.

2.1.5 Australia's Experience on Asphalt Mix Design

Australia is currently using the Marshall and Superpave methods for asphalt mix design. They are setting up a suite of performance tests to evaluate workability, rutting and cracking of asphalt mixtures is under investigation. Overall, three levels of testing have been envisioned by researchers in Australia as shown in Figure 2.2 and Figure 2.3 (Grobler, Rebbechi, & Denneman, 2018):

- Level 1 Testing: Volumetric properties based on gyratory compaction (using the Gyropac device).
- Level 2 Testing: Fatigue resistance, modulus, creep, and moisture sensitivity (optional) of the asphalt mix prepared at the design binder content determined in Level 1.
- Level 3 Testing: Refusal density and permanent deformation characteristics of the asphalt mix prepared at the design binder content.
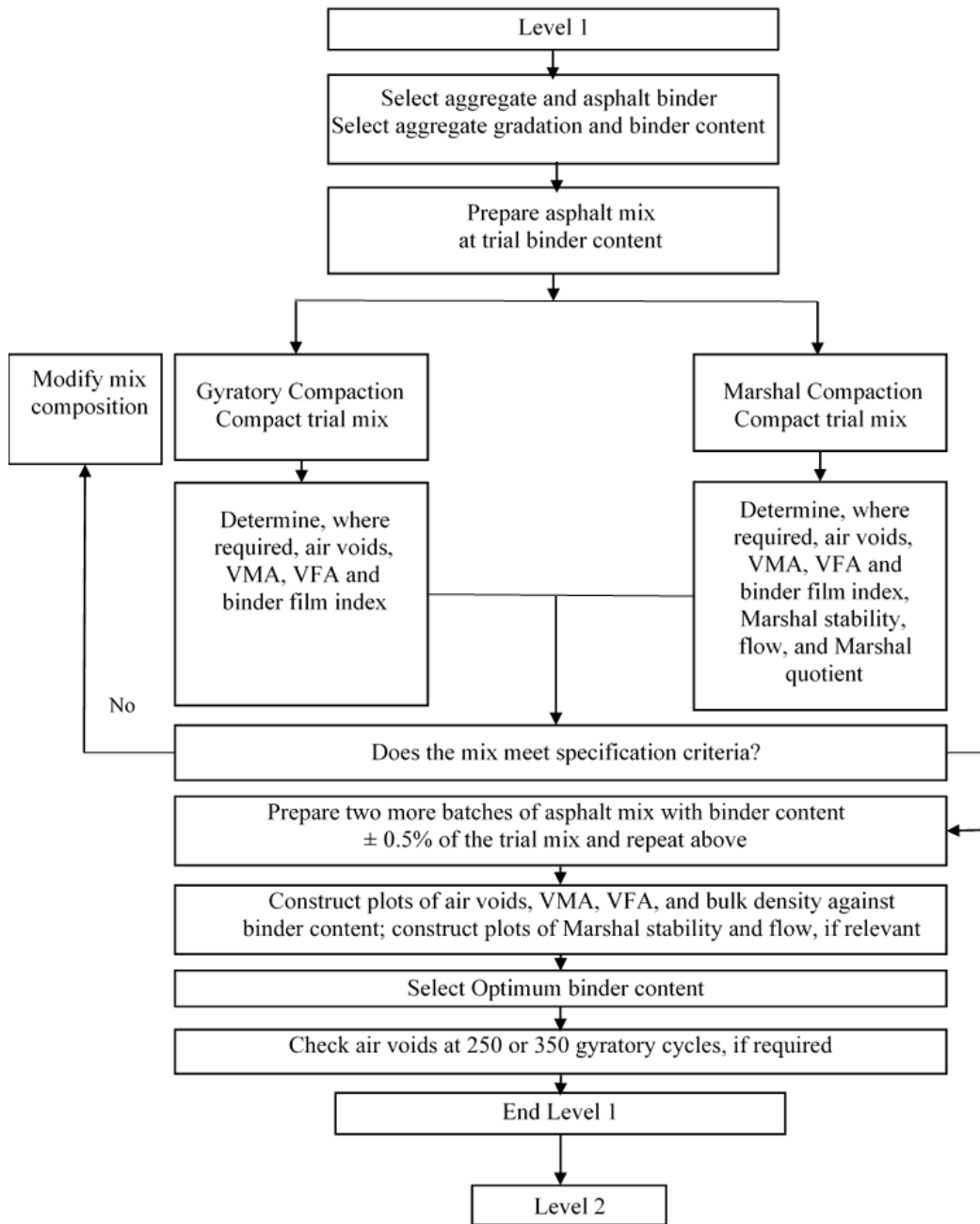
Figure 2.2 Level 1 of Australia's Asphalt Mix Design (Grobler, 2018).
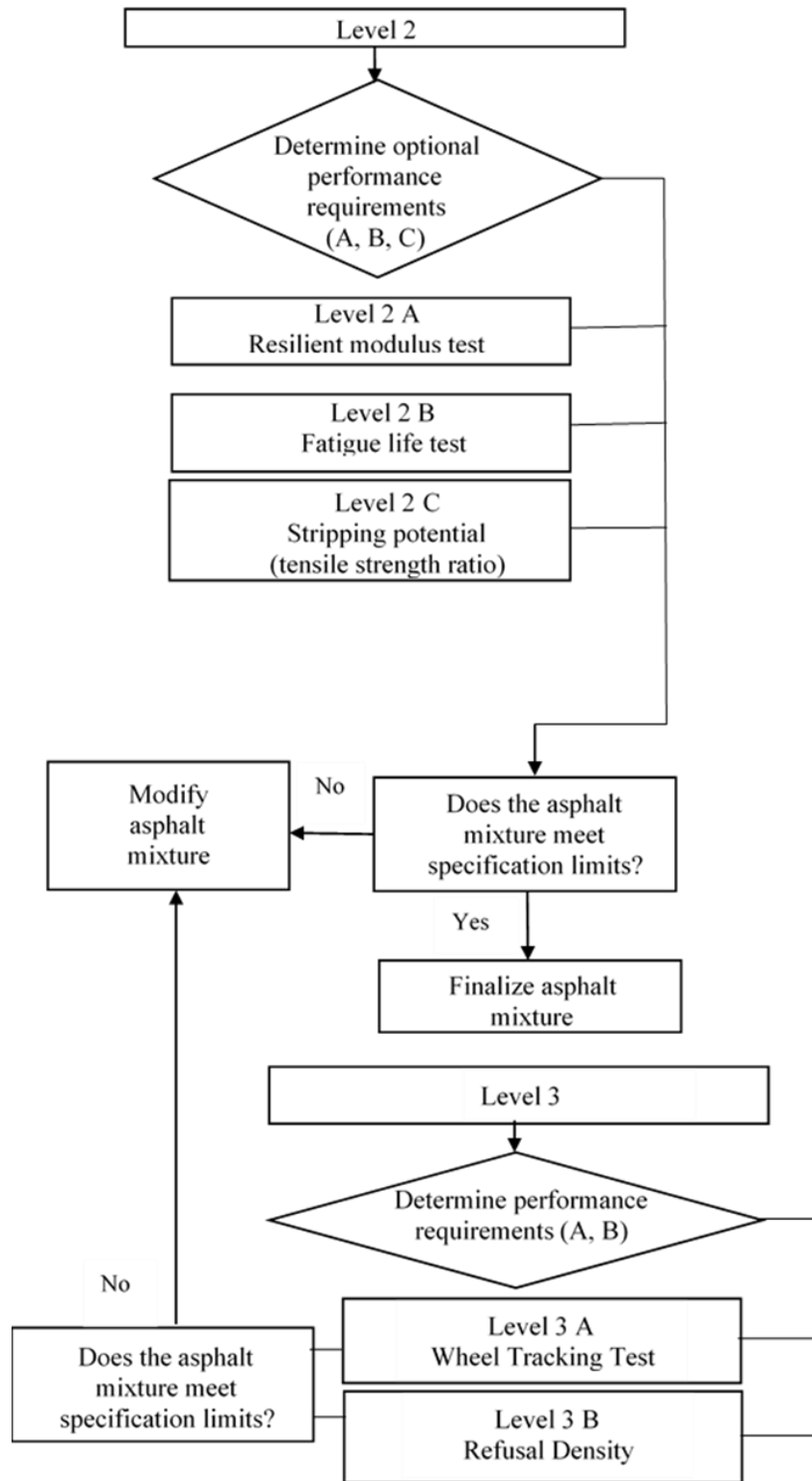
Figure 2.3 Level 2 and Level 3 of Australia's Asphalt Mix Design (Grobler, 2018).

2.1.6 Balanced Mix Design (BMD) Method

The BMD method, initiated by researchers at the Texas Transportation Institute (TTI), is defined as a method that helps asphalt mix designers provide an asphalt mixture using volumetric properties and performance testing so that the asphalt mixture will not have issues with rutting and premature cracking during the service life for which it has been designed (Bonaquist, 2014). Generally, BMD specifies a minimum amount of asphalt binder based on the cracking criterion and a maximum amount of asphalt binder based on the rutting criterion (Newcomb & Zhou, 2018). Overall, there are three main methods in BMD, shown in Figure 2.4, that are currently being used in some states in the United States, including Texas, Illinois, Louisiana, and New Jersey (Bennert, 2018), (Zhou F. , 2017), (Cooper & Mohammad, 2018), (Ozer & Al-Qadi, 2018), (Newcomb & Zhou, 2018). Figure 2.5, Figure 2.6, and Figure 2.7 show BMD space diagrams utilized in three different research (Zhou, 2018), (Ozer & Al-Qadi, 2018), (Cooper & Mohammad, 2018).

2.1.6.1 BMD Considering Volumetric Design with Performance Verification

In this approach, first, a mix design is determined according to volumetric parameters within AASHTO M322 standard limits. Then, the mix design needs to satisfy the required performance testing criteria for rutting and cracking regulated by highway agencies. If so, the mix design is verified, and if not, the mix design must be adjusted until it satisfies the required performance testing criteria while satisfying AASHTO M322 limits. Once the mix design satisfies rutting and cracking criteria as well as the volumetric requirements, it must pass moisture damage evaluation before becoming the Job Mix Formula (JMF).

2.1.6.2 BMD Considering Performance-Modified Volumetric Design

In this approach, the initial binder content of a mix design is determined according to AASHTO M322 before conducting performance tests. If the mix design produced does not satisfy the desired criteria of performance testing, the binder content or mix proportions must be changed until the mix design satisfies the desired criteria. A moisture damage evaluation test must be conducted to assure the durability of asphalt mixture. The final volumetric properties are allowed not to be within AASHTO M322 standard limits.

2.1.6.3 BMD Considering Performance Design

In this approach, performance testing is conducted at different binder contents to determine at what binder content all the required performance testing criteria are met. Volumetric properties are not mandatory to be within AASHTO M322 limits.
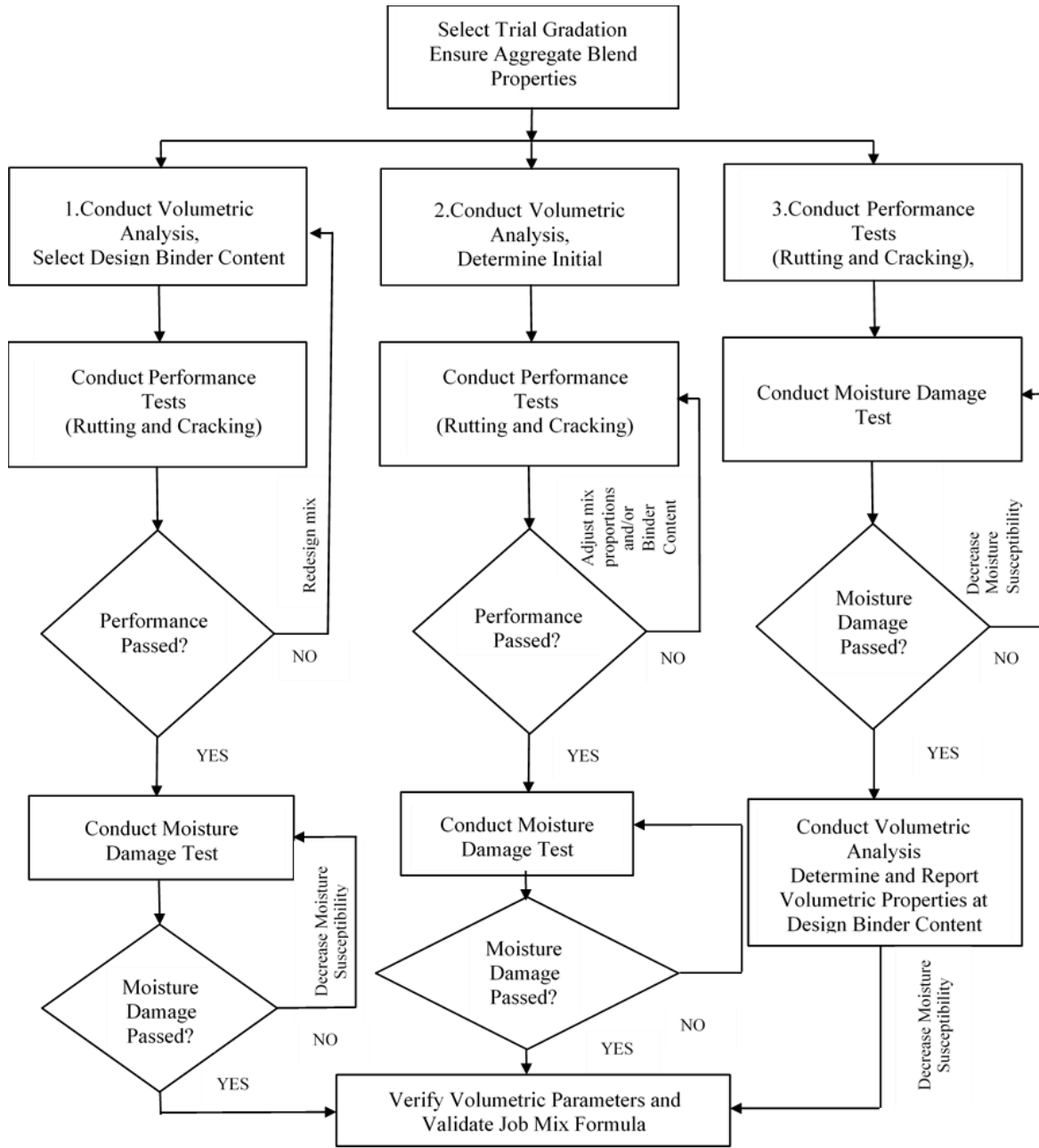
Figure 2.4 The three BMD approaches (Newcomb, 2018).
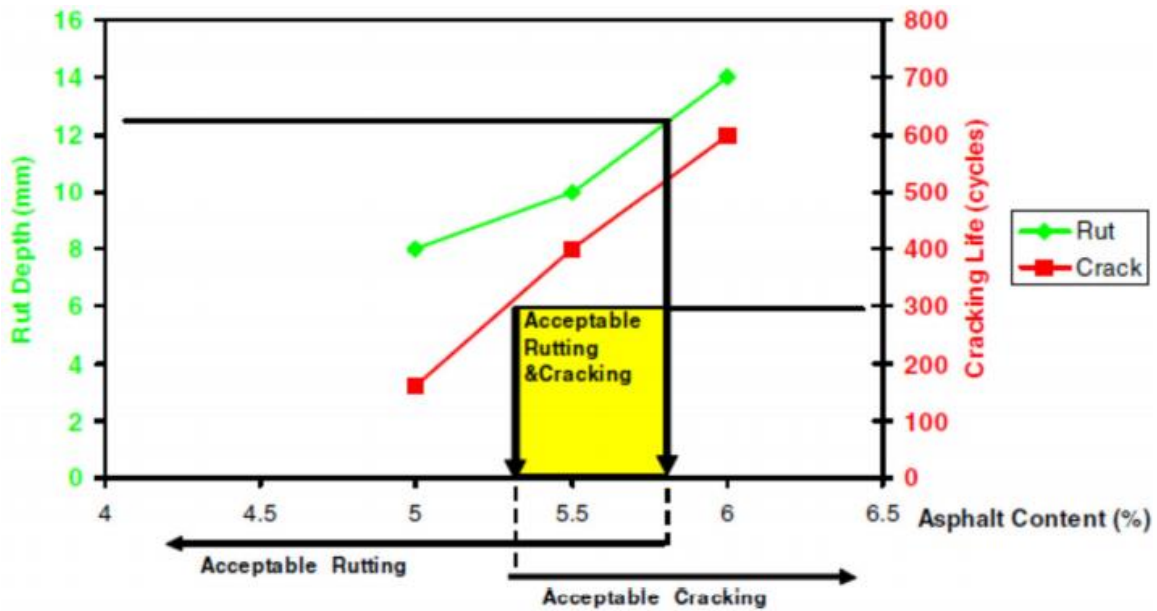
Figure 2.5 BMD Space Diagram using Texas Overlay and Hamburg Wheel Tracking Tests (Zhou, 2018).
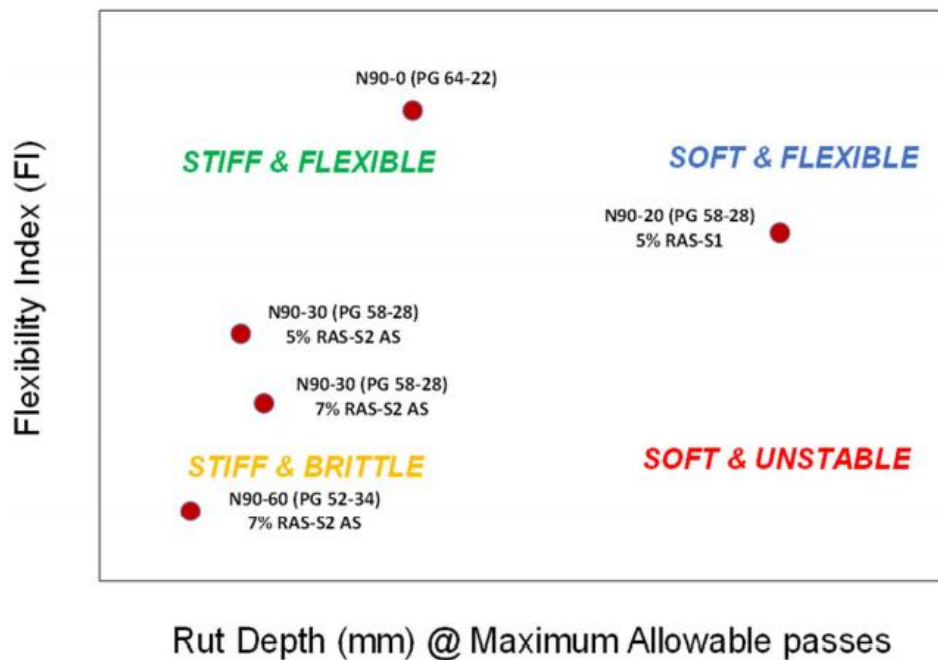
Figure 2.6 BMD Space Diagram using I-FIT and Hamburg Wheel Tracking (Ozer & Al-Qadi, 2018).
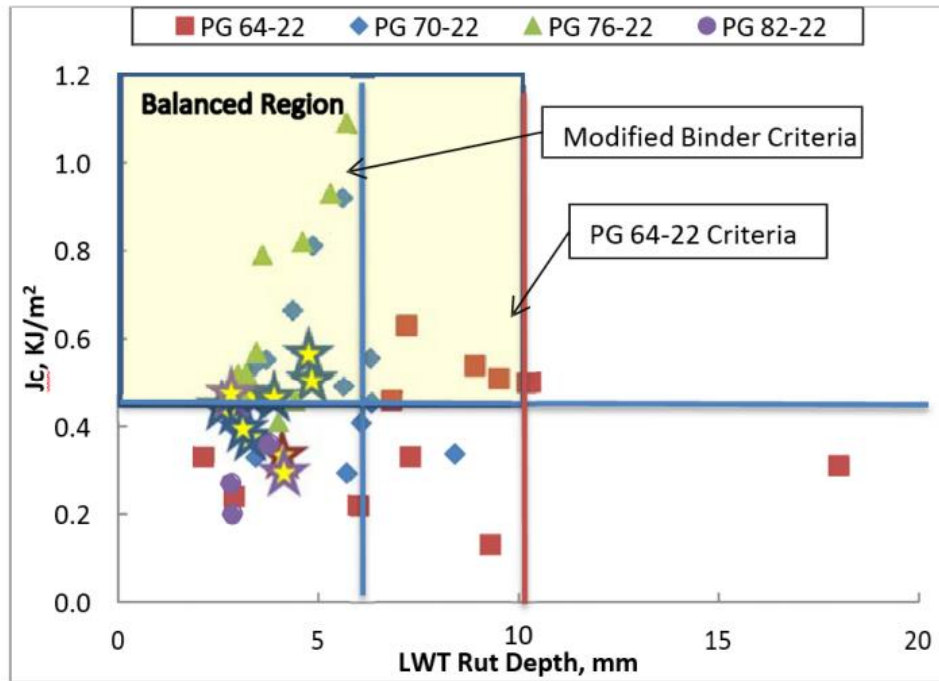
Figure 2.7 BMD Space Diagram using SCB and Hamburg Wheel Tracking Tests (Cooper & Mohammad, 2018).

2.2 Asphalt Pavement Distresses

2.2.1 Permanent Deformation (Rutting)

Permanent deformation or rutting occurs as a result of irrecoverable strains accumulated, especially when the repeated slow-moving traffic loads at high temperatures have been applied to the asphalt pavement. Overall, two main causes of rutting are subgrade failure and insufficient asphalt mixture stability which are shown in Figure 2.8. The most common form of permanent deformation is asphalt mixture instability which manifests in the form of wheel path rutting. Generally, the internal friction and interlock created by the aggregate skeleton and the cohesion provided by the asphalt binder are two main factors contributing to the resistance to permanent deformation. The interlock among aggregate particles mainly depends on the shape, texture, and angularity of coarse and fine aggregate and aggregate gradation, while the stiffness and the bond strength of asphalt binders govern the cohesion. Overall, the aggregate interlock and cohesion in asphalt mixtures prevents to a certain degree the aggregate particles

19

sliding past one another by the shear force exercised by moving traffic, thus resulting in a rutting resistant asphalt pavement. Currently, in the Superpave test method, rutting susceptibility of asphalt mixtures is controlled by characteristics of aggregate (shape, texture and angularity of coarse and fine aggregate) and characteristics of asphalt binders by using Dynamic Shear Rheometer (DSR) (measuring $G^*/\sin \delta$) and Multiple Stress Creep Recovery (MSCR) (measuring J_{nr} and Re%) tests. Overall, examining the aggregate and asphalt binder characteristics separately is not adequate to address rutting issue, and asphalt mixtures must be evaluated by an appropriate performance test.
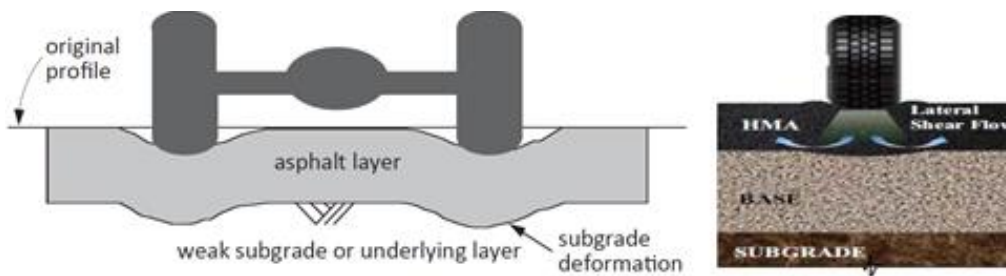
Figure 2.8 Rutting Distress due to Weak Subgrade (*left*) (Asphalt Institute, 2014) and Instability of Asphalt Mixture (*right*) (Faruk, 2015)

Table 2.2 summarizes asphalt mixture performance tests that have been employed to characterize rutting susceptibility of asphalt mixtures by researchers and highway agencies. Generally, performance tests listed in Table 2.2 can be divided in four groups: 1) simulative test, including Hamburg Wheel Tracking test, Asphalt Pavement Analyzer test, and French Rutting Tester, 2) static creep test, including Flow Time Test, 3) cyclic creep test, including Flow Number Test and Superpave Shear Tester, and 4) empirical test, including Marshall Stability Test, Hveem Stabilometer and IDEAL RT test.

Table 2.2 Summarized asphalt mixture performance tests to characterize rutting susceptibility (Zhou, 2020), (West, 2018), (Bhasin, Button, & Chowdhury, 2003), (Witczak, Kaloush, Pellinen, & El-Basyouny, 2002), (Aschenbrener, 1992), (Izzo & Tahmoressi, 1999)

Laboratory tests for Rutting	Equipment and Cost	Test Analysis Complexity	Practicality for Mix Design and QA	Correlation to Field Performance	Test Variability
Hamburg Wheel Tracking Test (AASHTO T324)	Hamburg Wheel-Tracking device and saw for cutting specimens $40,000-70,000 US	Simple	Good	Good correlation to pavement sections in Colorado and Texas	Medium COV<20%
Asphalt Pavement Analyzer (AASHTO T340)	Asphalt Pavement Analyzer $120,000 US	Simple	Good	Good correlation to pavement sections on FHWA ALF, WesTrack, NCAT Test Track, MnRoad, and in Georgia and Nevada	Medium COV<20%
French Rutting Tester EN 12697-22	French Rutting Tester $85,000	Simple	Good	Good correlations to pavement sections in Colorado	Medium COV<20%
Flow Time Test (AASHTO TP79)	Asphalt Mixture Performance Tester, Core drill, environmental chamber, saw for cutting specimens $112,000 US	Fair	Fair	Good correlation to pavement sections on FHWA ALF, WesTrack, and MnRoad	High COV>20%

Laboratory tests for Rutting	Equipment and Cost	Test Analysis Complexity	Practicality for Mix Design and QA	Correlation to Field Performance	Test Variability
Superpave Shear Tester (AASHTO T320)	Superpave Shear Tester, Environmental chamber, saw for cutting specimens

The cost of testing device is unknown | Fair | Fair | Good correlation to pavement sections on FHWA ALF, WesTrack, and MnRoad | Unknown |
Flow Number Test (AASHTO TP79)	Testing Frame, Core drill, environmental chamber, saw for cutting specimens $100,000 US	Fair	Fair	Good correlation to pavement sections on FHWA ALF, WesTrack, and MnRoad	High COV>20%
Marshal Stability Test ASTM D6926	Testing Device $5,000 US	Simple	Good	Unknown	Medium COV<15%
Hveem Stabilometer ASTM D1561	Testing Device $13,000 US	Simple	Good	Unknown	Medium COV<20%
IDEAL Rutting Test (IDEAL RT)	Testing Frame (Same as SCB and Ideal CT), Ideal RT Jig

$10,000 US | Simple | Good | Good | Medium COV<15% |

2.2.2 Cracking in Asphalt Materials

An asphalt mixture is a heterogeneous composite material having complexities, due to construction activities, related to loading rate and temperature dependency besides aging and non-uniformity. Cracking related distresses occurring in asphalt pavements are the consequence of fracturing in an asphalt layer or debonding between two asphalt layers, or an asphalt layer and unbounding layers in an asphalt pavement structure. Fatigue and thermal cracking, prevalent on the highways and roads, are two types of cracks in the asphalt layer. Due to recent significant progresses in laboratory characterization, analytical and computational modelling of fracture mechanics in asphalt materials, testing notched specimens (according to fracture mechanics concepts) have shown promising to characterize cracking resistance of asphalt mixtures through localized crack initiation and propagation. In order to understand the concepts of fracture energy that will be used in this research, the following section explains some concepts related to the fracture energy.

2.2.2.1 Fracture Mechanics Concepts

In contrast to the traditional approach of structural design, in which two variables, applied stress and tensile strength, are compared, fracture mechanics quantifies the critical combination of three variables, including applied stress, flaw size or crack and fracture toughness (Braham & Underwood, 2016).

Inglis can be considered as one of the pioneers of fracture mechanics because of his research conducted to investigate the stress concentration on the edge of an elliptical hole located on the major axis in a plate (Figure 2.9).
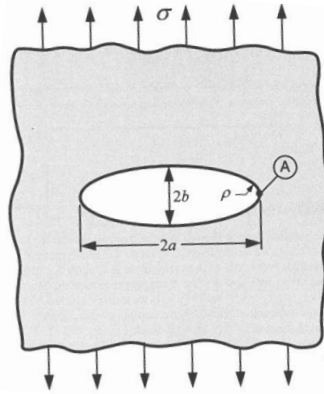
Figure 2.9 Stress at the tip of the major axis (Braham & Underwood, 2016).

Inglis postulated that the geometry of the elliptical hole is not influenced by the plate boundary (the plate width >>2a and the plate height >>2b), and the stress at the edge of hole (point A) can be calculated by Equation 1.

$$\sigma_A = \sigma\left(1 + \frac{2a}{b}\right) \tag{1}$$

In the plate, if the major axis increases relative to the minor axis, the elliptical hole turns into a sharp crack that must fail by applying an extremely small load. The issue encouraged Griffith to develop a fracture theory based on energy balance. The Griffith energy balance arose from the first law of thermodynamics. Griffith theorized that a system transforms from a non-equilibrium state to an equilibrium state on the condition that there exists a reduction in energy. Therefore, a crack can form or grow if the total energy decreases or remains constant. Equation 2 shows Griffith's theory,

$$\frac{dE}{dA} = \frac{d\Omega}{dA} + \frac{dWs}{dA} = 0 \; or \; -\frac{d\Omega}{dA} = \frac{dWs}{dA} \tag{2}$$

where E = total energy, dA = incremental increase in crack area, Ω = potential energy created by internal strain energy and external forces, and Ws = work required to create new surfaces.

The theory can be stated from another perspective such that a crack will propagate when the energy available for crack propagation equals the energy required for crack propagation. Therefore, the equation can be expressed as Equation 3,

$$\frac{\pi\sigma^2 a}{E} = -\frac{d\Omega}{dA} = \frac{dWs}{dA} = 2\gamma_s \tag{3}$$

where σ = stress, a = half-length of elliptical hole, E = Young's modulus, and γ_s = surface energy.

In 1956, Irwin proposed a simpler theory that is similar to Griffith's theory, but easier to be applied for solving engineering problems. Irwin defined an elastic energy released rate (G), which is a measure of the energy available for an increment of crack extension. Equation 4 describes Irwin's theory,

$$G = \frac{d\Omega}{dA} = \frac{d(U - F)}{dA} \tag{4}$$

where G = elastic energy release rate, Ω = potential energy of the elastic body, U = strain energy stored, and F = work done by external force.

The term of rate in "energy released rate" in not referred to a derivative with respect to time, and it simply defines the change of potential energy with the extension of crack area. G also can be called the crack extension force or the crack driving force.

For an elastic material, a relationship between G and K_I can be established as in Equation 5,

$$G = \frac{K_I^2}{E} \tag{5}$$

where G= elastic strain energy release rate K_I = intensity factor and E = Young's modulus.

The stress intensity factor is the magnified amount of remote stress causing the local stress close to the tip of crack surpasses the yield strength of the material. The intensity factor causes the crack initiates and develops at the tip of crack. Furthermore, the stress intensity factor is applied to quantify the local stress and the stress field around a crack tip (Figure 2.10). Fracture toughness (K_C) is the critical or maximum value of K under which a crack gets unstable and propagates. K_I and K_{IC} are the intensity factor and fracture toughness for the first mode of cracking (Figure 2.11). The relationship between K_I and K_{IC} is similar to the

25

relationship between stress and strength of a material. K_I is calculated according to Equation 6,

$$K_I = \sigma\beta\sqrt{\pi a} \tag{6}$$

where K_I = intensity factor, a= crack length and β = the geometry factor.

$$\sigma_{xx} = \frac{K_I}{\sqrt{2\pi r}}\cos\left(\frac{\theta}{2}\right)\left[1-\sin\left(\frac{\theta}{2}\right)\sin\left(\frac{3\theta}{2}\right)\right]$$

$$\sigma_{yy} = \frac{K_I}{\sqrt{2\pi r}}\cos\left(\frac{\theta}{2}\right)\left[1+\sin\left(\frac{\theta}{2}\right)\sin\left(\frac{3\theta}{2}\right)\right]$$

$$\tau_{xy} = \frac{K_I}{\sqrt{2\pi r}}\cos\left(\frac{\theta}{2}\right)\sin\left(\frac{\theta}{2}\right)\cos\left(\frac{3\theta}{2}\right)$$
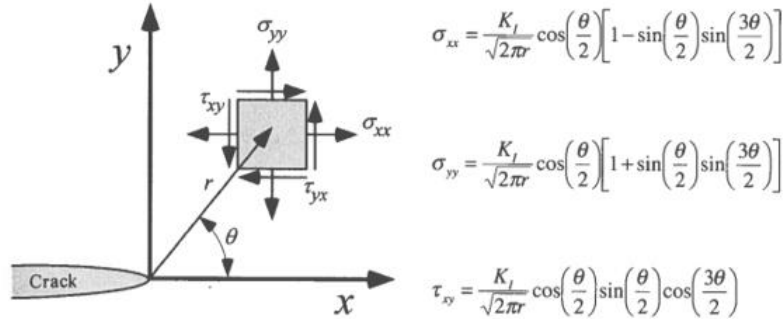
Figure 2.10 Stresses near a crack tip in an elastic material (Anderson, 2005).
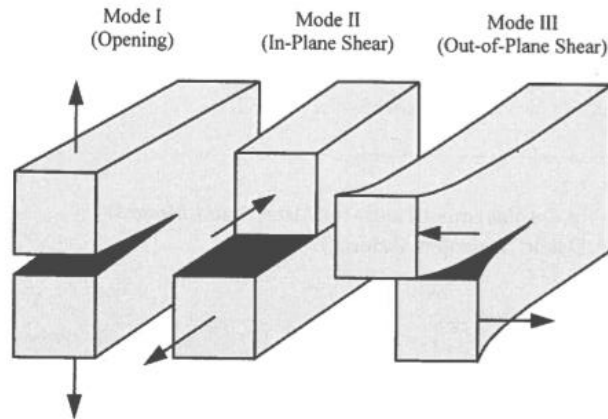
Figure 2.11 The three modes of cracking that can be applied to a crack (Anderson, 2005).

The J-integral (Figure 2.12) is defined as a line or surface integral surrounding a crack tip from one crack surface to the other that can be applied to characterize the local stress-strain field around the crack tip (ASTM E1820). The J integral is given in Equation 7,

$$J = \int_{\Gamma} wd_y - T_i \frac{\delta U_i}{\delta_x} d_s \tag{7}$$

26

where w = strain energy density, T_i = components of the traction vector, U_i = displacement vector components, d_s = length increment along the contour Γ.
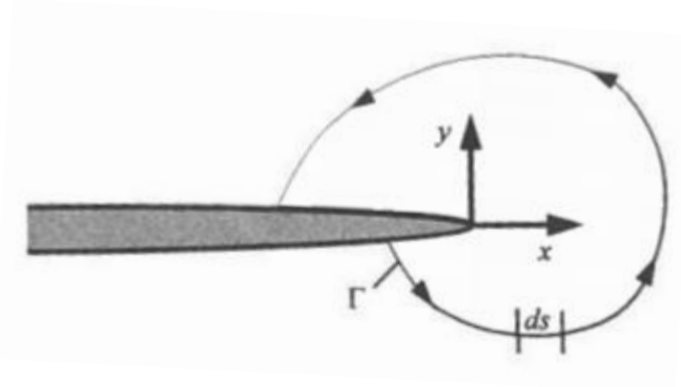
Figure 2.12 Arbitrary contour around the tip of a crack (Anderson, 2005).

Based on the J integral, the energy balance concept in fracture mechanics can include both linear elastic behavior and elastic-plastic behavior. J integral representing elastic-plastic strain energy release rate is related to the area under load-displacement curve divided by the product of advanced cracking length and specimen thickness (Equation 8),

$$J = -\frac{1}{B}\left(\frac{\delta U}{\delta a}\right) \tag{8}$$

where U = strain energy, B = specimen thickness and a = length of advanced cracking.

One easy way to obtain crack extension length is using samples with different initial crack sizes such that the difference between initial crack sizes is length of crack extension.

2.2.2.2 Fatigue (intermediate temperature) cracking

Fatigue cracking can be classified into two modes: bottom-up and top-down fatigue cracking. Bottom-up fatigue cracking, initiating at the bottom of asphalt layer and propagating toward asphalt layer, is the consequence of repetitive axle loading being applied to the asphalt pavement surface that results in a tensile strain level at the bottom of asphalt layer below which the tensile strain level causing a crack by a single load application (Zhou, 2016).

In general, major factors causing bottom-up fatigue cracking are the following (Zhou, 2016):

- Traffic: Traffic loading is the main cause of fatigue cracking due to the stress or strain induced in asphalt layer. The heavier the tire loads and the higher traffic volume, the earlier fatigue cracking happens.

- Environmental conditions: Temperature can influence the stiffness of asphalt mix by which the stress and strain in the pavement layer changes. Furthermore, stiffening of asphalt binder caused by aging can increase the brittleness of asphalt layer and reduce its cracking resistance.

- Pavement structural combination: Pavement structure, including the thickness of asphalt layer and base layer and their elastic modulus influences the location of fatigue cracking.

- Asphalt mixture material and volumetrics: The asphalt mixture type, gradation, modified or unmodified asphalt binder, asphalt binder content, and air voids have direct influence on material properties such as stiffness, viscoelastic properties, and fracture characteristics.

Top-down cracking is longitudinal cracks forming and initiating outside of the wheel path that propagates downward into asphalt layer. Top-down cracking has three stages: in the first stage, longitudinal cracks start outside of the wheel path. In the second stage companion parallel cracks develop within 12 to 40 inches to the initial cracks, and in the third stage, short transverse cracks connect the longitudinal cracks. Top-down cracking can be classified into two categories: the first is construction related top-down cracking mainly caused by aggregate segregation in the asphalt mixture, and the second category is load-related top-down cracking caused by the bending-induced surface tension away from the tire. Similar to bottom-up fatigue cracking, major factors causing top-down cracking are traffic, environmental condition, pavement structural combination and asphalt mixture material and volumetrics (Zhou, 2016).

In general, performance tests to evaluate fatigue cracking resistance of asphalt mixtures have been conducted on bulk specimens of asphalt mixtures. These tests can simulate crack initiation and propagation in specimens globally, however, recently fracture mechanics-based tests on notched specimens to evaluate crack resistance of asphalt mixtures at intermediate

temperature have been conducted. In general, tests on the notched specimens can simulate crack propagation locally (crack initiates at the tip of the notch and develops).

2.2.2.2.1 Fatigue (intermediate temperature) cracking

Performance tests on bulk specimens that have been used to evaluate fatigue crack resistance of asphalt mixtures can be divided into two groups: The first group includes performance tests in which stress distribution in specimens under test is not homogeneous (Table 2.3) and the second group includes performance tests in which stress distribution in specimens under test is homogeneous (Table 2.4).

In the first group, the classical fatigue criterion, 50 percent drop in initial stiffness and following that dissipated energy approaches have been applied to find the number of cycles to failure. The criterion of 50 percent drop in initial stiffness is an arbitrary definition that does not evaluate the various mechanisms by which a material responds to the energy input while subjected to the loading. Therefore, researchers began applying dissipated energy to describe the fatigue behavior of asphalt mixes. Dissipated energy approaches, described in Table 2.5, are as follow: Initial dissipated energy (IDE), cumulative dissipated energy (CDE), dissipated energy ratio, and ratio of dissipated energy change (RDEC). The research conducted in fatigue behavior of asphalt mixes have shown that rate of change in dissipated energy per load cycle is a better indicator of fatigue (DER and RDEC approaches). (American Society of Civil Engineers, 2009)

Table 2.3 Fatigue tests on bulk specimens with non-homogeneous stress distribution.
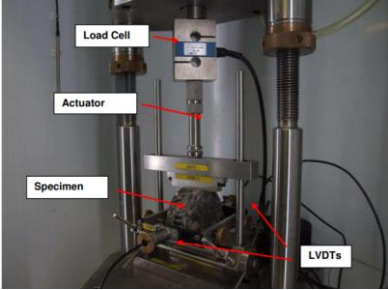
Test name	Type of loading and test description	Test standard	Mode	Test configuration and Analysis
Four-point bending	Sinusoidal Non-homogeneous A prismatic specimen of asphalt mix is subjected to repetitive sinusoidal strain levels (140-220 micro strain) at 10 Hz and 20 ℃ until its stiffness drops to 50% of initial stiffness.	AASHTO T321	Strain controlled	$N_f = k_1 (1/\varepsilon)^{k2}$ Wohler curve and ε_6
Two-point bending	Sinusoidal Non-homogeneous A trapezoidal specimen of asphalt mix, at its narrow end, is subjected to repetitive sinusoidal strain levels (140-220 micro strain) at 15 Hz and 25 Hz, and 10 ℃ until its stiffness drops to 50% of initial stiffness.	EN 12697-24	Strain controlled	$N_f = k_1 (1/\varepsilon)^{k2}$ Wohler curve and ε_6
Indirect Tensile	Haversine Non-homogeneous A cylindrical specimen of asphalt mix is subjected to repetitive haversine diametral load at 10 ℃ and 20 ℃ with loading and resting time of 0.1s and 0.4s respectively until its stiffness drops to 50% of initial stiffness.	EN 12697-26	Stress controlled	$N_f = k_1 (1/\sigma)^{k2}$ Wohler curve and ε_6

Table 2.4 Fatigue tests on bulk specimens with homogeneous stress distribution.

Test name	Type of loading and stress distribution	Test standard or Designed by	Mode	Test configuration and Analysis
Cyclic (continuum damage)	Sinusoidal Homogeneous	DGCB approach ENTPE	Strain controlled	a_F vs. ε plot and ε_6
Cyclic (continuum damage)	Sinusoidal Homogeneous	AASHTO TP79	Strain controlled	C-S curve, S_{app} and D_R parameters

Table 2.5 Dissipated energy ratio approaches.

Dissipated Energy Approach	Analysis
Initial dissipated energy	The dissipated energy measured at initial loading cycles (usually at 50th cycle). $N_f = 2.365 \ e^{0.069 \ VFB} \ (W_0)$ $W_0 = 0.25 \ \pi \ \varepsilon_0^2 \ (E_0 \ \sin\phi_0)$ N_f = the fatigue life, W_0 = the initial dissipated energy at the 50th cycle VFB = the percentage void filled with asphalt
Cumulative dissipated energy (CDE)	The total dissipated energy (the sum of all hysteresis loops) until the failure of material. $W_{total} = A \ (N_f)^Z$ W_{total} = the cumulative dissipated energy to failure N_f = the number of cycles to failure A and Z = constant coefficients dependent on the mixture
Dissipated energy ratio (DER)	The ratio of dissipated energy at a specific cycle to the total dissipated energy up to that cycle. The plot of DER vs. number of cycles defines cycle N in which widening of hair crack and crack growth starts happening. $DER = W_i \ / \Sigma \ W_i$ DER = dissipated energy ratio W_i = dissipated energy at cycle i $\Sigma \ W_i$ = total dissipated energy up to cycle i
Ratio of dissipated energy change (RDEC)	The dissipated energy is history dependent and the damage accumulation in a material subjected to fatigue must be accompanied by a change in the dissipated energy. RDEC approach can indicate damage. $RDEC = \frac{W_{n+1} - W_n}{W_n}$ RDEC = ratio of dissipated energy change per load cycle W_n = dissipated energy produced in load cycle n W_{n+1} = dissipated energy produced in load cycle n+1 The plot of RDEC vs. number of cycles has three stages in which the point where stage II turns in stage III is considered the beginning of macro cracking and failure.

In the second group, continuum damage mechanics is applied to describe the behavior of asphalt specimens subjected to cyclic loading and fatigue. Currently, there are two approaches for continuum damage: DGCB approach (Department of Building and Civil Engineering) of "ENTPE" according to Di Benedetto's research (Baaj, 2005) and Simplified Visco-Elastic Continuum Damage (S-VECD) according to North Carolina State University (NCSU) (American Society of Civil Engineers, 2009).

2.2.2.2.2 DGCB Approach

This approach has been used and verified by use in various research; one of them was the interlaboratory fatigue test campaign conducted by the RILEM 182 PEB technical committee (Baaj, 2005). According to DGCB method, there are three distinctive phases in an experimental fatigue test (Figure 2.13). In phase I, a drastic decrease in stiffness occurs due to heating and thixotropy. Phase II is considered as the true evolution of fatigue damage, however, bias effects such as heating are assumed to be existent in this phase. Therefore, the value of stiffness must be corrected in order to eliminate the bias effects. In phase III, macro cracks initiate and progress until the failure at the end of this phase. The damage parameter (D_{exp}) at a specific cycle Number N is calculated according to Equation 9,

$$D_{exp} = 1 - \frac{(E_0 - E_N)}{E_0} \tag{9}$$

where E_0 = initial stiffness and E_N = stiffness at cycle N.

In the DGCB approach, two intervals are selected in the second phase of fatigue (Figure 2.14), and the value of a_T is calculated by dividing the slope of the regression line divided by E_{00i} for the specific interval. The experimental slope (a_T) needs to be corrected due to changes in dissipated energy per cycle for fatigue testing in two different modes of controlled stress and controlled strain. Therefore, a_T is separated into two parts based on Equation 10 in which a_F is true fatigue and a_B is the bias effect.

$$a_T = a_F + a_B \tag{10}$$

Equation 11 shows the proposed law to determine the corrected fatigue slope (a_F),

$$a_F = a_T + a_W, C_i \frac{(E_0 - E_{00i})}{E_{00i}} \qquad (11)$$

where the value E_{00i} of the dissipated energy is obtained from a linear extrapolation to the first cycle of loading (Figure 2.13). C_i is a coefficient that considers damage evolution (C_1 and C_2 are 3/4 and 2/3 respectively). After finding a_F for each interval (1 and 2) at specific stain levels, the plot of strain level versus a_F shows the rate of damage (the slope of regression line) for asphalt mixes (Figure 2.15). $\varepsilon_{6\text{-}i}$ that can be found for each interval (1 and 2) is defined as the strain level resulting in a damage of 50% after 1,000,000 cycles (Figure 2.15). In Equation 11, a_T is the slope of the dissipated energy in the considered interval normalized by the value W_{00i} of the dissipated energy obtained from a linear extrapolation to the first cycle of loading (Figure 2.15). C_i is a coefficient that considers damage evolution (C_1 and C_2 are 3/4 and 2/3 respectively). After finding a_F for each interval (1 and 2) at specific stain levels, the plot of strain level versus a_F shows the rate of damage (the slope of regression line) for asphalt mixes (Figure 2.15). $\varepsilon_{6\text{-}i}$ that can be found for each interval (1 and 2) is defined as the strain level resulting in a damage of 50% after 1,000,000 cycles (Figure 2.15).
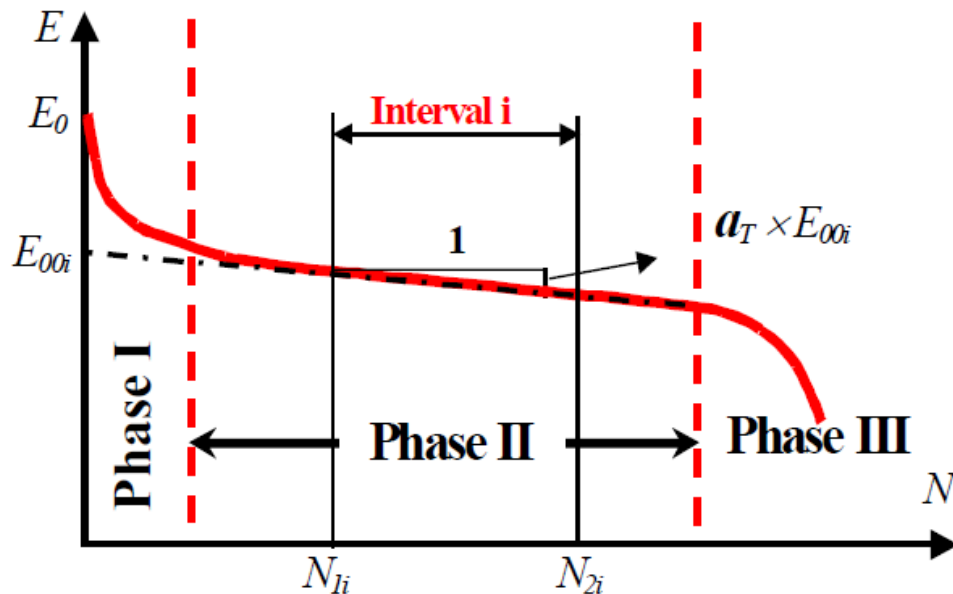
Figure 2.13 Determination of E_{00i} and a_T from stiffness evolution curve (Baaj, 2005).
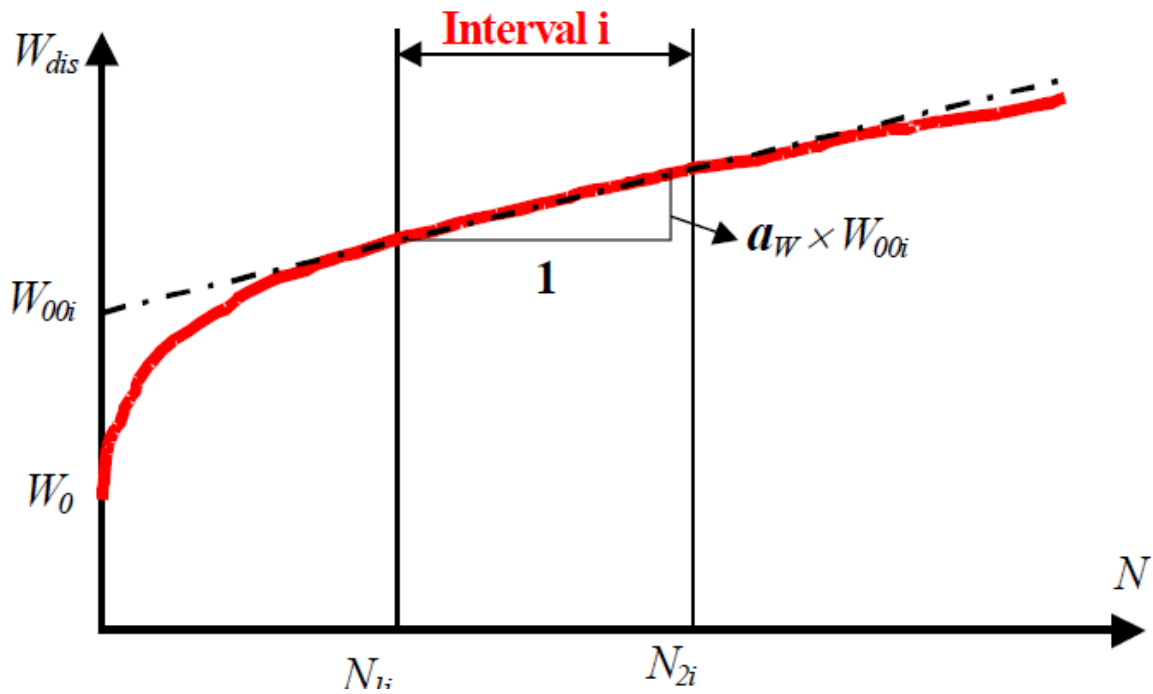
Figure 2.14 Determination of W_{00i} and a_W from the dissipated energy curve (Baaj, 2005).
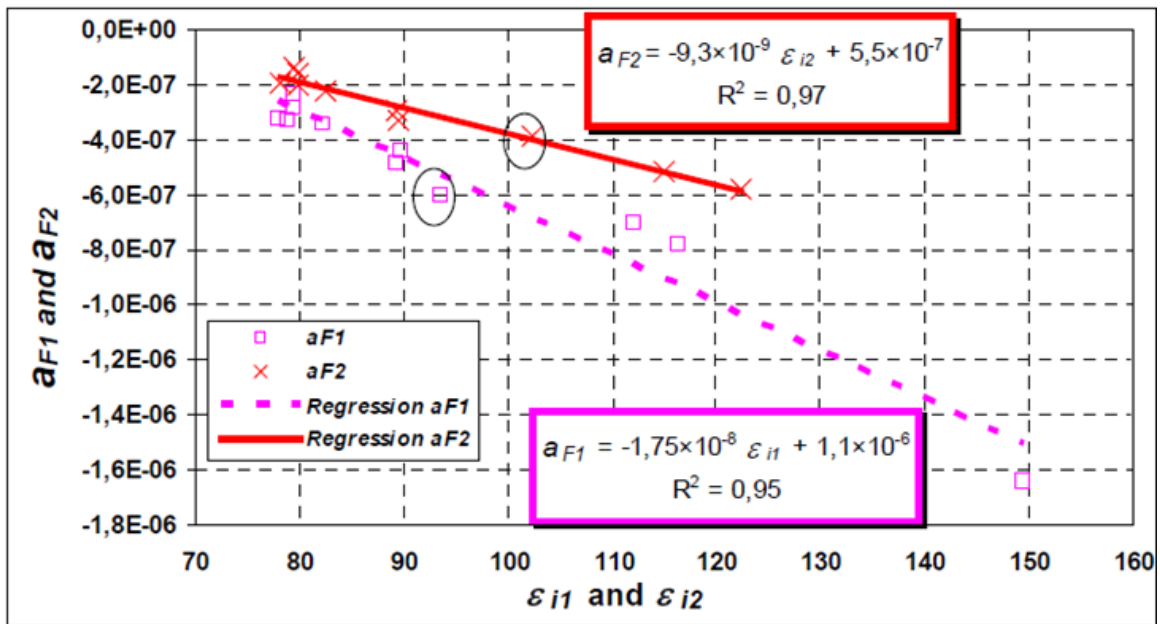
Figure 2.15 Damage rates and corresponding regression lines (Baaj, 2005).

35

2.2.2.2.3 <u>S-VECD Approach</u>

Simplified viscoelastic continuum damage is a VECD model that has been applied for cyclic loading using an asphalt mixture performance tester (AMPT) or a system that meets or surpasses the requirements for the Simple Performance Test System mentioned in NCHRP Report 629 (Appendix E) in order to characterize the fatigue behavior of asphalt mixtures (Michael, 2008). VECD was developed based on three essentials: (1) the time-temperature superposition (TTS) principle with growing damage in order to find the effect of temperature on constitutive behavior, (2) the elastic-viscoelastic correspondence principle, and (3) continuum damage mechanics in order to investigate the effect of microcracking and degradation on the constitutive behavior.

The first essential was verified by Chehab's research in which asphalt specimens were simply subjected to a wide range of monotonic constant cross head tensile strain levels at different temperatures (Chehab, Kim, Schepary, Witczack, & Bonaquist, 2003). The continuous plot of stress at different temperatures versus the reduced time at a constant tensile strain level simply verified the TTS with growing damage beyond linear viscoelastic (LVE) region. The importance of the TTS with growing damage is underscored by the reduction in testing for VECD model.

The second essential is elastic-viscoelastic correspondence principle developed by Schapery in which using pseudo variables instead of physical strain and stress can transform the constitutive equations for viscoelastic materials into the same equivalent equations as elastic materials (Equations 12, 13 and 14) (Schapery, 1984) and (Lee & Y, 1998).

$$Elastic\ body\ without\ damage: \sigma = E\ \varepsilon \tag{12}$$

$$Viscoelastic\ body\ without\ damage: \sigma = E^R\ \varepsilon^R \tag{13}$$

$$Pseudostrain\ \varepsilon^R = \frac{1}{E_R}\int_0^t E(t-\tau)\frac{d_\varepsilon}{d_\tau} \tag{14}$$

The third essential is using continuum damage mechanics in order to examine the effect of microcracking and degradation phenomenon on the constitutive behavior. In continuum damage mechanics, the body damaged is considered as a homogeneous continuum on a macroscopic scale such that the effect of damage is exhibited by reduction in strength or stiffness of the material. Therefore, Equations 12 and 13 are transformed into Equations 15 and 16 considering continuum damage mechanics such that C and S are respectively representative of stiffness (integrity) and damage.

$$Elastic\ body\ with\ damage: \sigma = C(S_m)E\varepsilon \tag{15}$$

$$Viscoelastic\ body\ with\ damage: \sigma = C(S_m)E^R\varepsilon^R \tag{16}$$

Schapery used the concept of thermodynamics of irreversible processes to obtain a method for describing the mechanical behavior of elastic materials with growing damage. Therefore, the extent of work needed to create an amount of damage was defined as a function of internal state variables (ISVs) considering the theory of thermodynamics of irreversible processes. Schapery utilized the work potential theory to elastic media in order to find the effect of damage on the constitutive behavior. The work potential theory is comprised of the following components:

1. Strain energy density function: $W = W(\varepsilon, S_m)$
2. Stress-strain relationship: $\partial W / \partial \varepsilon = \sigma$
3. Damage evolution law: $-\partial W / \partial S = \partial Ws / \partial S_m$

Considering that σ = stress, ε = strain, S_m internal state variable (damage), W = work of strain energy and W_s dissipated energy due to microstructural damage.

The S-VECD model is used as a material model characterizing the constitutive relationships as fatigue damage grows (Daniel & Y., 2002), (Chehab, Kim, Schepary, Witczack, & Bonaquist, 2003), (Underwood, Kim, & Guddati, Characterization and

Performance Prediction of ALF Mixtures Using a Viscoelastic Continuum Damage Model, 2006), (Underwood, 2012) VECD model initiated by Kim and Little by using the time-domain one-dimension VECD model for asphalt mixes in cyclic domain in order to develop a uniaxial constitutive equation to predict the effects of loading (Kim, 1990). By applying Schapery's elastic-viscoelastic correspondence principle, Kim presented a viscoelastic constitutive model with growing damage (Schapery, 1984).

To identify the linear viscoelastic (LVE) characteristics of an asphalt mix, first, dynamic modulus value |E*| is determined, and then the uniaxial fatigue testing is conducted to obtain the fatigue data. The main results of S-VECD method can be presented in the form of damage characteristic curve (C-S), the D^R failure criterion, and the apparent damage capacity referred to as S_{app} (Wang, 2018 and 2020).

Although the analysis of S-VECD fatigue testing is conducted using the FlexMat excel sheet provided by North Carolina State University (NCSU), Equation 17, 18, 19 and 20 are the primary relationships used to analyze obtained data and determine C-S (Underwood, 2011).

$$\varepsilon_R = \begin{cases} \varepsilon_R = \dfrac{1}{E_R} \displaystyle\int_0^{\xi} \int E(\xi - \tau) \dfrac{d\xi}{d\tau} & \xi \leq \xi_P \\[4mm] \varepsilon_{0,ta_{cycle\,i}}^R = \dfrac{1}{E_R} \dfrac{\beta+1}{2} \left((\varepsilon_{0,pp})_i |E^*|_{LVE} \right) & \xi > \xi_P \end{cases} \tag{17}$$

$$C \begin{cases} C = \dfrac{\sigma}{\varepsilon^R DMR} & \xi \leq \xi_P \\[4mm] C^* = \dfrac{\sigma_{0,ta}}{\varepsilon_{0,ta}^R DMR} & \xi > \xi_P \end{cases} \tag{18}$$

$$dS = \begin{cases} (dS_{transient})_{timestep\,j} = \left(-\dfrac{DMR}{2} (\varepsilon^R)_j \Delta C_j \right)^{\frac{\alpha}{1+\alpha}} (\Delta \xi_j)^{\frac{1}{1+\alpha}} & \xi \leq \xi_P \\[4mm] (dS_{cyclic})_{cycle\,i} = \left(-\dfrac{DMR}{2} (\varepsilon_{0,ta}^R)^2 \Delta C_j \right)^{\frac{\alpha}{1+\alpha}} (\Delta \xi_p K_1)^{\frac{1}{1+\alpha}} & \xi > \xi_P \end{cases} \tag{19}$$

$$K_1 = \frac{1}{\xi_f - \xi_i} \int_{\xi_i}^{\xi_f} \left(f(\xi)\right)^{2\alpha} d\xi \tag{20}$$

where $\varepsilon_{0,ta}^R$= Tension amplitude of pseudo strain for given cycle, β = quantity to determine proportion of tensile loading in cycle, C^* = pseudo secant modulus in cycle portion, DMR = dynamic modulus ratio from LVE testing, $\varepsilon_{0,pp}$= peak to peak strain for given cycle, ξ_P= pulse time, $\sigma_{0,ta}$ = tension amplitude of stress for given cycle, and $f(\xi)$ = loading function.

D^R, a new fatigue failure criterion determined by Wang and Kim, is the average loss of integrity per cycle throughout an asphalt mix's life remains constant regardless of temperature, mode of loading and load amplitude (Wang, 2018). D^R can be determined by Equation 21.

$$D^R = \frac{\int_0^{N_f}(1 - C)dN}{N_f} = \frac{sum\ (1 - C)}{N_f} \tag{21}$$

According to Equation 21, D^R is the slope of the linear relationship between the sum of (1-C) and N_f. Wang and Kim demonstrated that D^R value is a parameter indicative of ductility and brittleness of an asphalt mix. High D^R value and low D^R value indicate that an asphalt mix is ductile and brittle, respectively.
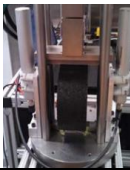
The corresponding S value on the damage characteristic curve when C is equal to (1- D^R) is defined as the apparent damage capacity (S_{app}). S_{app} is determined by Equation 22.

$$S_{app} = 1000^{\frac{\alpha}{2}-1} \times a_T^{\frac{1}{\alpha+1}} \left(\frac{D^R}{C_{11}}\right)^{\frac{1}{C12}} \tag{22}$$

2.2.2.2.4 Performance Tests to Evaluate Intermediate Crack Propagation

Although fatigue characterization techniques using cyclic loading either in flexural or uniaxial mode have been long established, the development of simple, timely, and affordable techniques that can evaluate the fracture properties of asphalt mixtures is considered to be very beneficial to the asphalt paving community. Such tests could be potentially utilized toward implementation of a Balanced Mix Design (BMD) process as well as a quality assurance tool, assisting with crack resistance evaluation of asphalt mixtures at the production level. Table 2.6 shows various fracture mechanics-based tests, and their test analysis that have been used by different researchers and highway agencies up to now.

Table 2.6 Cracking resistance tests at intermediate temperature (West, 2018).

Laboratory tests for Cracking	Equipment and Cost	Specimen Fabrication	Test Results and Data Analysis Complexity	Practicality for Mix Design and QA	Correlation to field performance	Test variability
Illinois Flexibility Index Test (I-FIT) AASHTO T 124	Stand-alone servo-hydraulic device, saw for cutting specimens, saw for notching specimens $20,000 US	Cylindrical specimen, three cuts and one notch	Flexibility Index Simple Analysis	Good	Good correlation to pavement sections in Illinois and on FHWA ALF	Medium COV=10-20%
Indirect Tensile Asphalt Cracking Test (IDEAL-CT) ASTM D8225	Stand-alone servo hydraulic IDEAL-CT device $15,000 US	Cylindrical specimen	Cracking test index (CT Index) Simple Analysis	Good	Good correlation to pavement sections in Texas and on FHWA ALF and MnROAD facilities	Medium COV=10-25%

Semi-Circular Bend Test (Louisiana method) ASTM D8044	Screw drive test, fixture, saw for cutting specimens, environmental chamber, saw for notching specimens $20,000 US	Cylindrical specimen, several cuts, three notches	J-integral Fair Analysis	Fair	Fair correlation to pavement sections in Louisiana	Medium COV=20%
Texas Overlay Test NJDOT B-10 Tex-248-F	Texas overlay tester, environmental chamber, saw for cutting specimens $55,000 US	Cylindrical specimen, four cuts, gluing base plates	Number of cycles to failure Simple Analysis	Good	Good correlation to pavement sections in Texas, New Jersey, on FHWA-ALF and NCAT test track	High COV=30-50%

2.2.2.3 Thermal (Low Temperature) Cracking

Generally, thermal cracking of asphalt pavements occurs in cold climate, especially in Canada and the Northern US due to cold temperature or temperature cycling. Thermal cracking caused by cold temperature is refereed to low temperature cracking, while thermal cracking caused by temperature cycling is refereed to thermal fatigue cracking. Low temperature cracking happens in Canada and in the northern United States. Meanwhile, thermal fatigue cracking happens in the southwestern USA where asphalt pavements experience large temperature difference between day and night-time.

The main reason giving a rise to thermal cracking is the contraction within an asphalt layer due to cold weather that results in building up tensile stress. When the tensile stress becomes equal to or greater than the tensile strength of the asphalt layer, thermal cracking happens (Zhou, 2016).

In general, major factors influencing thermal cracking are as follows:

- Temperature: The colder the temperature of the asphalt pavement surface, the higher the potential of thermal cracking. The main reason is that at cold temperature the asphalt mixture becomes stiffer and more brittle.
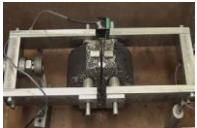
- Cooling rate: The greater the cooling rate, the greater potential of thermal cracking.
- Asphalt binder: The lower the PG grade low end, the higher the resistance of the asphalt binder to thermal cracking.
- Coefficient of thermal contraction: The greater the coefficient of thermal contraction, the higher the potential of thermal cracking.
- Pavement thickness: the thicker the asphalt pavement layer, the lower potential of thermal cracking.
- Aging: The more asphalt binder is aged, the higher the frequency of thermal cracking.
- Subgrade type: Sand subgrade causes more thermal cracking than cohesive soil.
- The reason is that more friction causes the asphalt layer not to slide.

Currently, the Superpave mix design method characterizes asphalt mixtures performance at low temperatures by conducting the Bending Beam Rheometer (BBR) test and controlling two parameters obtained from the test: creep stiffness (S) and the rate of change of creep stiffness (m) at 60 s in the linear viscoelastic region. However, to investigate the resistance of asphalt mixtures to thermal cracking, not only is the characteristics of an asphalt binder as a component of asphalt mixtures significant, but also the aggregate gradation, the physical and chemical interaction between asphalt binder and aggregate, asphalt binder adhesion, and cohesion of the entire asphalt mixture must be taken into consideration. Therefore, in addition to conducting asphalt binder testing to characterize thermal cracking resistance of asphalt mixtures, suitable asphalt mixture performance tests must be employed to examine the resistance of asphalt mixtures to thermal cracking. Over the past decades, several asphalt mixture performance tests such as the Thermal Stress Restrained Specimen Test (TSRST) and the Indirect Tension Test (IDT), Disk-Shaped Compact Tension (DC(T)) test and the Semi-Circular Bend (SCB) test have been used to capture thermal cracking resistance of asphalt mixtures (Christensen D. R., 2004; Marasteanu, 2007 and 2012; Dave, 2016; Braham A. F., 2007; Hill, 2013; Bashir, 2020; Salehi-Ashani, 2020; Rahbar-Rastegar, 2018; Jahangiri, 2019; Li, 2009. DC(T) and SCB tests known as fracture mechanics-based tests can better simulate thermal cracking evolution in asphalt pavements which is a function of

42

temperature and time. Generally, temperature and time in DC(T) and SCB tests can be identified by controlling testing temperature and crack mouth opening displacement (CMOD), respectively.

Table 2.7 summarizes asphalt mixture performance tests that have been applied to characterize thermal cracking susceptibility of asphalt mixtures by different researchers and highway agencies.

Table 2.7 Performance Tests to Characterize Low Temperature Cracking Resistance.

Laboratory tests for Cracking	Equipment and Cost	Specimen Fabrication	Test Results and Data Analysis Complexity	Practicality for Mix Design and QA	Correlation to field performance	Test variability
Disc-Shaped Compact Tension Test ASTM D7313	Stand-alone DCT test system, core drill, saw for cutting specimens Saw for notching specimens $ 60,000 US	Cylindrical specimen, three cuts, one notch, two loading holes, gluing gauge points	Fracture energy Simple Analysis	Good	Good correlation to pavement sections in New York, Iowa, Illinois, and on UIUC-ATLAS APT and MnROAD	Low (10%)
IDT Creep Compliance and Strength Test AASHTO T 322	Loading device, data acquisition system, specimen deformation measuring device, environmental chamber, saw for cutting specimens $ 156,000 US	Cylindrical specimen, two cuts, gluing gage points	IDT creep compliance IDT tensile strength Complex Analysis	Fair	Good (inputs to TCModel and MEPDG)	Medium (7-11%)

Semi-Circular Bend Test AASHTO TP 105	Loading device, data acquisition system, bend test fixture, environmental chamber, saw for cutting specimens, saw for notching specimens $ 145,000 US	Cylindrical specimen, three cuts, one notch and gluing gauge points	Fracture energy Simple Analysis	Fair	Good correlation to pavement sections in Illinois, Minnesota, and Wisconsin	Medium (20%)
Uniaxial Thermal Stress Restrained Specimen Test	Stand-alone UTSRST system, core drill, saw for cutting specimens $100,000 US	Cylindrical specimen, coring, and gluing	CTC, fracture strength/temperature, Crack initiation stress, UTSST Resistance Index, or other thermo-viscoelastic properties Complex Analysis	Fair	Good correlation to pavement sections in Nevada	Unknown
Thermal Stress Restrained Specimen Test BS EN 12697-46	Stand-alone TSRST testing apparatus, slab compactor, saw for cutting specimens $ 170,000 US	Beam specimen, four cuts, gluing end platens	Fracture temperature Fair Analysis	Poor	Fair correlation to pavement sections in Alaska, Pennsylvania, and on MnROAD	Medium (COV = 10-20%)

2.2.3 Moisture Damage

Moisture damage or stripping is a cause of failure of asphalt pavements that brings about costly repair and rehabilitations activities. Generally, there are a few possible mechanisms causing moisture damage listed as follows (Asphalt Institute, 2014):

- Scouring effect: This phenomenon happens in consequence of hydraulic pressure fluctuations within interconnected voids in asphalt pavements containing water

caused by passing traffic. The scouring effect removes the asphalt binder from the surface of aggregate.

- Adhesion failure between asphalt binder and aggregate: Since aggregate has a higher affinity for water than the asphalt binder, existing water in an asphalt pavement can replace the asphalt binder film and causes stripping.

- Cohesion failure within asphalt binder: The pressure of evaporated water within an asphalt pavement can remove the bond between asphalt binder molecules.

- Cohesive failure within the aggregate: The action of water within an asphalt pavement can cause the breakage of aggregate.

- Spontaneous emulsification: The presence of water in the asphalt pavement followed by high temperatures and high shear stresses can weaken the bond between asphalt binder molecules.

- Freezing: The expansion of entrapped water within the asphalt pavement can damage the asphalt pavement.

Table 2.8 summarizes asphalt mixture performance tests that have been applied to characterize moisture damage susceptibility of asphalt mixtures by different researchers and highway agencies.

Table 2.8 Performance Tests to Evaluate Moisture Damage of Asphalt Mixtures.

Laboratory tests for Moisture Damage	Equipment and Cost	Specimen Fabrication	Test Results and Data Analysis Complexity	Practicality for Mix Design and QA	Correlation to field performance	Test variability
Moisture Induced Stress Tester ASTM D7870	Moisture conditioning system $18,000 US	Cylindrical specimen	Changes in the bulk specific Simple Analysis	Good	Unknown	Unknown

Test	Equipment / Cost	Specimen	Output / Analysis		Correlation	COV
Tensile Strength Ratio AASHTO T 283	Vacuum container, water bath, freezer, mechanical testing machine, Lottman breaking head $8,500 US	Cylindrical specimen	IDT strength, TSR Simple Simple Analysis	Good	Unknown	Low COV=10%
Hamburg Wheel Tracking Test (AASHTO T324)	Hamburg Wheel-Tracking device and saw for cutting specimens $40,000-70,000 US	Cylindrical and slab specimens	Stripping inflection point, stripping slope Simple Analysis	Good	Good correlation to pavement sections in Colorado and Texas	Medium COV=10-30%
Asphalt Pavement Analyzer (AASHTO T340)	Asphalt Pavement Analyzer $120,000 US	Cylindrical and slab specimens	Stripping inflection point, stripping slope Simple Analysis	Good	Good correlation to pavement sections on FHWA ALF, WesTrack, NCAT Test Track, and in Georgia and Nevada	Medium COV=20%

2.3 Construction Quality Assurance Terms

Generally, Quality Assurance (QA) specifications are a combination of End Result Specifications (ERS) and materials and methods specifications. ERS are defined as specifications that hold the contractors responsible for providing a product.

Overall, performance specifications describe how a finished product should perform during its service time. Performance specifications can be divided into two primary groups: Performance-Based-Specifications (PBS) and Performance-Related Specifications (PRS). PBS are QA specifications that describe the desired level of fundamental engineering

properties and can be used in performance prediction, while PRS are QA specifications that that describe the desired levels of key materials and construction quality characteristics that have been found to correlate with fundamental engineering properties that predict performance (Tighe, 2013).

Table 2.9 shows some of performance tests and their specifications that have been set up or that are still under development in some Departments of Transportation (DOTs) in the US. These tests have been proposed to be used for QA or BMD activities (West, 2018).

Table 2.9 Performance Specifications Set up by Some DOTs for QA and BMD Activities (West, 2018).

State	Description	Cracking Criteria	Rutting Criteria
California	Performance-Based Specifications (PBSs) and the CalME (Caltrans' Mechanistic Empirical Design Program)	Bending Beam Fatigue Test (AASHTO T 321)	Determining the Permanent Shear Strain and Stiffness of Asphalt Mixtures Using the Superpave Shear Tester (SST) (AASHTO T 320) Hamburg Wheel Track Test (AASHTO T324)
Florida	Research in progress	IDT Energy Ratio Texas Overlay	Flow Number Hamburg Wheel Track (HWT) Test (AASHTO T324) Rutting and Moisture Damage Asphalt Pavement Analyzer (APA) Test @64 ℃ (AASHTO T340) Acceptance Criteria: Maximum rut depth of 4.5 mm at 8000 cycles

Georgia	Research in progress	————————————	Hamburg Wheel Track (HWT) Test (AASHTO T324) Rutting and Moisture Damage Asphalt Pavement Analyzer (APA) Test (AASHTO T340)
Iowa	Research in progress	Bending Beam Fatigue Test (AASHTO T 321) Minimum threshold of 100,000 cycles to failure at 2,000 micro strain For High Performance Thin Overlay (HPTO) Disk-shaped compact tension (DC(T)) test (ASTM 7313)	Hamburg Wheel Track (HWT) Test (AASHTO T324) @40°C for PG 58-xx asphalt binders and 50°C for higher binder grades Acceptance Criteria: Maximum 8 mm rut depth at 8,000 passes Minimum HWTT stripping inflection point (SIP) of 10,000 for plant produced mixtures with traffic designation Standard (S), and 14,000 for mixtures with traffic designations High (H) and Very High (V)
New Mexico	Research in progress	————————————	Hamburg Wheel Track (HWT) Test AASHTO T324 @40°C, 50°C and 60°C

Ohio	Research in progress	Bending Beam Fatigue Test (AASHTO T321) Acceptance Criteria: Minimum of 100,000 cycles at 1500micro strain for Bridge deck waterproofing surface course	Asphalt Pavement Analyzer (APA) Test (AASHTO T340) 48.9°C for non-polymer asphalt binder mixes and 54.4°C for all heavy surface and high stress area mixes Acceptance Criteria: The maximum APA rut depth is 5.0 mm at 8,000 cycles for most mixes, and 3.0 mm for high stress mixes
Oklahoma	Research in progress	IFIT	Hamburg Wheel Track (HWT) Test AASHTO T324 @50°C Acceptance Criteria: Minimum passes at 12.5 mm rut depth Binder Number of Pass PG64-XX 10000 PG70-XX 15000 PG76-XX 20000
Minnesota	Research in progress	Disk-shaped compact tension (DC(T)) test (ASTM 7313) Acceptance Criteria: ESALs>30M FE=690J/m^2 30M>ESALs>10M FE=460J/m^2 ESALs<10M FE=400J/ m^2	_____

Texas	BMD-Volumetric Design with Performance Verifications A space diagram including both rut depth of HWT test and minimum number of cycles of OT test is used during mix design and acceptance	Texas Overlay Test (Tex-248-F) Acceptance Criteria: Asphalt Mix Number of Cycles Porous Friction Course >200 SMA >200 Thin Overlay (PG70-XX) >300 Thin Overlay (PG76-XX) >300 Hot-in-place recycling >150	Hamburg Wheel Track (HWT) Test AASHTO T324 @50°C Acceptance Criteria: Minimum passes at 12.5mm rut depth Asphalt Mix Minimum Passes Porous Friction Course 10000 SMA 20000 Thin Overlay (PG70-XX) 15000 Thin Overlay (PG76-XX) 20000 Hot-in-place recycling 10000
South Dakota	Research in progress	Disk-shaped compact tension (DC(T)) test (ASTM 7313) SCB Low Temperature (AASHTO TP105)	Asphalt Pavement Analyzer (APA) Test (AASHTO T340) @ Binder's high temperature PG Acceptance Criteria: Maximum Rut Depth at 8000 Cycles Truck ADT Rut Depth <75 <8mm 76-250 <7mm 251-650 <6mm 651-1200 <5mm >1200 <5mm

Utah	Research in progress	IFIT Test (AASHTO TP124) Bending Beam Rheometer (AASHTO TP125)	Hamburg Wheel Track (HWT) Test AASHTO T324 Acceptance Criteria: Maximum 10mm rut depth @20000 cycles Binder Temperature PG58-XX 46°C PG64-XX 50°C PG70-XX 54°C
Louisiana	BMD-Volumetric Design with Performance Verifications A space diagram including both rut depth of HWT test and minimum critical strain energy release of SCB test is used during mix design and acceptance	ASTM D8044 Minimum critical strain energy release (J_c) kJ/m^2 Acceptance Criteria: Minimum of 0.6 and 0.5 kJ/m^2 of critical strain energy released for level 1 and 2 of traffic respectively	Hamburg Wheel Track (HWT) Test AASHTO T324 @50 ºC Acceptance Criteria: Minimum number of passes at 12 mm rut depth Binder Number of Pass PG58-XX 12000 PG64-XX 20000 PG70-XX (OGFC) 7500

Illinois	BMD-Volumetric Design with Performance Verifications A space diagram including both rut depth of HWT test and minimum Flexibility Index (FI) of SCB test is used during mix design and acceptance	I-FIT AASHTO TP124 Flexibility Index (FI) Acceptance Criteria: FI≥8	Hamburg Wheel Track (HWT) Test AASHTO T324 @50 ºC Acceptance Criteria: Maximum rut depth 12.5mm Binder Number of Pass PG58-XX 5000 PG64-XX 7500 PG70-XX (OGFC) 15000 PG76-XX 20000
Wisconsin	Research in progress	Disk-shaped compact tension (DC(T)) test (ASTM 7313) Low-temperature semi-circular bend test (AASHTO TP105) Extracted Binder (ΔT_C) Binder $\quad$ ΔTC DC(T)FE(J/m^2) PG58-XX $\quad$ <5°C $\quad$ >400 PG64-XX $\quad$ <5°C $\quad$ >400	Hamburg Wheel Track (HWT) Test (AASHTO T324) Acceptance Criteria: @45 ºC Minimum passes to 12.5 mm Low traffic 7500 passes Medium traffic 11250 passes High traffic 15000 passes

New Jersey	Flexural beam test is used if the mode of cracking is dependent on the flexural properties of the pavement and OT test is used if the expansion-contraction of concrete slab underlying asphalt mix is causing the cracking	Texas Overlay (OT) test (TX-248-F) Acceptance Criteria: Minimum of 700 cycles for Binder-rich intermediate course and 170 cycles for High RAP mixes and Flexural Beam Fatigue Test (AASHTO T321) Acceptance Criteria: Minimum of 100,000 cycles @15 ℃ and 1500micro strain for Bridge deck waterproofing surface course and Minimum of 100,000,000 cycles @15 ℃ and 100micro strain for Bottom rich base course	Rutting and Moisture Damage Asphalt Pavement Analyzer (APA) Test (AASHTO T340) @64 ℃ 100-psi hose pressure, 100-lb wheel loads and 8000 cycles Acceptance Criteria: Maximum of 4mm rut depth for High-performance thin overlay Maximum of 6mm rut depth for Binder-rich intermediate course Maximum of 3mm rut depth for Bridge deck waterproofing surface course Maximum of 5mm rut depth for Bottom-rich base course Minimum of 4mm for High RAP mix with PG70-22 and minimum of 7mm for High RAP mix with PG64-22
Alabama	Research in progress	_____	Asphalt Pavement Analyzer (APA) Test (AASHTO T340) Acceptance Criteria: Rut depth @ 8000 cycles @67 ℃ Traffic Max Rut Depth 30M>ESALs>10M 4.5 mm
South Carolina	Research in progress	_____	Asphalt Pavement Analyzer (APA) Test (AASHTO T340) Acceptance Criteria: Rut depth @ 8000 cycles Binder Max Rut Depth PG76-22 @64 ℃ 3mm PG64-22 @64 ℃ 5mm

2.4 Summary and Research Gap

As mentioned earlier, the volumetric properties of asphalt mixtures are not sufficient to predict the long-term performance of asphalt pavements, and performance testing not only can predict the long-term performance of asphalt pavements, but it can also facilitate the use of new materials and technologies in the asphalt pavement industry. Therefore, to find the most suitable performance tests and to provide a basis for implementation of performance specifications for rutting and cracking resistance of asphalt mixtures in Ontario is critical.

Based on the literature review, the Hamburg Wheel Tracking test as a simulative test is an appropriate test to evaluate rutting and moisture damage susceptibility of asphalt mixtures that can be applied in Ontario. However, the appropriate testing temperature and rut depth specification must be investigated in terms of asphalt binder PG grade.

To date, several laboratory tests, including flexural beam fatigue test, trapezoidal test, indirect tension test, and uniaxial fatigue test have been developed and applied to address fatigue cracking. Even though fatigue characterization techniques using cyclic loading have been long established, development of a simple, timely, and affordable laboratory test that can capture the fracture properties of asphalt mixtures is considered very beneficial for evaluation of durability. Therefore, it is important to compare cyclic tests with simple fracture tests such as I-FIT and IDEAL-CT. Given that 1) the default testing temperature for I-FIT is specified at 25 ℃, 2) there are two methods for pre-test conditioning of I-FIT specimens (water bath and environmental chamber), 3) I-FIT can be conducted with or without a chamber set up at 25 ℃, 4) asphalt binders manifest a level of temperature susceptibility derived from their Performance Grade (PG), and 5) long-term aging drastically affects long-term in-service of asphalt pavements, it is crucially important to investigate the temperature sensitivity of I-FIT parameters, especially Flexibility Index, due to the likely variability in testing temperature occurring in practice. Furthermore, it is important to investigate the effect of long-term aging on I-FIT parameters.

To overcome the shortcoming of Superpave specifications regarding thermal cracking, two fracture-mechanics based tests, DC(T) and SCB, which have shown promise were selected for further investigation. Since testing temperature for DC(T) and SCB tests has been specified

at 10°C higher than low PG asphalt binder, it is important to investigate the testing temperature sensitivity of these tests. Moreover, it is important to provide a statistical comparison of DC(T) and SCB tests on a variety of asphalt mixtures and to provide a correlation between DC(T) and SCB. Furthermore, the effect of long-term aging on either DC(T) or SCB must be investigated. In the end, the preliminary specifications for the performance tests selected must be recommended.

Chapter 3
Methodology and Materials

This research has been conducted in collaboration with the Ministry of Transportation Ontario (MTO). To fulfil the objectives of this research, the experimental work began with the characterization of five plant-produced surface course asphalt mixtures collected from five distinctive regions across Ontario (Figure 3.1). The five plant-produced SP12.5 surface course asphalt mixtures paved in Ontario have a wide range of PG (Performance Grade) asphalt binder, including SP12.5 PG52-40, SP12.5FC1 PG58-34, SP12.5FC2 PG64-34 20%RAP, SP12.5FC2 PG64-28 20%RAP and SP12.5FC2 PG70-28. It should be noted that for SP12.5FC1 and SP12.5FC2 asphalt mixtures, FC means "friction course" and the aggregate for these asphalt mixtures must be obtained from pre-approved sources listed on the MTO (Ministry of Transportation Ontario) Designated Sources for Materials (DSM). FC1 requires that only the coarse aggregate fraction for the asphalt mix must be obtained from DSM list, while FC2 requires that both coarse and fine aggregates for the asphalt mixture must be obtained from DSM list. Generally, FC1 and FC2 asphalt mixtures provide superior rutting and skid resistance performance and are used on the highways carrying medium to high volume of traffic.

Figure 3.1 Regional Map of Ontario (MTO, 2021).

To characterize the aforementioned asphalt mixtures, extraction and recovery tests followed by Dynamic Shear Rheometer, Multiple Stress Creep Recovery (MSCR) and Bending Beam Rheometer tests were conducted in order to determine recovered aggregate gradation, recovered asphalt binder content, recovered continuous high temperature grade, recovered percent recovery (R3.2 (%)), recovered permanent deformation (J_{nr}3.2) and recovered continuous low temperature grade. Furthermore, Hamburg Wheel Tracking, I-FIT, IDEAL-CT, complex modulus, cyclic, DC(T) and SCB tests were conducted, and the tests results were analysed. Generally, the statistical analysis using the Minitab software and employing analysis of variance (ANOVA) test, t-test, and Tukey's HSD (Honest Significant Difference) test were applied where necessary.

A survey was also conducted in order to investigate whether asphalt mixture laboratories in Ontario which are working and collaborating with MTO have the testing equipment required for asphalt mixture performance testing. The survey was prepared at the University of Waterloo and was distributed by MTO among asphalt mixture laboratories to investigate the capability of asphalt laboratories to conduct I-FIT and DC(T) tests (Appendix A).

According to the analysis of test results from five plant-produced asphalt mixtures, and the data collected from the survey, three performance tests were selected for the last part of this research. Sixteen plant-produced asphalt mixtures were then characterized by using the three selected performance tests and preliminary specifications for the performance tests were recommended in the end. Appendix B shows the JMF (Job Mix Formula) of sixteen asphalt mixtures used in this research, and Figure 3.2 shows the outline of the research methodology.

3.1 Designs of Experiments (DOEs)

Table 3.1, Table 3.2, Table 3.3 and Table 3.4 show DOEs used for this research conducted in the different sections of this thesis. Altogether 115, 120, 210, 176 specimens were fabricated and tested through research conducted in Chapter 4, Chapter 5, Chapter 6 and Chapter 7, respectively.

Table 3.1 DOE used in Chapter 4.

Research Variable	Number of levels	Levels [Number of specimens per experiment]
Performance-related test	7	DC(T) [3] SCB [3] I-FIT [4] IDEAL-CT [3] Complex Modulus [3] Cyclic [3] HWT [4]
Asphalt mixture	5	Mix1 (SP12.5 PG52-40) Mix2 (SP12.5FC1 PG58-34) Mix3 (SP12.5FC2 PG64-34 20%RAP) Mix4 (SP12.5FC2 PG64-28 20%RAP) Mix5 (SP12.5FC2 PG70-28)

Table 3.2 DOE used in Chapter 5.

Research Variable	Number of levels	Levels [Number of specimens per experiment]
Performance-related test	2	DC(T) [3] SCB [3]
Asphalt Mixture	5	Mix1 (SP12.5 PG52-40) Mix2 (SP12.5FC1 PG58-34) Mix3 (SP12.5FC2 PG64-34 20%RAP) Mix4 (SP12.5FC2 PG64-28 20%RAP) Mix5 (SP12.5FC2 PG70-28)
Temperature	3	-18 ℃ -24 ℃ -30 ℃
Aging method	2	Short-term aged Long-term aged

Table 3.3 DOE used in Chapter 6.

Research Variable	Number of levels	Levels [Number of specimens per experiment]
Performance-related test	1	I-FIT [4]
Testing device	2	Hydraulic Screw-driven
Asphalt Mixture	5	Mix1 (SP12.5 PG52-40) Mix2 (SP12.5FC1 PG58-34) Mix3 (SP12.5FC2 PG64-34 20%RAP) Mix4 (SP12.5FC2 PG64-28 20%RAP) Mix5 (SP12.5FC2 PG70-28)
Temperature sensitivity	4	23 ℃ 24 ℃ 25 ℃ Intermediate temperature based on PG
Aging method	2	Short-term aged Long-term aged

Table 3.4 DOE used in Chapter 7.

Research Variable	Number of levels	Levels [Number of specimens per experiment]
Performance-related test	3	I-FIT [4] DC(T) [3] HWT [4]
Asphalt Mixture	16	Mix1 (SMA12.5 PG70-28) Mix2 (SMA12.5 PG70-28) Mix3 (SP12.5 FC2 PG70-28) Mix4 (SP12.5 FC2 PG70-28 20% RAP) Mix5 (SP12.5 FC2 PG70-28 20% RAP) Mix6 (SP12.5 FC2 PG64-28 20% RAP) Mix7 (SP12.5 FC2 PG64-34 20% RAP) Mix8 (SP12.5 FC2 PG64-34) Mix9 (SP12.5 FC2 PG58-28) Mix10 (SP12.5 FC2 PG58-28) Mix11 (SP12.5 FC1 PG58-34) Mix12 (SP12.5 FC1 PG58-34) Mix13 (SP12.5 PG58-34) Mix14 (SP12.5 PG52-40) Mix15 (SP12.5 PG52-40) Mix16 (SP12.5 PG52-40)
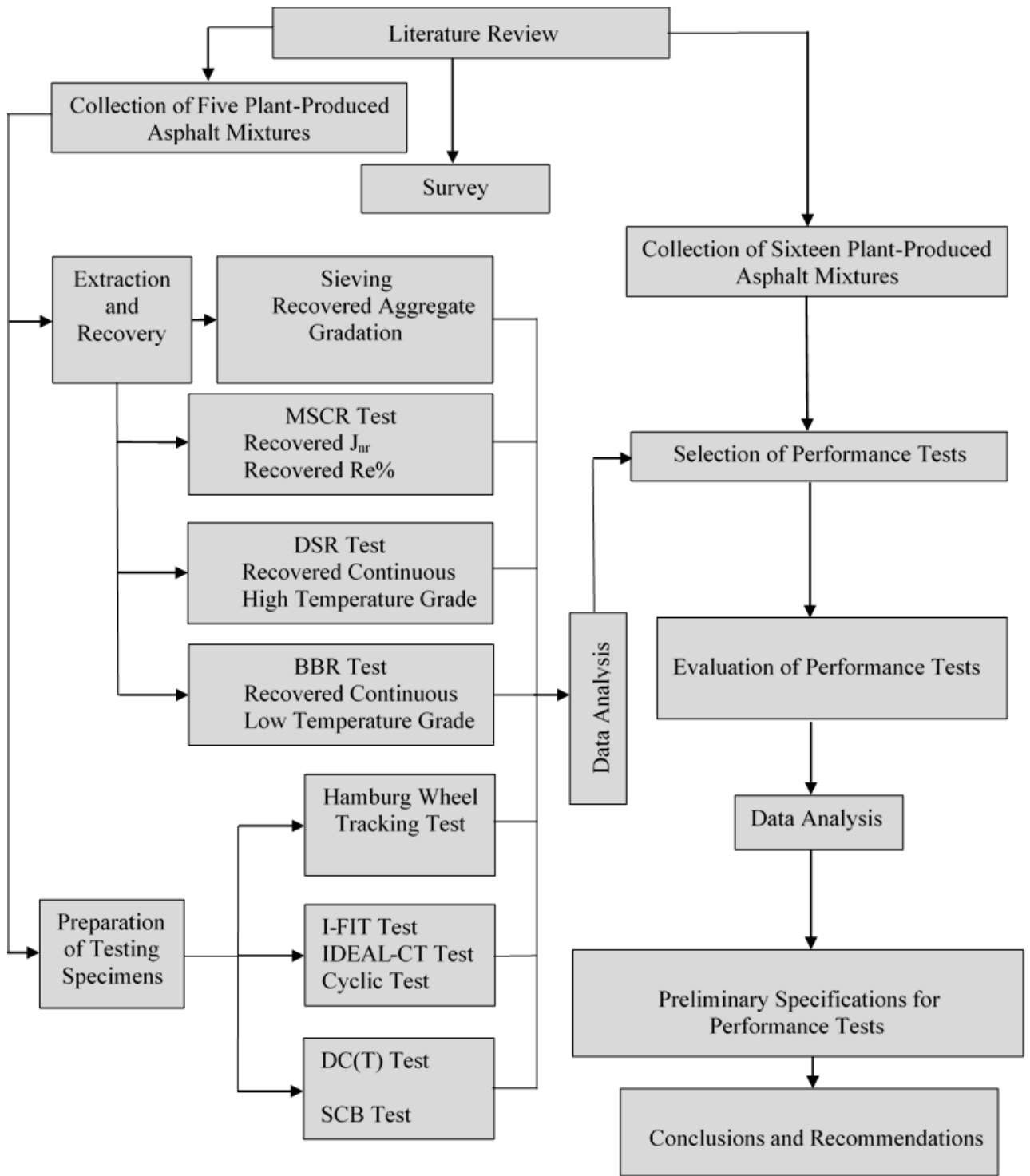
Figure 3.2 Research Methodology Outline.

61

3.2 Characterization of Recovered Asphalt Binders

To characterize the recovered asphalt binders, first, asphalt binders were extracted from asphalt mixtures according to LS-282 test method. Then, asphalt binders were recovered from the mixture of solution and asphalt binders based on, LS-284 test method. Dynamic Shear Rheometer (DSR) test was conducted according to ASHTO T315 to determine continuous high temperature of the recovered asphalt binders. Bending Beam Rheometer (BBR) test was conducted on the pressure aged vessel residue of the recovered binders to determine the continuous low temperatures. Furthermore, Multiple Stress Creep and Recovery (MSCR) test was conducted according to AASHTO T350 t0 determine Re3.2kPa and J_{nr}3.2kPa^{-1}.

3.3 Test Procedures

3.3.1 DC(T) Test (ASTM D7313)

DC(T) test can be used as a performance test to compute fracture energy of asphalt mixtures and evaluate prevalent crack-related distresses such as thermal, reflective and block cracking. The DC(T) test produces a fracture energy value which can be used to evaluate the asphalt mixture's resistance to low temperature cracking. Testing specimens must have a diameter in the range of 150 ± 10 mm, thickness of 50 ± 5 mm, a notch depth of 62 ± 3 mm and a notch width of 1.5 ± 0.5 mm. To conduct the DC(T) test, a specimen is conditioned for 8-16 hours in a freezer at 10 ℃ higher than the low temperature grade of the PG asphalt binder used in the mixture. Then, the specimen is mounted in the loading frame of the testing equipment (Figure 3.3) and pulled apart from loading holes in a Crack Mouth Opening Displacement (CMOD) controlled mode with a displacement rate of 1 mm/min. As soon as the post-peak load reaches 0.1 kN, the test stops. The fracture energy (G_f) (J/m^2) is calculated by determining the area under the Load-CMOD displacement curve normalized by the product of ligament length and thickness of a specimen. The larger the G_f value, the more resistant the asphalt mixture is to low temperature cracking. For specimen thicknesses other than 50 mm, a thickness correction factor needs to be applied, in order to arrive at the fracture energy that would have been

62

measured using a specimen with thickness of 50 mm. Equation 23 was used to correct fracture energy data for thickness,

$$CF_t = 21.965B^{-0.788} \tag{23}$$

where B is the specimen thickness.

Figure 3.3 DC(T) Test Loading Fixture.

To fabricate a DC(T) testing specimen according to ASTM D7313 standard, first, two discs of 50mm thickness were cut and extracted from the middle of Superpave gyratory briquettes. If the discs produced contained 7±0.5% air voids, each disc was edge-cut with a tile-saw to create a flat edge surface for placing knife edges and the mounting crack mouth opening displacement (CMOD) gauge. After creating the flat edge surface, two loading holes of 25 mm diameter were drilled with a water-cooled drilling device and following that a notch of 62.5 mm length was saw-cut with a tile-saw from the flat edge surface toward center of the disc passing through the middle of loading holes. Finally, the knife edges were glued on the flat surface of each specimen (Figure 3.4).
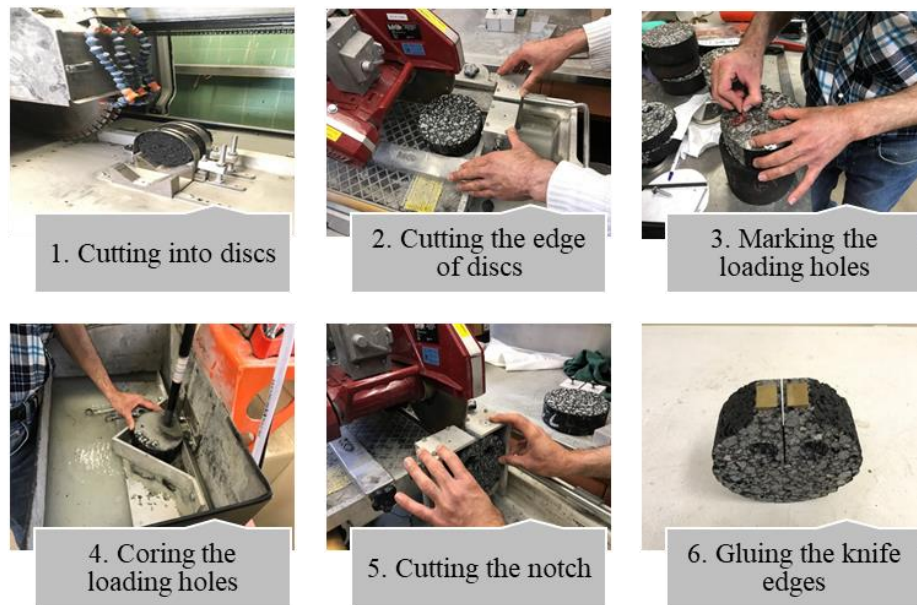
Figure 3.4 DC(T) Testing Specimen Preparation Procedure.

3.3.2 SCB Test (AASHTO TP105)

The SCB test is conducted on a half disc specimen of 150±9 mm in diameter and of 24.7±2 mm thickness with a 15±1 mm notch length that is aligned with the direction of loading. To conduct an SCB test, a half-disc specimen is mounted on its flat side on two roller supports on the testing frame (Figure 3.5). First, a small contact load of 0.3±0.02 kN with a displacement rate of 3 mm/min is applied. Next, a seating load of 0.6±0.02 kN is applied with a displacement rate of 0.3 mm/min. Then, the test is executed in stroke control with a rate of 0.06 mm/min resulting in an initial load of 1±0.1 kN. As soon as the initial load is reached, the system switches to Crack Mouth Opening Displacement (CMOD) control and the load is applied with a CMOD rate of 0.03 mm/min for the rest of the test. The test stops when the load drops to 0.5 kN or the CMOD reaches to its range limit, and the remainder of the curve is extrapolated by the method explained in AASHTO TP105. During the test process, the load, the CMOD and the load line displacement (LLD) on both sides of the specimen are measured and recorded. The CMOD measurement is used to maintain the test stability in the post peak region of the test. G_f (J/m^2) is calculated by determining the area under the load-load line displacement divided by the product of initial ligament length and thickness of the specimen.

64

To fabricate an SCB testing specimen according to AASHTO TP105 standard, first, two discs of 25mm thickness were cut and extracted from the middle of Superpave gyratory briquettes. If the discs produced contained 7±0.5% air voids, each disc was cut in half with a tile-saw to create two semi-circular bending test specimens. Then, a notch length of 15 mm was cut in the middle and on the flat side of each half disc. After cutting the notch, the gauge points and the knife edges were glued to the specimens (Figure 3.6).

Figure 3.5 SCB Test Loading Fixture.
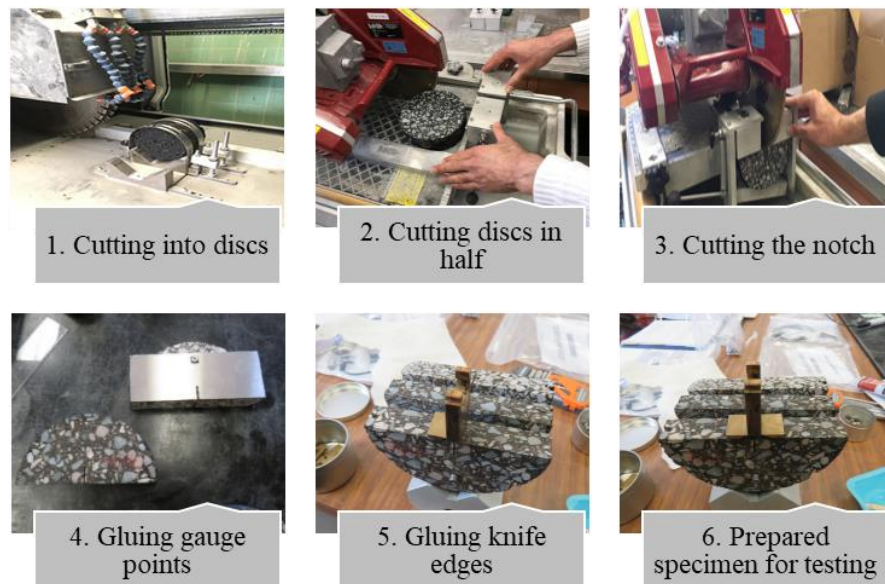
Figure 3.6 The procedure of SCB Testing Specimen Preparation.

3.3.3 IDEAL-CT Test (ASTM D8225)

The IDEAL-CT (*ind*irect t*e*nsile *a*sphal*t* *c*racking *t*est) test can be conducted by a regular indirect tensile strength test equipment on cylindrical specimens of 150 mm diameter and 62±1 mm height at 25 ºC with loading rate of 50 mm/min (Figure 3.7). The IDEAL-CT test does not require cutting, coring, gluing or instrumentation. The analysis of the load-displacement curve of IDEAL-CT test defines a parameter called CT_{index} that was derived from the laws of crack propagation. The larger the CT_{index} value, the more resistant the asphalt mixture is to intermediate crack propagation.

Figure 3.7 IDEAL-CT Test Loading Fixture.

3.3.4 I-FIT Test (AASHTO TP124)

The Flexibility Index Test (I-FIT) produces three parameters, fracture energy, post-peak load slope, and the flexibility index (FI) to evaluate asphalt mixtures' resistance to intermediate temperature cracking according to the AASHTO TP124 test method (AASHTO TP124, 2016). To conduct the FIT test, a half-disc specimen is conditioned at 25±0.5 ºC for 2h±10 min in an environmental chamber or water bath. The specimen is then mounted on its flat side on two roller supports on the testing frame and tested at 25 ºC (Figure 3.8). The testing machine applies a monotonic load with a rate of 50 mm/min until the crack initiates at the tip of the notch and propagates upwards. As soon as the post-peak load reaches 0.1 kN, the test stops. To compute

the FI value, the work of fracture (W_f) is calculated as the area under the load-load line displacement curve. The fracture energy (G_f) (J/m^2) is then calculated by dividing W_f by the ligament area. Finally, the FI value is determined using G_f and the absolute slope of the load-displacement curve at the first inflection point between the peak load and the end of the curve. The higher the FI, the more resistant asphalt mixture is to intermediate temperature cracking.

To fabricate an I-FIT specimen according to AASHTO TP124 standard, first, two discs of 50mm thickness were cut and extracted from the middle of Superpave gyratory briquettes. If the discs produced did not contain 7±0.5% air voids, they were discarded. Discs were cut in half by using a tile-saw to provide two SCB replicates. Then, a notch with the length and the width of 15±0.5 mm and 1.5±0.5 mm, respectively, was cut in the middle on the flat side of each half disc (Figure 3.9). Overall, four SCB replicates were obtained for testing from a gyratory briquette.
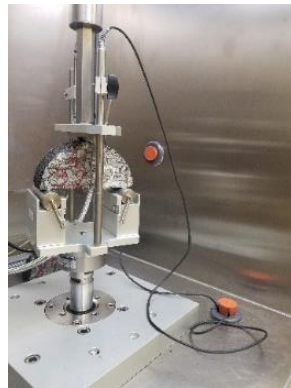
Figure 3.8 I-FIT Test Setup.

Figure 3.9 The procedure of I-FIT Specimen Preparation.

3.3.5 Complex Modulus and Cyclic Testing (AASHTO TP132 and AASHTO TP133)

Complex modulus and cyclic tests were conducted on small specimens of 38 mm in diameter by 110 mm in height according to AASHTO TP132 and AASHTO TP133 test methods (Figure 3.10). To identify the linear viscoelastic (LVE) characteristics of an asphalt mixture, complex modulus testing is conducted on three cylindrical specimens of an asphalt mixture at three temperatures (4°, 20°, and 38° or 40° C) and three frequencies (0.1, 1.0 and 10 Hz) by applying the sinusoidal loading and measuring the deformations. Furthermore, cyclic testing was conducted according to AASHTO TP133 test method.

Figure 3.10 Complex Modulus Test (*left*) and Cyclic Test (*right*).

3.3.6 Hamburg Wheel Tracking (HWT) Test (AASHTO T324)

Hamburg Wheel Tracking Device (HWTD) is employed to evaluate the rutting resistance and moisture susceptibility of asphalt mixtures. The test is conducted in accordance with AASHTO T324 in which the testing device tracks a 158 lb (705 N) load steel wheel across the surface of specimens submerged in a hot water bath at 50°C (Figure 3.11). During the test, the deformation of specimens is recorded as a function of the number of passes. The result of HWT test is a plot of number of passes vs. rut depth comprising post-compaction consolidation, the creep slope, the stripping slope, and stripping inflection point. The post-compaction consolidation measured as the rut depth (mm) at 1000-wheel passes is due to the densification of specimens within the first 1000-wheel passes. The creep slope defined as the inverse of the rate of deformation, between post compaction consolidation and stripping inflection point, and is a measure of rutting susceptibility of specimens. The stripping slope defined as the inverse of the rate of deformation, after stripping inflection point is a measure of moisture damage susceptibility of specimens. The stripping inflection point defined as the number of passes at the intersection of creep slope and stripping slope is a measure of resistance of specimens to moisture damage.

Figure 3.11 Hamburg wheel tracking device.

Chapter 4

Characterization of Five Plant-Produced Asphalt Mixtures

Five plant-produced asphalt mixtures were characterized by conducting laboratory testing on recovered asphalt binders and Plant-Produced Laboratory Compacted (PPLC) specimens. To characterize the recovered asphalt binders, first, asphalt binders were extracted from asphalt mixtures according to the LS-282 standard. Then, the asphalt binders were recovered from the mixture of solution and asphalt binder based on LS-284 standard. Dynamic Shear Rheometer (DSR) and Multiple Stress Creep and Recovery (MSCR) tests according to AASHTO T315 and AASHTO T350 test methods, respectively, were conducted on the recovered asphalt binders in order to determine continuous high temperature grades, average percent recovery (Re) at 3.2 kPa, and non-recoverable creep compliance (J_{nr}) at 3.2 kPa. Bending Beam Rheometer (BBR) test according to AASHTO T313 test method was conducted on the recovered asphalt binders after long-term aging in order to determine the continuous low temperature grades. The recovered intermediate temperature grades were calculated by adding 4°C to the average of continuous high and low temperature grades. To characterize the low-temperature cracking resistance of asphalt mixtures, DC(T) and SCB tests were conducted according to ASTM D7313 and AAHTO TP105 test methods, respectively, on the PPLC specimens, while I-FIT and IDEAL-CT tests were conducted according to AASHTO TP124 and ASTM D8225 test methods, respectively, to characterize intermediate crack propagation resistance of the asphalt mixtures. Moreover, complex modulus and cyclic tests were conducted according to AASHTO TP132 and AASHTO TP133 to characterize the fatigue cracking resistance of the asphalt mixtures. Furthermore, Hamburg Wheel Tracking (HWT) test according to AASHTO T324 was conducted in order to characterize rutting and moisture susceptibility of the asphalt mixtures.

4.1 Asphalt Binder Characterization Results

Table 4.1 shows the recovered aggregate gradation and the recovered asphalt binder contents of the asphalt mixtures. Figure 4.1 shows the results of the BBR tests, including S, m-value and ΔT_c temperatures, and Figure 4.2 presents the results of continuous high, low, and

70

intermediate temperature grades. Moreover, Figure 4.3 shows the results of Re, and J_{nr} obtained from MSCR test.

Table 4.1 Recovered Aggregate Gradation and Asphalt Binder Content.

Sieve Size (mm)	Mix1. SP12.5 PG52-40	Mix2. SP12.5FC1 PG58-34	Mix3. SP12.5FC2 PG64-34 20%RAP	Mix4. SP12.5FC2 PG64-28 20%RAP	Mix5. SP12.5FC2 PG70-28
19.0	100	100	100	100	100
12.5	94.90	98.80	98.60	96.50	96.35
9.5	77.30	89.90	80.20	85.10	84.30
4.75	46.20	63.60	52.10	58.70	58.05
2.36	34.90	51.30	46.20	43.90	45.40
1.18	27.20	41.40	31.70	35.00	38.55
0.6	19.20	28.10	20.80	27.30	33.35
0.3	10.20	12.60	12.40	17.00	17.30
0.15	4.90	7.50	6.00	7.80	8.35
0.075	2.50	4.40	3.00	3.70	4.50
Recovered Asphalt Binder Content (%)	4.86	5.05	5.23	5.01	5.03
Job Mix Formula Asphalt Binder Content (%)	4.90	4.90	5.00	4.90	5.20
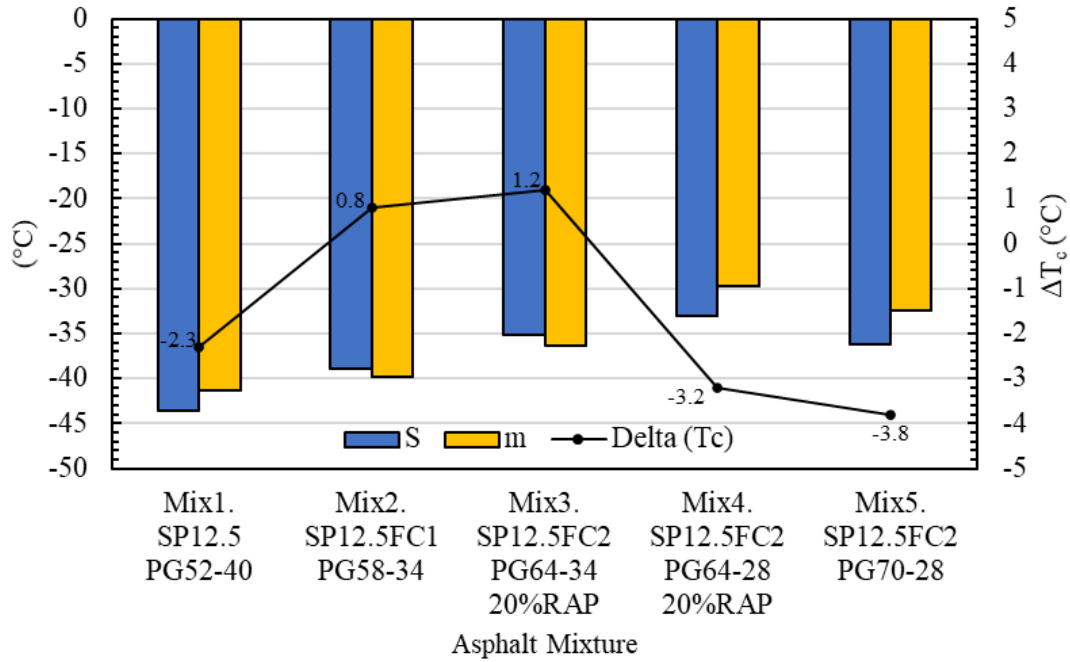
Figure 4.1 Recovered S, m, and ΔTc Temperatures.
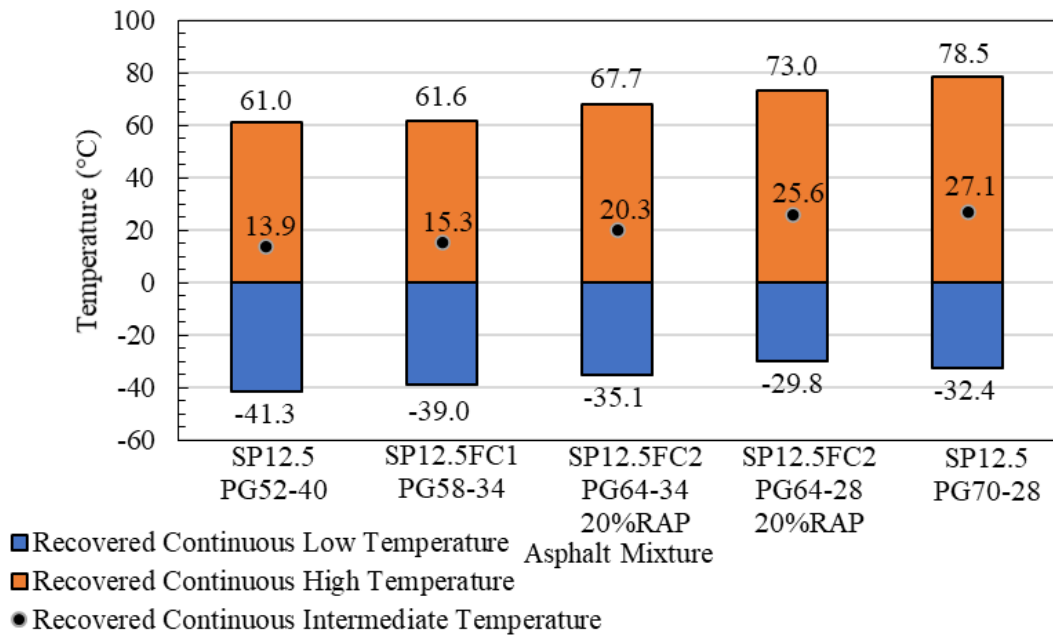
Figure 4.2 Recovered Continuous High, Intermediate and Low Temperatures.
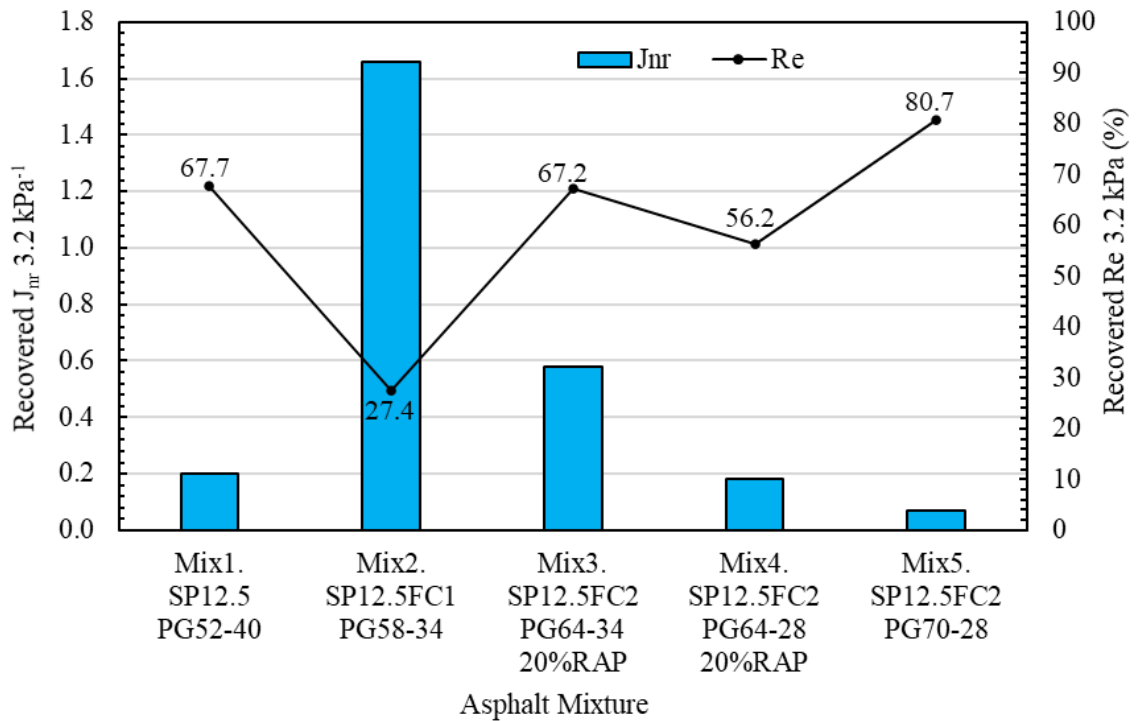
Figure 4.3 Recovered Re and Jnr.

4.2 Asphalt Mixture Characterization Results

4.2.1 DC(T) Test Results

DC(T) testing was carried out according to ASTM D7313 test method at 10 ℃ higher than the low temperature PG of the asphalt binder used in the asphalt mixtures on triplicate. Figure 4.4 shows the bar charts of average fracture energy in conjunction with one standard deviation error bar from the average fracture energy and the continuous low temperature grade of asphalt mixtures. Also, Table 4.2 shows Coefficient of Variation (C.V) and Ranking of asphalt mixtures based on Tukey's HSD test. As shown in Figure 4.4, even though low temperature continuous PG determined from the recovered asphalt binders meet the BBR test requirements, DC(T) fracture energy values indicate that Mix5 and Mix2 outperform the other asphalt mixtures. In general, the results show that the average fracture energy of DC(T) test is associated with the low temperature continuous PG. In order to clarify this matter, it should be

noted that the low temperature continuous PG of Mix5 and Mix2 are -32.4 ℃ and -39.0 ℃, respectively, which are lower than their corresponding low temperature PG, i.e. -28 ℃ and -34 ℃. The aforementioned difference between the low temperature continuous PG and the low temperature PG could contribute to high fracture energy and high low temperature cracking resistance of Mix5 and Mix2. On the other hand, the difference between the low temperature continuous PG and the low temperature PG for Mix1, Mix3 and Mix4 is not as considerable as that for Mix5 and Mix2. The low temperature continuous PG of Mix1, Mix3 and Mix4 measured at -41.3 ℃, -35.1 ℃ and -29.8 ℃, respectively, are almost close to their corresponding low temperature PG, namely -40 ℃, -34 ℃ and -28 ℃. As can be seen in Figure 4.4, Mix3 and Mix4 have the lowest value of fracture energy among the asphalt mixtures. The reason is likely due to the existing RAP in Mix3 and Mix4 causing them to have a brittle behaviour at low temperature. Even though the difference between the low temperature continuous PG and the low temperature PG is not considerable for Mix1, the average fracture energy for Mix1 is higher than that for Mix3 and Mix4. This could stem from the virgin materials used in Mix1. Furthermore, as seen in Table 4.2, the repeatability of DC(T) is good with a C.V less than 20%, and DC(T) test was able to distinguish low temperature cracking resistance of the asphalt mixtures.
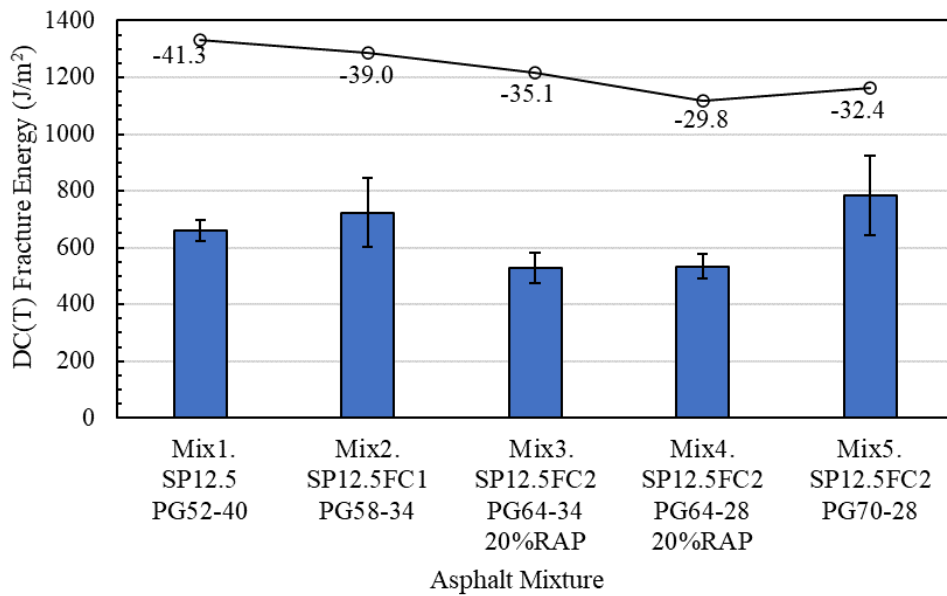
Figure 4.4 DC(T) Fracture Energy at 10℃ Higher than Low Temperature Grade.

Table 4.2 C.V and Ranking of Asphalt Mixtures for DC(T) Test.

Asphalt Mixture	10°C Higher than Low Temperature PG	
	C.V (%)	Ranking
Mix1.SP12.5 PG52-40	5.5	AB
Mix2.SP12.5FC1 PG58-34	16.7	AB
Mix3.SP12.5FC2 PG64-34 20%RAP	10.1	B
Mix4.SP12.5FC2 PG64-28 20%RAP	8.2	B
Mix5.SP12.5FC2 PG70-28	18.1	A

4.2.2 SCB Test Results

SCB testing was conducted according to AASHTO TP105 test method at 10 ºC higher than the low temperature PG of the asphalt binders used in the asphalt mixtures on triplicate. Figure 4.5 displays the bar charts of average fracture energy in conjunction with one standard deviation error bar from the average fracture energy and the continuous low temperature grade of asphalt mixtures. Furthermore, Table 4.3 shows C.V and Ranking of asphalt mixes based on Tukey's HSD test. As shown in Figure 4.5, similar to DC(T) results, even though low temperature continuous PG determined from the recovered asphalt binders meet the BBR test requirements, SCB fracture energy values indicate that Mix5 and Mix2 outperform the other asphalt mixtures, and the average fracture energy of SCB test is associated with the low temperature continuous PG. As can be seen in Figure 4.5, Mix3 and Mix4 have the lowest value of fracture energy among the asphalt mixtures. Furthermore, as seen in Table 4.3, the repeatability of SCB is also good with a C.V less than 12%, and SCB test was able to distinguish low temperature cracking resistance of the asphalt mixtures. Furthermore, a statistical paired t-test between the results of fracture energy from DC(T) and SCB tests showed that their results are statistically the same (P-value = 0.775).
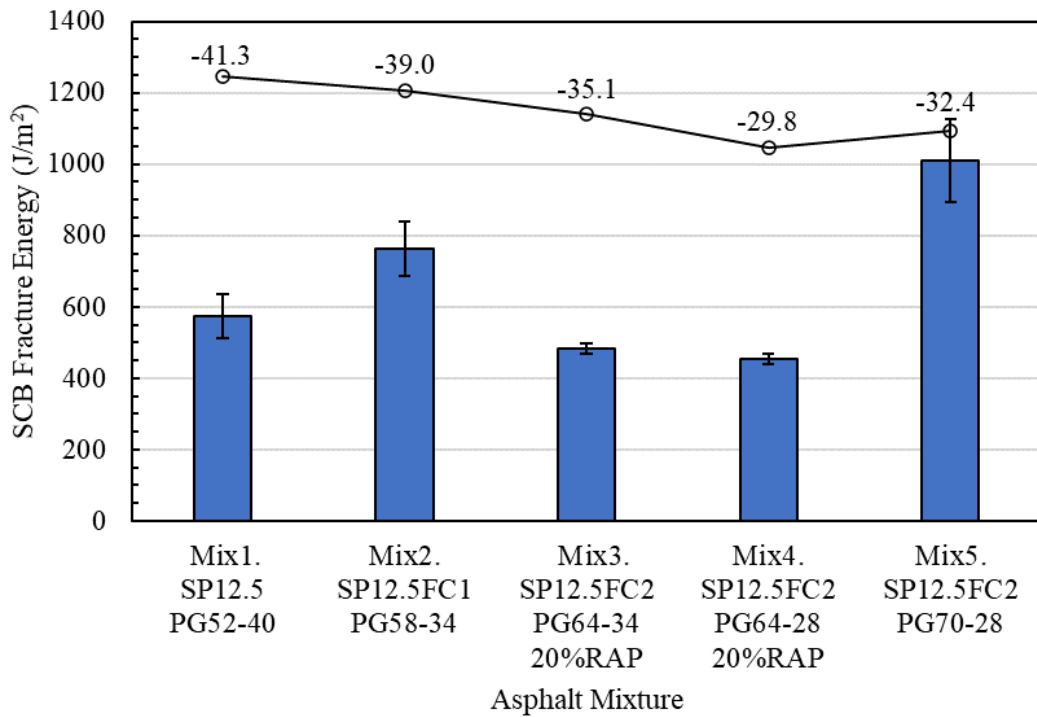
Figure 4.5 SCB Fracture Energy at 10°C Higher than Low Temperature Grade.

Table 4.3 C.V and Ranking of Asphalt Mixtures for SCB Test.

Asphalt Mix	10°C Higher than Low Temperature PG	
	C.V (%)	Ranking
Mix1.SP12.5 PG52-40	10.6	C
Mix2.SP12.5FC1 PG58-34	10.2	B
Mix3.SP12.5FC2 PG64-34 20%RAP	3.1	C
Mix4.SP12.5FC2 PG64-28 20%RAP	2.9	C
Mix5.SP12.5FC2 PG70-28	11.5	A

4.2.3 I-FIT Test Results

I-FIT testing was conducted according to the AASHTO TP124 test method on quadruplicate at two testing temperatures, namely 25°C and the intermediate temperature based on PG asphalt binder (average of high and low temperature grades plus 4°C). To decrease the variability of FI, one test result out of four, having an FI value further from the average, was discarded. Then, the average, standard deviation, and coefficient of variation (C.V) relevant to

the three remaining test results were determined. Figure 4.6 presents the results of average FI at two testing temperatures, and the error bars represent one standard deviation from the average. Table 4.4 shows C.V and Ranking of asphalt mixtures based on Tukey's HSD test. As seen in Figure 4.6, at 25°C, Mix3 containing 20%RAP has the highest value of FI among the asphalt mixtures. This can be attributed to the soft PG binder (PG64-34) and high content of asphalt binder (5.2%) in Mix3 compared to other asphalt mixtures. Moreover, Mix4 and Mix5 have the lowest FI among the asphalt mixtures. The existing RAP in Mix4 could give a rise to the low value of FI, while regarding Mix5, the asphalt binder content (5.03%) is lower than the designed asphalt binder content reported in Job Mix Formula (5.2%). Similar to the test results at 25°C, Mix4 and Mix5 have the lowest value of FI at intermediate temperature, while Mix1, Mix2 and Mix3 have statistically the same value of FI and the same ranking. Table 4.4 shows that asphalt mixtures containing RAP tend to show more variability in FI results. For instance, Mix4 has a C.V of 25.3% at intermediate temperature.
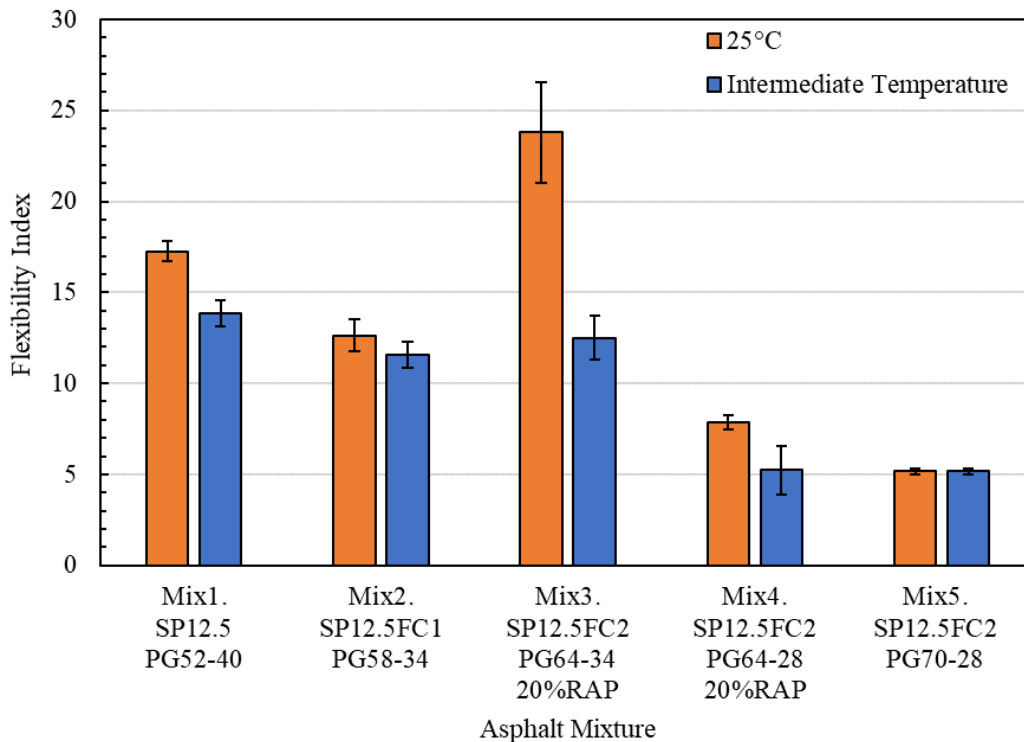
Figure 4.6 Flexibility Index at 25°C and Intermediate Temperature.

Table 4.4 C.V and Ranking of Asphalt Mixtures for I-FIT Test.

Asphalt Mix	25°C		Intermediate Temperature	
	C.V (%)	Ranking	C.V (%)	Ranking
Mix1.SP12.5 PG52-40	3.1	B	5.1	A
Mix2.SP12.5FC1 PG58-34	6.9	C	6.2	A
Mix3.SP12.5FC2 PG64-34 20%RAP	11.8	A	9.7	A
Mix4.SP12.5FC2 PG64-28 20%RAP	4.8	D	25.3	B
Mix5.SP12.5FC2 PG70-28	3.3	D	3.3	B

4.2.4 IDEAL-CT Test Results

The IDEAL-CT test was conducted according to the ASTM D8025 test method on triplicate at two testing temperatures, namely 25°C and the intermediate temperature based on PG asphalt binder (average of high and low temperature grades plus 4°C). Figure 4.7 illustrates the results of average CT Index at two testing temperatures. The error bars represent one standard deviation from the average. Table 4.5 shows C.V and Ranking of asphalt mixtures based on Tukey's HSD test. As can be seen in Figure 4.7 and Table 4.5, similar to I-FIT results, Mix3 outperforms other asphalt mixtures at 25°C with having the highest value of CT Index, while Mix4 and Mix5 have the lowest values of CT Index among asphalt mixtures. However, unlike the I-FIT results at intermediate temperature where Mix1, Mix2 and Mix3 have the same ranking, based on IDEAL-CT test results, Mix3 outperforms other asphalt mixtures. Table 4.5 shows that Mix3 and Mix4 containing 20% RAP have high variability in CT Index results.
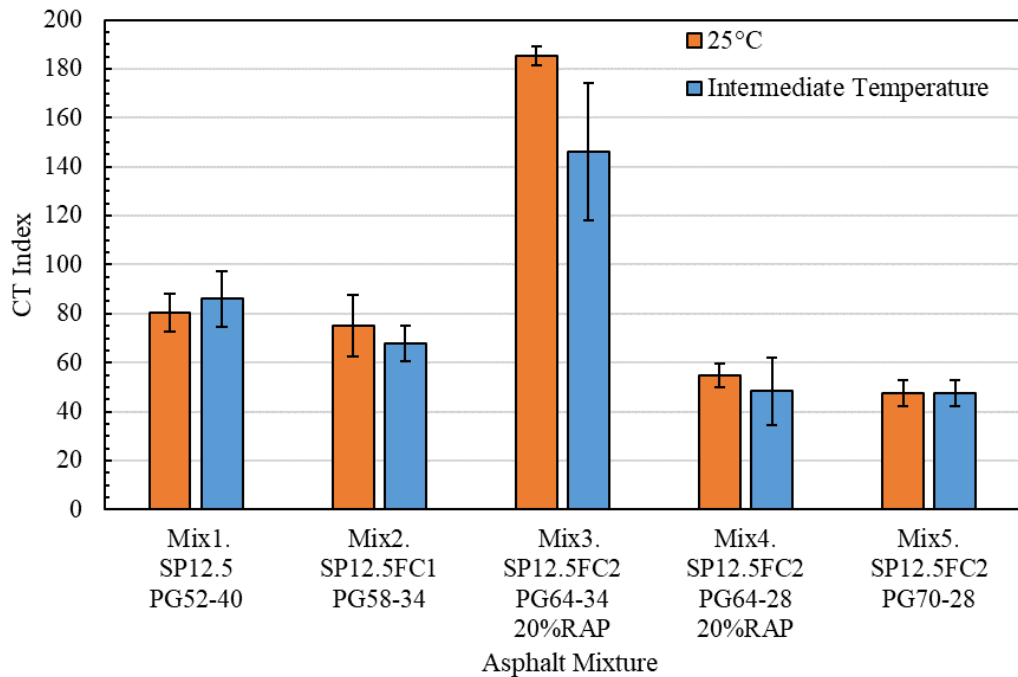
Figure 4.7 CT Index at 25°C and Intermediate Temperature.

Table 4.5 C.V and Ranking of Asphalt Mixtures for IDEAL-CT Test.

Asphalt Mix	25°C		Intermediate Temperature	
	C.V (%)	Ranking	C.V (%)	Ranking
0101Mix1.SP12.5 PG52-40	9.7	B	13.2	B
Mix2.SP12.5FC1 PG58-34	16.9	BC	10.8	B
Mix3.SP12.5FC2 PG64-34 20%RAP	2.1	A	19.2	A
Mix4.SP12.5FC2 PG64-28 20%RAP	8.7	CD	29.0	B
Mix5.SP12.5FC2 PG70-28	11.4	D	11.4	B

4.2.5 Relationship Between I-FIT and IDEAL-CT Tests Results

Figure 4.8 and Figure 4.9 illustrate the plots of the relationship between the average FI and CT-Index of I-FIT and IDEAL-CT tests, respectively. The horizontal and vertical axes represent the average FI and CT-Index, respectively. As seen in Figure 4.8 and Figure 4.9, linear fits suggest a good and moderate correlation between FI and CT-Index values at 25°C and intermediate temperature, respectively ($R^2=0.826$ and $R^2=0.496$, respectively).
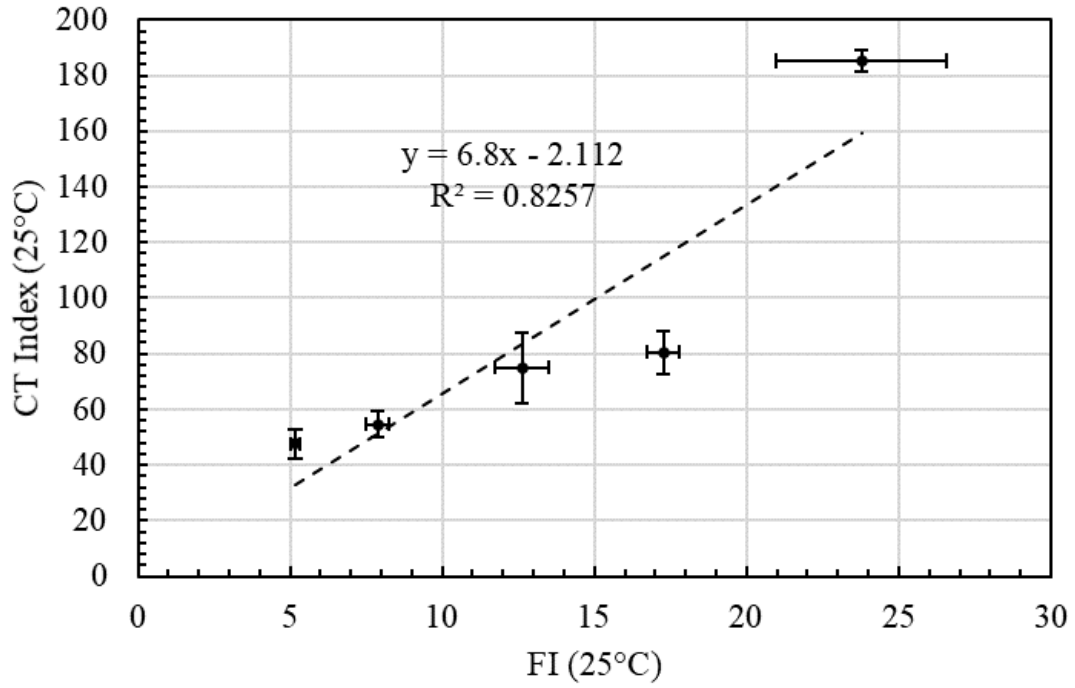
Figure 4.8 Relationship between FI and CT-Index Results at 25°C.
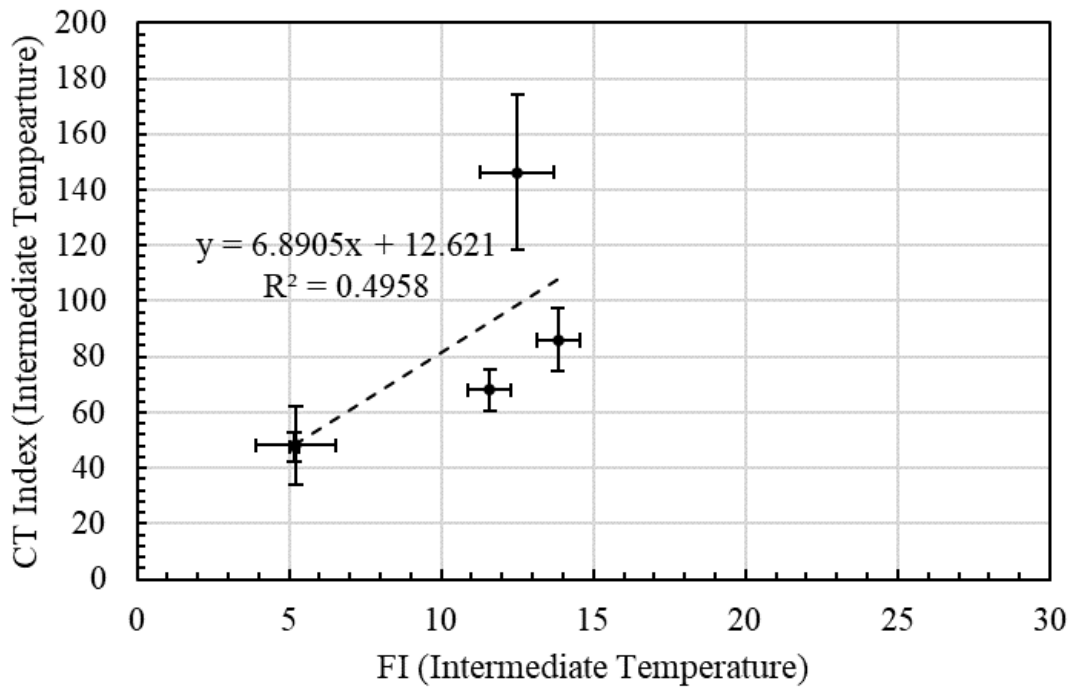
Figure 4.9 Relationship between FI and CT-Index Results at Intermediate Temperature.

4.2.6 Complex Modulus and Cyclic Tests Results

The complex modulus test was conducted on small specimens according to AASHTO TP132 test method. Figure 4.10 shows the dynamic modulus master curves at 20°C which was constructed according to AASHTO R62 standard. As shown in Figure 4.10, Mix1 with PG52-40 asphalt binder and Mix2 with PG58-34 asphalt binder, in order, have the softest response than other asphalt mixtures, i.e., they have the lowest dynamic modulus values. Mix3 and Mix4 almost have similar master curves, while Mix5 with PG70-28 has the stiffest response, i.e., the highest dynamic modulus value among the asphalt mixtures.
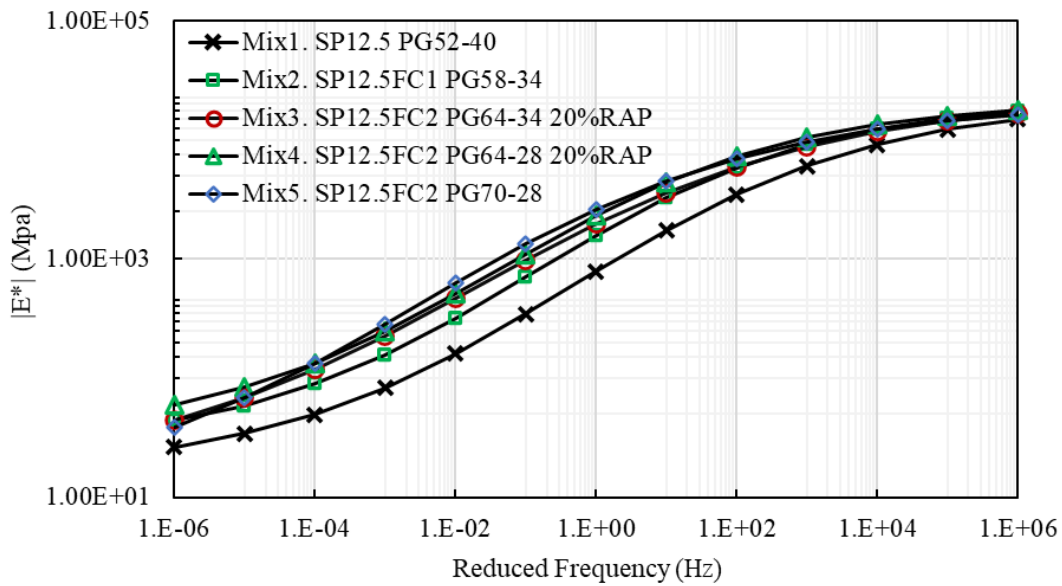
Figure 4.10 Dynamic Modulus Master curves at 20°C.

The cyclic test was conducted on small specimens according to AASHTO TP133 test method. Testing temperatures were 12°C for Mix1 and Mix3, and 18°C for Mix2, Mix3 and Mix4. Figure 4.11 shows the damage characteristic curves (C vs. S curves) for the asphalt mixtures. Figure 4.12 shows S_{app} values and D^R criterion for the asphalt mixtures. Generally, S_{app} values for the asphalt mixtures were determined according to the intermediate temperature of the locations where the asphalt mixtures have been paved (12°C for Mix1, 16°C for Mix2 and Mix3, and 19°C for Mix4 and Mix5). As seen in Figure 4.12, Mix1 and Mix2 have the highest ductility (D^R=0.76 and 0.75, respectively) among the asphalt mixtures, while Mix4 has

81

the lowest ductility (D^R =0.68). Moreover, Mix3 and Mix4 has the highest and lowest values of S_{app} (S_{app} = 30 and 21.8, respectively). Overall, Mix3 has the best fatigue performance among the asphalt mixtures.
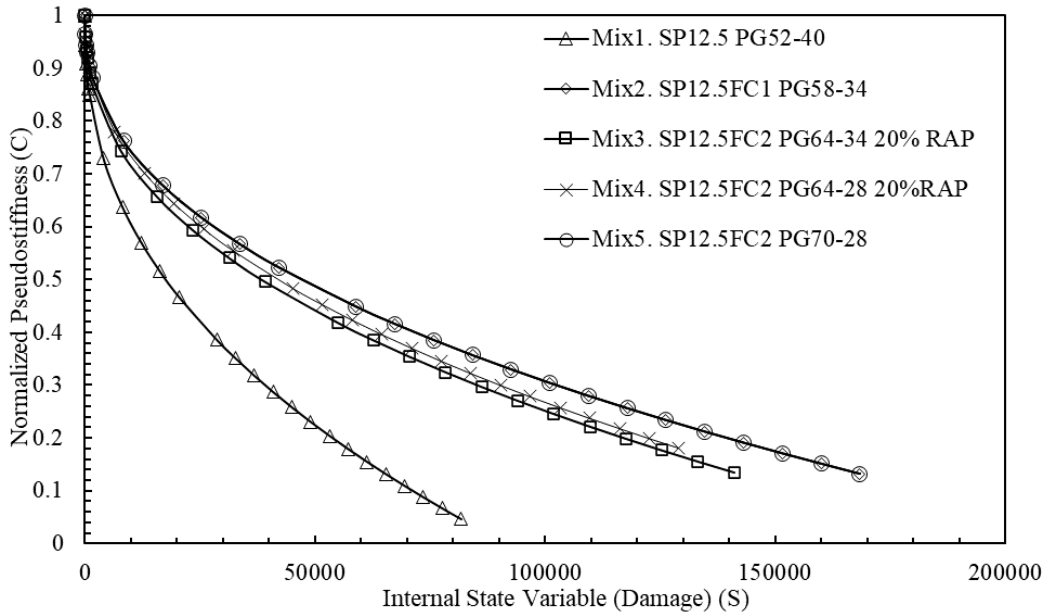
Figure 4.11 Damage Characteristic Curve (C vs. S) Curves.
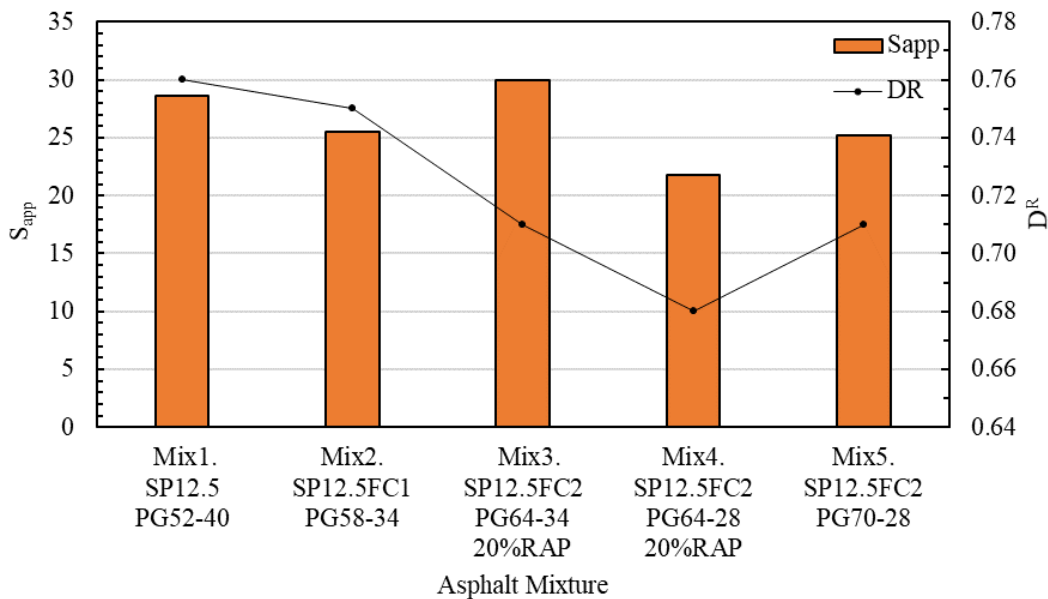
Figure 4.12 Sapp Values at Intermediate Temperature and DR criterion.

4.2.7 Hamburg Wheel Tracking Test Results

The Hamburg Wheel Tracking (HWT) test procedure specified in the AASHTO T324 was used to investigate rutting and moisture susceptibility of PPLC specimens in this study. Currently, the specimens are loaded at test temperatures ranging from 46-50°C for a maximum number of passes or until reaching a certain rut depth as specified by various agencies. A maximum 20000 passes and 12.5 mm rut depth are commonly used.

With respect to the test criteria determined by various agencies, either a maximum rut depth at a specific number of wheel passes or a minimum number of wheel passes to reach a certain rut depth are required.

For this part of study, first, the HWT test was conducted on PPLC specimens compacted at 7±0.5% air void submerged in water at 50°C. The test specimens received 20,000 passes or when a total rut depth of 12.5 mm was reached over a wheel path distance of 200 mm. Figure 4.13 shows rut depth vs. number of wheel passes. As seen in Figure 4.13, Mix5 performed well by completing the test and reaching a total rut depth of 1.85 mm, without having moisture susceptibility. Furthermore, Mix4 completed the test by reaching total depths of 10.7 mm, with showing moisture susceptibility, while Mix3 failed the test by reaching total depths of 13.5 mm at 15200 passes. Moreover, Figure 4.13 shows that asphalt binder stiffness predominantly influences HWT results for Mix1 and Mix2 containing softer PG binder grades (i.e., PG52-40 and PG58-34) such that they reached to rut depth of 12.5 mm at low number of passes. Various highway agencies have specified HWT test temperature ranging from 40 to 46°C for asphalt mixtures containing PG58-XX and lower. For instance, Iowa, Montana, Colorado, and Utah are testing at 40°C, 44°C, 45°C and 46°C, respectively. Therefore, HWT tests were repeated on Mix1, Mix2 at 44°C to compare the results between 50°C and 44°C for these asphalt mixtures, and to determine whether 44°C is an appropriate testing temperature for asphalt mixtures containing softer binders (PG58-XX and PG52-XX). Figure 4.13 demonstrates that Mix1 and Mix2 have low value of post-compaction consolidation at 44°C compared to 50°C, i.e., asphalt binder stiffness predominantly did not impact HWT results at 44°C, therefore, Mix1 and Mix2 pass HWT test at 20,000 passes with the rut depth of 3.6 mm and 6.7 mm, respectively.
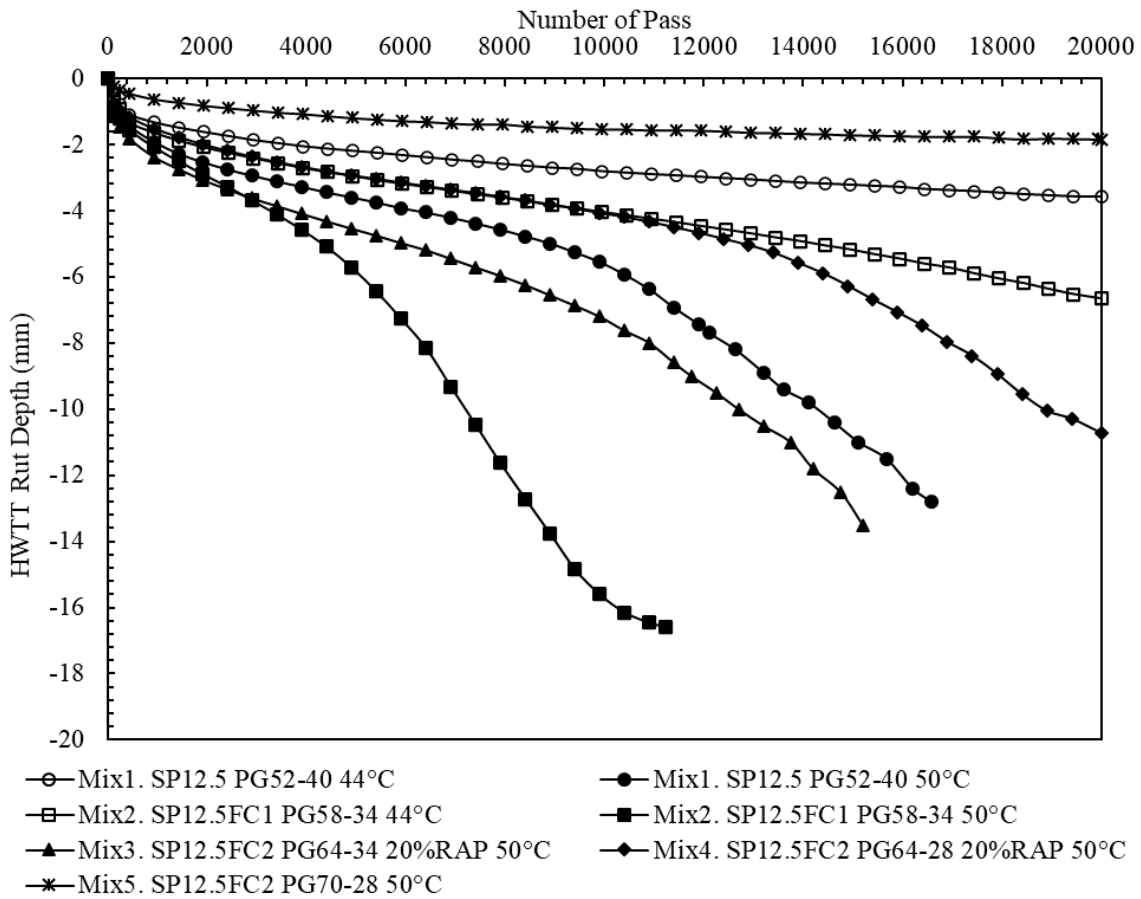
Figure 4.13 Rut Depth vs. Number of Passes.

4.2.8 Relationship Between HWT and MSCR Tests Results

Figure 4.14 and Figure 4.15 illustrate the plots of the relationship between recovered Re% and 10,000 passes rut depth at 50°C and recovered J_{nr} and 10,000 passes rut depth at 50°C, respectively. As seen in Figure 4.14 and Figure 4.15, logarithmic fits suggest a good correlation (R^2=0.861 and R^2=0.918, respectively).
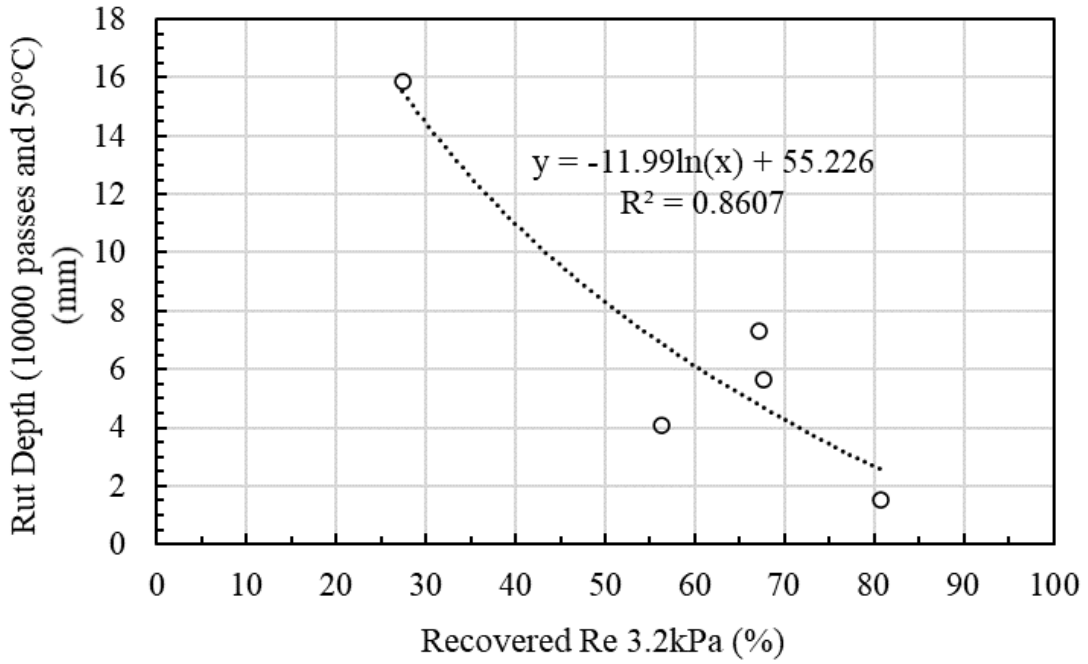
Figure 4.14 Relationship between Re% and Rut Depth (10,000 passes and 50°).
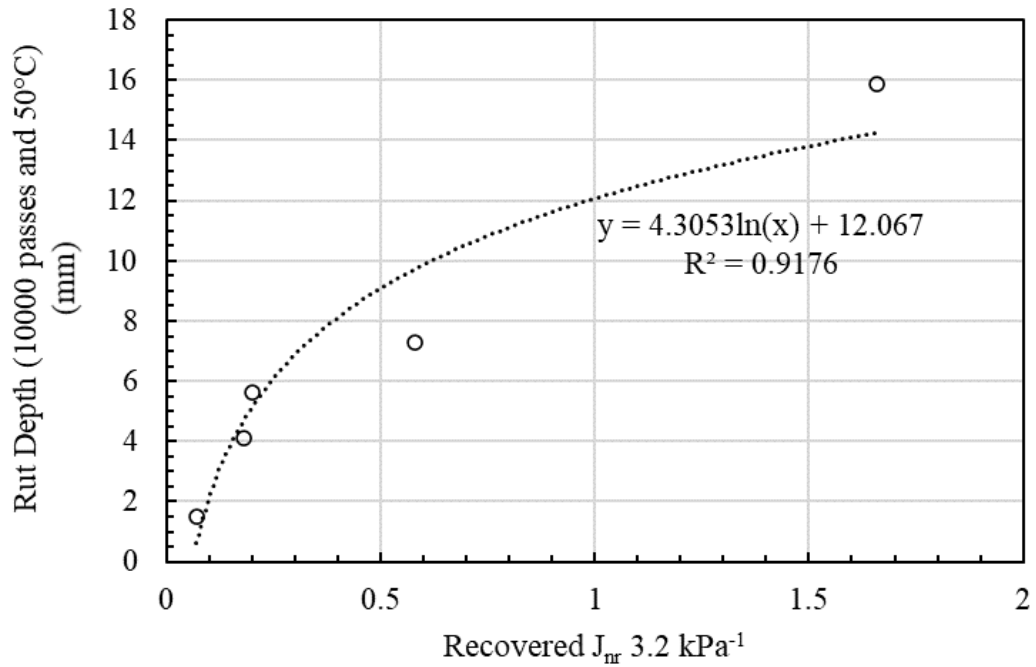
Figure 4.15 Relationship between Jnr and Rut Depth (10,000 passes and 50°).

4.3 Survey

A survey was conducted in order to investigate whether asphalt mixture laboratories in Ontario are capable of conducting asphalt mixture performance tests employed in this research.

The survey was prepared at the University of Waterloo and was distributed by MTO among asphalt mixture laboratories across Ontario to assess whether the laboratories are capable of conducting152

I-FIT and DC(T) tests. Another survey was conducted internally by MTO to assess capability of laboratories to conduct HWT test. Figure 4.16 shows the outcome of the surveys. Since the same testing device and instrumentation can be used for I-FIT and IDEAL-CT tests, IDEAL-CT test can be considered as a feasible performance test for the laboratories. As can be seen in Figure 4.16, as of now, nine laboratories can conduct I-FIT and IDEAL-CT tests, while four and seven laboratories can conduct DC(T) and Hamburg Wheel Tracking tests, respectively.
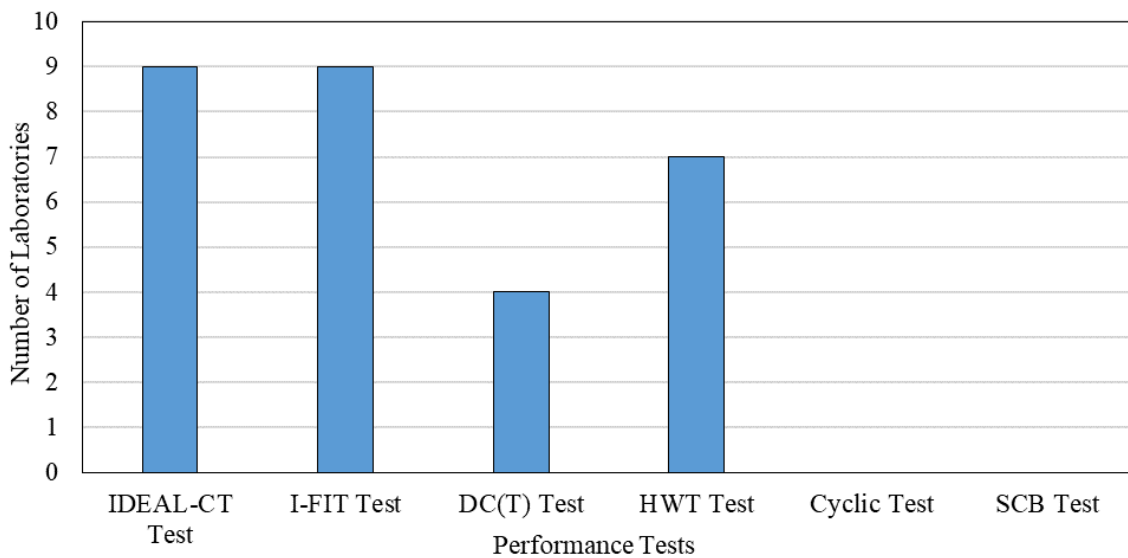
Figure 4.16 Survey Results.

4.4 Conclusions

The following conclusions can be drawn based on the experimental results and discussions provided in this chapter:

- Mix3 showed the highest S_{app} value among the asphalt mixtures in terms of cyclic test, and it also had the highest values of FI and CT Index at 25°C in terms of I-FIT and IDEAL CT tests, respectively. This could be attributed to the soft PG asphalt binder (PG64-34) and the content of recovered asphalt binder (5.2%).

- Mix1 and Mix2 had higher values of FI and CT Index than those of Mix4 and Mix5 according to I-FIT and IDEAL CT tests, however, Mix2 and Mix5 had similar S_{app} values according to cyclic test. The discrepancy between characterization of Mix2 and Mix5 in terms of cyclic test, and I-FIT and IDEAL CT could be attributed to two different modes of testing (cyclic vs. monotonic), test configurations and geometry of specimens.

- Mix1, Mix2 and Mix5 had higher fracture energy values than those of Mix3 and Mix4 according to DC(T) and SCB tests. Low values of Fracture energy in Mix3 and Mix4 could be attributed to the existing RAP in those asphalt mixtures.

- DC(T) and SCB tests were able to rank the asphalt mixtures similarly at 10°C warmer than the low PG grade.

- I-FIT and IDEAL-CT tests were able to distinguish and rank the asphalt mixtures similarly at 25°C, however, they were not able to distinguish asphalt mixtures at the intermediate temperature based on the climate of location where they were paved.

- There was a good linear correlation between I-FIT and IDEAL-CT at 25°C with R^2=0.826.

- Hamburg Wheel Tracking (HWT) test must be conducted at a temperature lower than 50°C for asphalt mixtures containing soft asphalt binders (58-YY and 52-YY), and 44°C seems to be an appropriate temperature.

- Logarithmic fits suggested a good correlation between recovered Re% and Jnr obtained from MSCR test and rut depth at 10000 passes and 50°C (R^2=0.861 and R^2=0.918, respectively).
- According to the survey data and the analysis of laboratory results from five plant-produced asphalt mixtures, DC(T), SCB, I-FIT and Hamburg Wheel Tracking (HWT) tests were selected for further research.

Chapter 5

The Evaluation of DC(T) and SCB Tests Using Five Plant-Produced Asphalt Mixtures

Parts of this chapter have been published in a paper submitted to the Canadian Technical Asphalt Association (CTAA) conference in 2020 (Salehi-Ashani, 2020). DC(T) and SCB tests were investigated in detail by conducting laboratory research on five plant-produced asphalt mixtures. DC(T) and SCB tests were conducted according to ASTM D7313 and AASHTO TP105 test methods, respectively, on triplicates. Although DC(T) and SCB test methods have specified the testing temperature at 10 ℃ higher than the low PG, in this research triplicates were tested at three temperatures, including -18 ℃, -24 ℃ and -30 ℃. Furthermore, to treat specimens equally, the ASTM D7313 test method was followed to condition both DC(T) and SCB specimens. Analysis of variance (ANOVA) and Tukey's HSD (Honest Significant Difference) tests were performed using the Minitab software to statistically evaluate the results of DC(T) and SCB tests. Therefore, a three-way ANOVA with three independent variables, including asphalt mixture (five levels), test method (two levels) and testing temperature (three levels) and one dependent variable (fracture energy) was designed and analysed. Furthermore, correlations between the fracture energies of DC(T) and SCB tests, and between fracture energies of DC(T) and SCB tests and low temperature properties of the recovered asphalt binders were investigated.

Moreover, the effect of long-term aging on the DC(T) test results were examined. Furthermore, Pearson Correlation Coefficient (PCC) test was employed to measure linear relationships between the fracture energies of DC(T) and SCB tests, and between fracture energies of DC(T) and SCB tests and low temperature properties of the recovered asphalt binders.

5.1 DC(T) and SCB Test Results

Figure 5.1 and Figure 5.2 show the bar charts of average fracture energy of DC(T) and SCB tests in conjunction with one standard deviation error bar from the average fracture energy of DC(T) and SCB tests, respectively. Furthermore, the tables below the bar charts summarize

the coefficient of variation (C.V) for fracture energy of DC(T) and SCB tests at three testing temperatures.

As seen in Figure 5.1 and Figure 5.2 there is a general trend whereby a reduction in testing temperature results in a decrease in the average fracture energy for all asphalt mixtures investigated. As the testing temperature decreases from -18 ℃ to -24 ℃, and from -24 ℃ to -30 ℃, the average fracture energy decreases, thus resulting in a reduction in low temperature cracking resistance of asphalt mixtures. This demonstrates that DC(T) and SCB tests are sensitive to the testing temperature, and a reduction in the testing temperature followed by the increase in the brittleness of the asphalt mixtures results in a smaller amount of energy to be dissipated to initiate and propagate the crack at the tip of the notch in the DC(T) and SCB testing specimens. Furthermore, a drop in the testing temperature from -18 ℃ to -30 ℃ causes a significant reduction in the average fracture energy for all asphalt mixtures. This implies that DC(T) and SCB tests can capture the transition from quasi-ductile to quasi-brittle behaviour in asphalt mixtures.

Figure 5.1 and Figure 5.2 also show that, in general, DC(T) and SCB tests are both able to distinguish asphalt mixtures containing RAP from those without RAP since Mix3 and Mix4 containing 20% RAP have the lowest average fracture energy compared to the other asphalt mixtures (Mix1, Mix2 and Mix5) at the three testing temperatures. Moreover, Mix3 has higher values of average fracture energy than those of Mix4 at the three testing temperatures due to using a softer PG asphalt binder (PG64-34 compared to PG64-28). This observation indicates that combining a softer PG asphalt binder with RAP results in reduced brittleness of asphalt mixtures at low temperatures.

Coefficient of Variation (C.V) of fracture energy values for five asphalt mixtures at three testing temperatures are, in most cases, less than 15% implying that DC(T) and SCB tests have a satisfactory repeatability.

90

	Mix1. SP12.5 PG52-40	Mix2. SP12.5FC1 PG58-34	Mix3. SP12.5FC2 PG64-34 20%RAP	Mix4. SP12.5FC2 PG64-28 20%RAP	Mix5. SP12.5FC2 PG70-28
-18°C	9.0	18.8	7.3	8.2	18.1
-24°C	6.2	16.7	10.1	6.8	11.5
-30°C	5.5	5.0	15.7	6.2	11.2
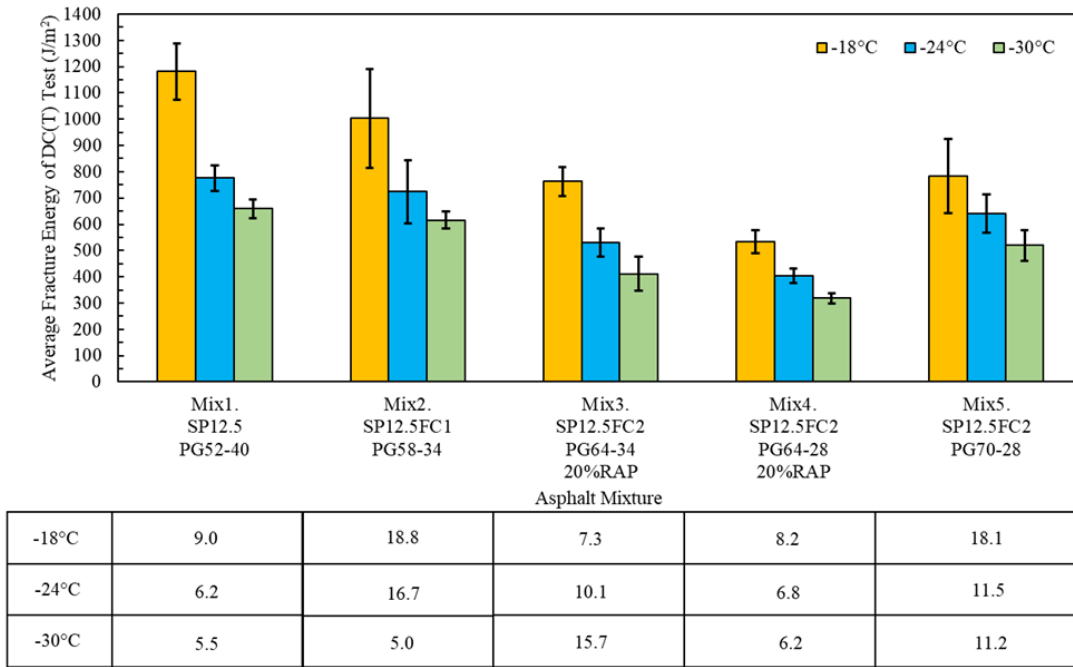
Figure 5.1 DC(T) Test Results at Three Testing Temperatures.

	Mix1. SP12.5 PG52-40	Mix2. SP12.5FC1 PG58-34	Mix3. SP12.5FC2 PG64-34 20%RAP	Mix4. SP12.5FC2 PG64-28 20%RAP	Mix5. SP12.5FC2 PG70-28
-18°C	7.3	15.7	8.8	2.9	11.5
-24°C	8.9	10.2	3.1	4.4	11.4
-30°C	10.6	14.8	5.3	24.1	16.6
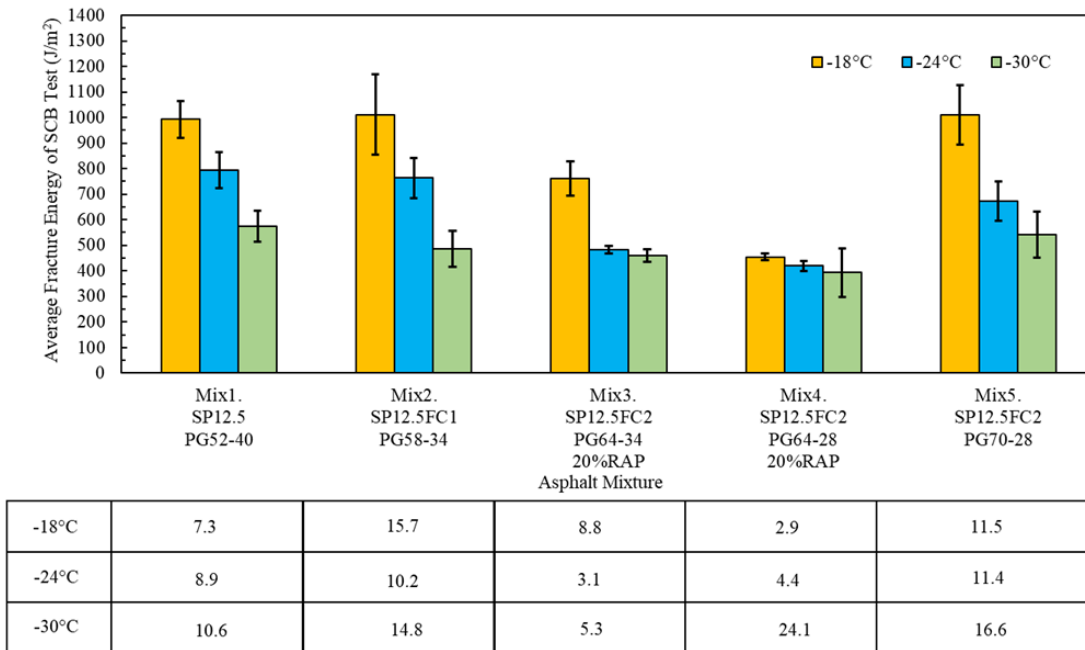
Figure 5.2 SCB Test Results at Three Testing Temperatures.

91

Figure 5.3 provides a closer look at the bar charts results of DC(T) and SCB fracture energies at 10°C higher than low PG coupled with the results of recovered continuous low temperature PG. As shown in Figure 5.3 fracture energy values of DC(T) and SCB tests indicate that Mix5 and Mix2 outperform the other asphalt mixtures. In general, the results show that the average fracture energy of DC(T) and SCB tests are associated with the recovered continuous low temperature PG. In order to clarify this matter, it should be noted that the continuous low temperature PG of Mix5 and Mix2 are -32.4 ℃ and -39.0 ℃, respectively, which are significantly lower than their corresponding low temperature PG, i.e. -28 ℃ and -34 ℃. The aforementioned difference between the recovered continuous low temperature PG and the low temperature PG could contribute to higher fracture energy and higher low temperature cracking resistance of Mix5 and Mix2 compared to other asphalt mixtures. On the other hand, the difference between the recovered continuous low temperature PG and the low temperature PG for Mix1, Mix3 and Mix4 is not as considerable as that for Mix5 and Mix2. The recovered continuous low temperature PG of Mix1, Mix3 and Mix4 measured at -41.3 ℃, -35.1 ℃ and -29.8 ℃, respectively, are almost close to their corresponding low temperature PG, namely -40 ℃, -34 ℃ and -28 ℃. As can be seen in Figure 5.3, Mix3 and Mix4 have the lowest value of fracture energy among the asphalt mixtures. The reason is likely due to the existing RAP in Mix3 and Mix4 causing them to have a brittle behaviour at low temperatures. Even though the difference between the continuous low temperature PG and the low temperature PG is not considerable for Mix1, the average fracture energy of Mix1 is higher than that of Mix3 and Mix4. This could stem from the virgin materials used in Mix1.
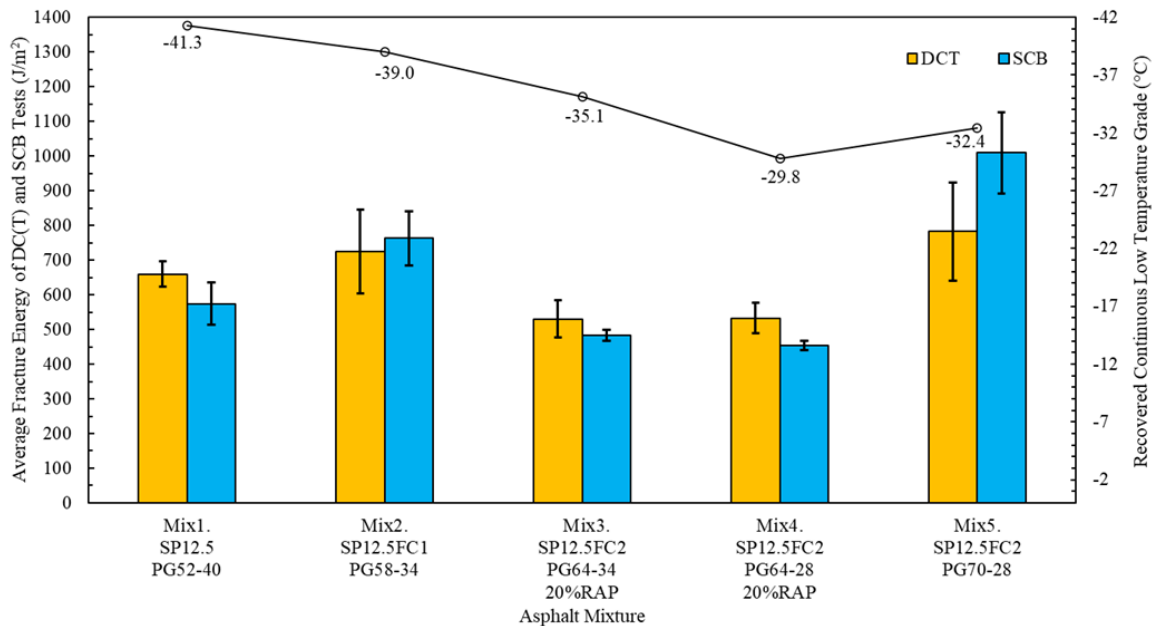
Figure 5.3 DC(T) and SCB Test Results at 10°C Higher than Low Temperature PG.

Table 5.1 summarizes the statistical analysis obtained from ANOVA confirming that asphalt mix and temperature as well as two interactions of asphalt mix-temperature and asphalt mix-test method are statistically significant parameters in fracture energy variation.

Table 5.1 Summarized Analysis of Variance (ANOVA).

Source	DF[1]	Adjusted SS[2]	Adjusted MS[3]	P-Value[4]	Statistically Significance
Asphalt Mix	4	1934559	483640	0.000	Yes
Temperature	2	1907100	953550	0.000	Yes
Test Method	1	204	204	0.862	No
Asphalt Mix-Temperature Interaction	8	228412	28552	0.000	Yes
Asphalt Mix-Test Method Interaction	4	74174	18544	0.035	Yes
Temperature-Test Method Interaction	2	2615	1307	0.823	No

Tukey's HSD (Honest Significant Difference) test using Minitab software was utilized at 5% confidence level to obtain statistical ranking of the asphalt mixtures based on fracture energy of DC(T) and SCB tests at 10°C warmer than low PG of asphalt binders as well as individual testing temperatures, namely -18°C, -24°C and -30°C. Table 5.2 summarizes the

93

statistical ranking of asphalt mixtures at 10°C warmer than low PG, -18°C, -24°C and -30°C. As presented in Table 5.2, at 10°C higher than low PG, based on DC(T) test, Mix5 statistically has the same ranking of resistance to low temperature cracking as Mix2 and Mix1, while it outperforms Mix3 and Mix4. Correspondingly, based on SCB test, Mix5 has the highest resistance to low temperature cracking and Mix3 and Mix4 have the lowest resistance to low temperature cracking. As shown in Table 5.2, based on DC(T) test, Mix5 at -24°C statistically has the same resistance to low temperature cracking as Mix1, Mix2 and Mix3, and considering SCB test, Mix5 has statistically the same low temperature cracking resistance as Mix1 and Mix2 and outperforms Mix3. As shown in Table 5.2, at -18°C, SCB test is not able to distinguish five asphalt mixtures as well as DC(T) test does. As can be seen in Table 5.2, based on DC(T) test, Mix1 and Mix2 statistically have higher average fracture energy than other asphalt mixtures at -30°C. Mix5 statistically has the same average fracture energy as Mix2 and Mix3. However, considering SCB test, all asphalt mixtures statistically have the same average fracture energy, and SCB test could not distinguish the low temperature cracking resistance of asphalt mixtures at -30°C. The main reason causing SCB test not to distinguish and rank low temperature cracking resistance of asphalt mixtures at -18 ºC and -30 ºC can be attributed to the behaviour of asphalt mixtures when they are too ductile and too brittle, respectively, and the discrepancies existing with DC(T) and SCB test methods: different geometry of testing specimens (the ligament area in DC(T) test is 4,125 mm^2, while the ligament area for SCB test is 1500 mm^2), different mode of loading considering compressive loading in SCB test while tensile loading in DC(T) test, different CMOD rates (1mm/min and 0.03mm/min for DC(T) and SCB tests, respectively).

Table 5.2 Summarized Analysis of Tukey's HSD Ranking.

Testing Temperature	Asphalt Mixture	DC(T) Test	SCB Test
10°C warmer than low PG	Mix1. SP12.5 PG52-40	A B	C
	Mix2. SP12.5FC1 PG58-34	A B	B
	Mix3. SP12.5FC2 PG64-34 20% RAP	B	C
	Mix4. SP12.5FC2 PG68-28 20% RAP	B	C
	Mix5. SP12.5FC2 PG70-28	A	A
-18°C	Mix1. SP12.5 PG52-40	A	A
	Mix2. SP12.5FC1 PG58-34	A B	A
	Mix3. SP12.5FC2 PG64-34 20% RAP	B C	A
	Mix4. SP12.5FC2 PG68-28 20% RAP	C	B
	Mix5. SP12.5FC2 PG70-28	B C	A
-24°C	Mix1. SP12.5 PG52-40	A	A
	Mix2. SP12.5FC1 PG58-34	A	A
	Mix3. SP12.5FC2 PG64-34 20% RAP	B C	B
	Mix4. SP12.5FC2 PG68-28 20% RAP	C	B
	Mix5. SP12.5FC2 PG70-28	A B	A
-30°C	Mix1. SP12.5 PG52-40	A	A
	Mix2. SP12.5FC1 PG58-34	A B	A
	Mix3. SP12.5FC2 PG64-34 20% RAP	C D	A
	Mix4. SP12.5FC2 PG68-28 20% RAP	D	A
	Mix5. SP12.5FC2 PG70-28	B C	A

5.2 Relationship Between DC(T) and SCB Tests Results

Figure 5.4 illustrates the plot of the relationship between the average fracture energy of DC(T) and SCB tests where the horizontal and vertical axes represent the average fracture energy of DC(T) and SCB tests, respectively. The data has been divided in three groups by the testing temperatures, namely -18 ºC, -24 ºC and -30 ºC. As seen in Figure 5.4, there is a trend in which the lower the testing temperature, the lower the spread of the data points such that at -30 ºC, data points cluster in the bottom left of the plot. Moreover, power fits suggest a strong correlation (R^2=0.843) between the fracture energy values of DC(T) and SCB tests as can be seen in Figure 5.4.
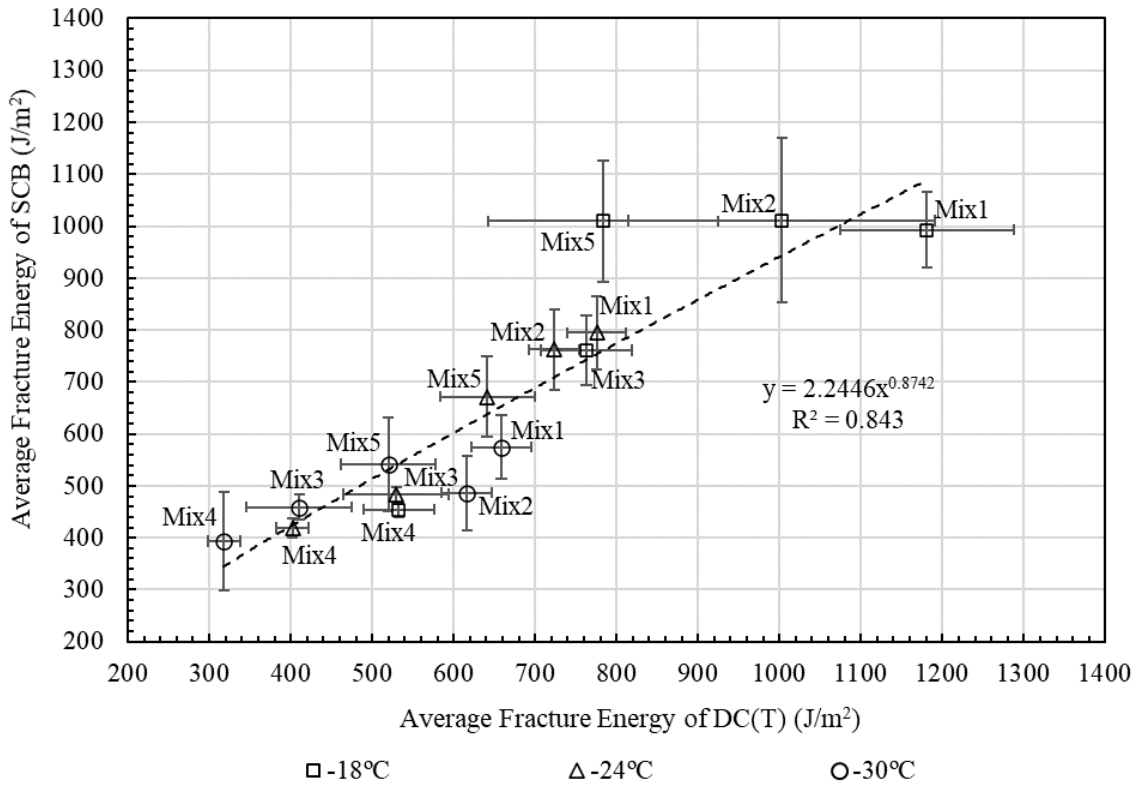
Figure 5.4 Relationship between the Fracture Energy Obtained from DC(T) and SCB Tests.

5.3 Relationship Between DC(T) and SCB Tests Results and Asphalt Binder Low Temperature Properties

Figure 5.5, Figure 5.6, and Figure 5.7 show the relationship between DC(T) fracture energy and recovered continuous low temperature grade, recovered m-value temperature and recovered stiffness temperature, respectively. As shown in the aforementioned figures, there is a negative correlation between recovered asphalt binder properties at low temperature and DC(T) fracture energy at three testing temperatures, namely -18°C, -24°C and -30°C such that a decrease in recovered asphalt binder properties results in an increase in DC(T) fracture energy. Linear fits indicate a strong correlation between DC(T) fracture energy and recovered asphalt binder properties at three testing temperatures.
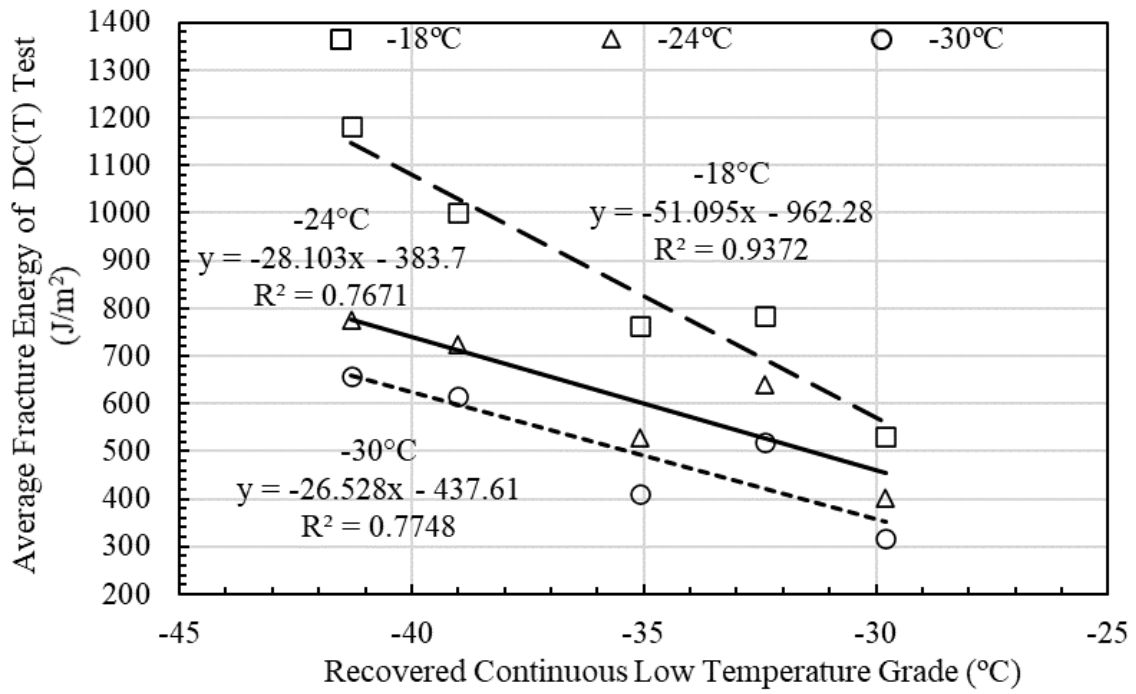
Figure 5.5 Relationship between the Fracture Energy of DC(T) and Recovered Continuous Low Temperature Grade.
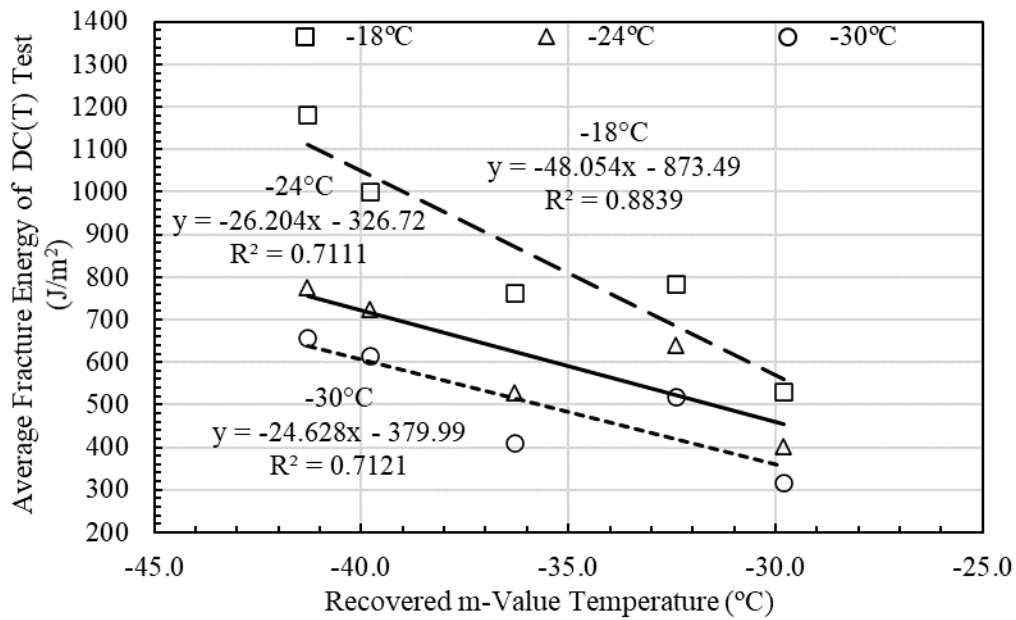
Figure 5.6 Relationship between the Fracture Energy of DCT Test and Recovered m-Value Temperature.
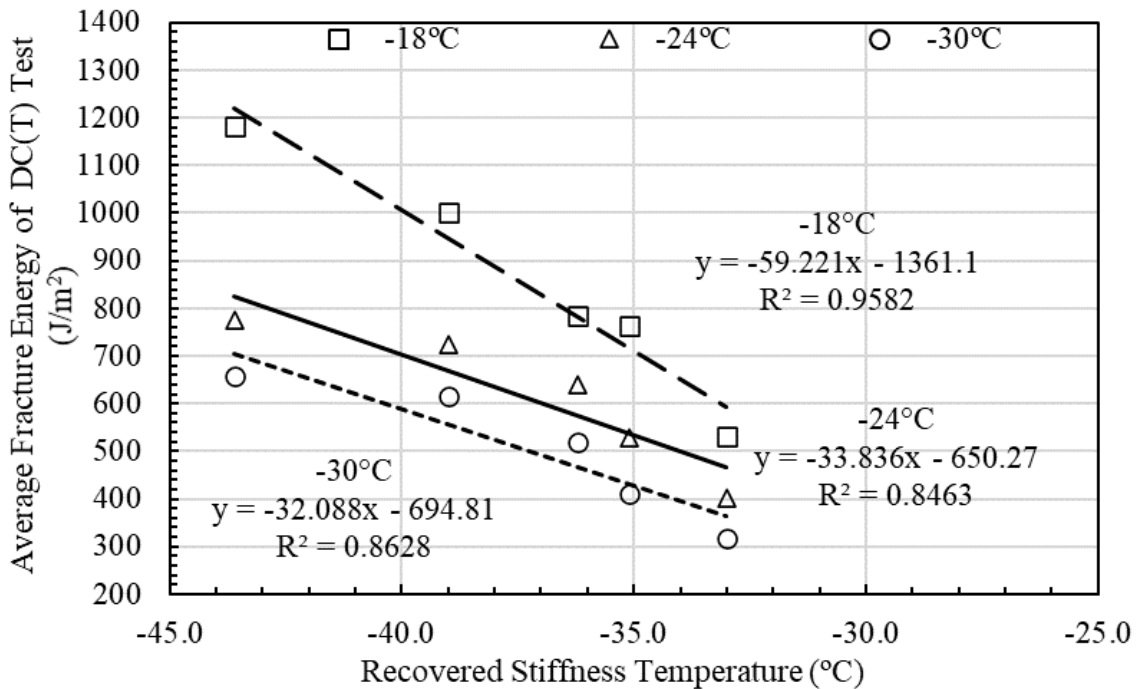
Figure 5.7 Relationship between the Fracture Energy of DC(T) Test and Recovered Stiffness Temperature.

Figure 5.8, Figure 5.9, and Figure 5.10 and illustrate the relationship between SCB fracture energy and recovered asphalt binder properties at low temperature. As shown in the aforementioned figures, linear fits indicate a moderate to poor negative correlation between SCB fracture energy and recovered asphalt binder properties at -18°C and -30°C, however, the correlation is almost strong at -24°C.
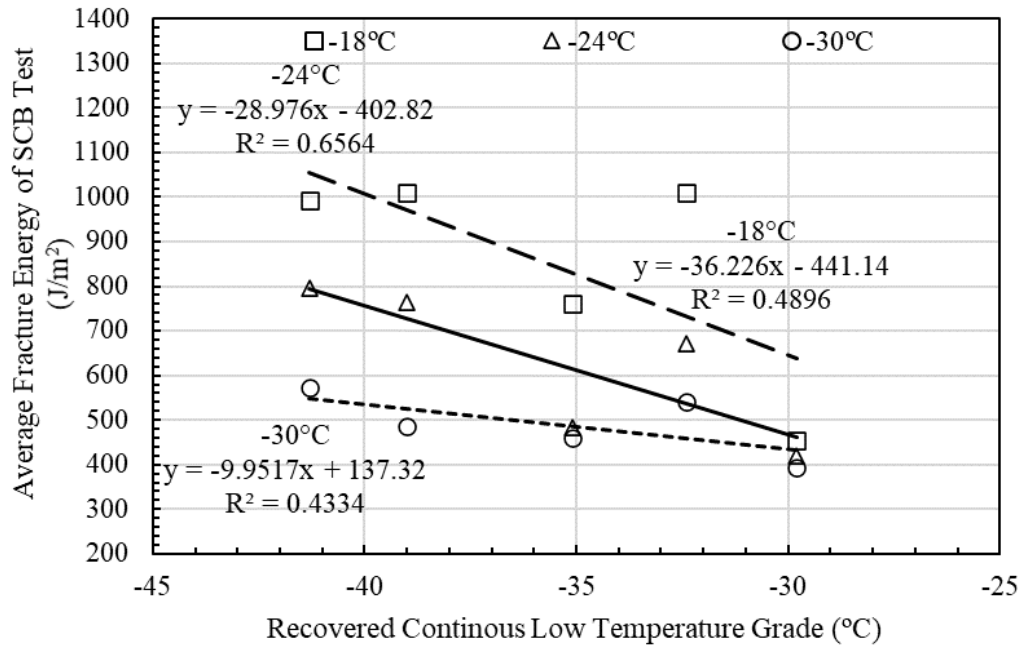
Figure 5.8 Relationship between the Fracture Energy of SCB Test and Recovered Continuous Low Temperature Grade.
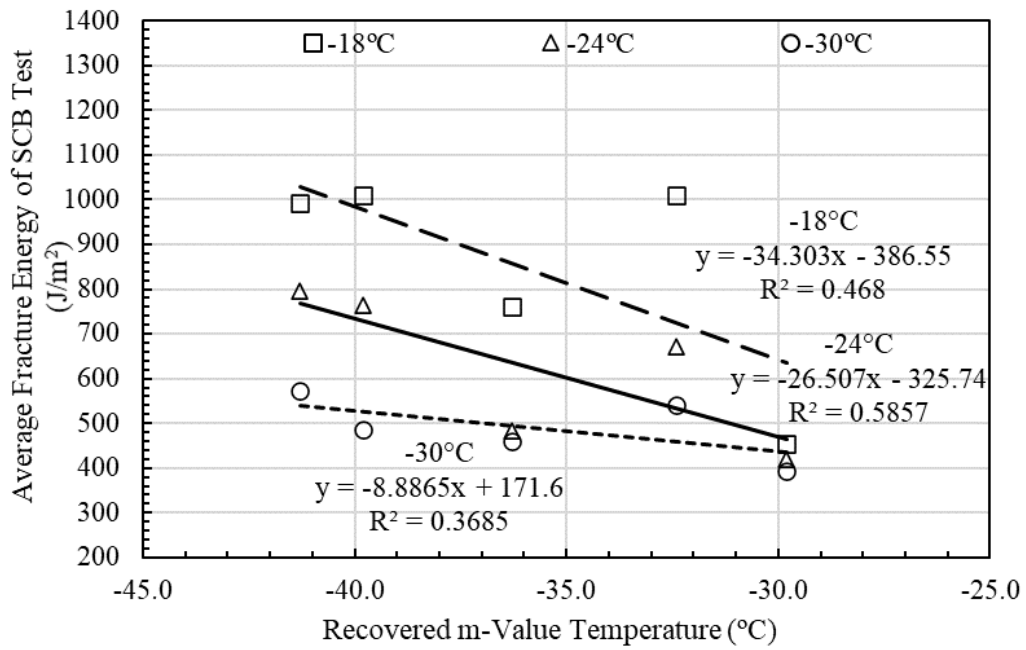
Figure 5.9 Relationship between the Fracture Energy of SCB Test and Recovered m-Value Temperature.
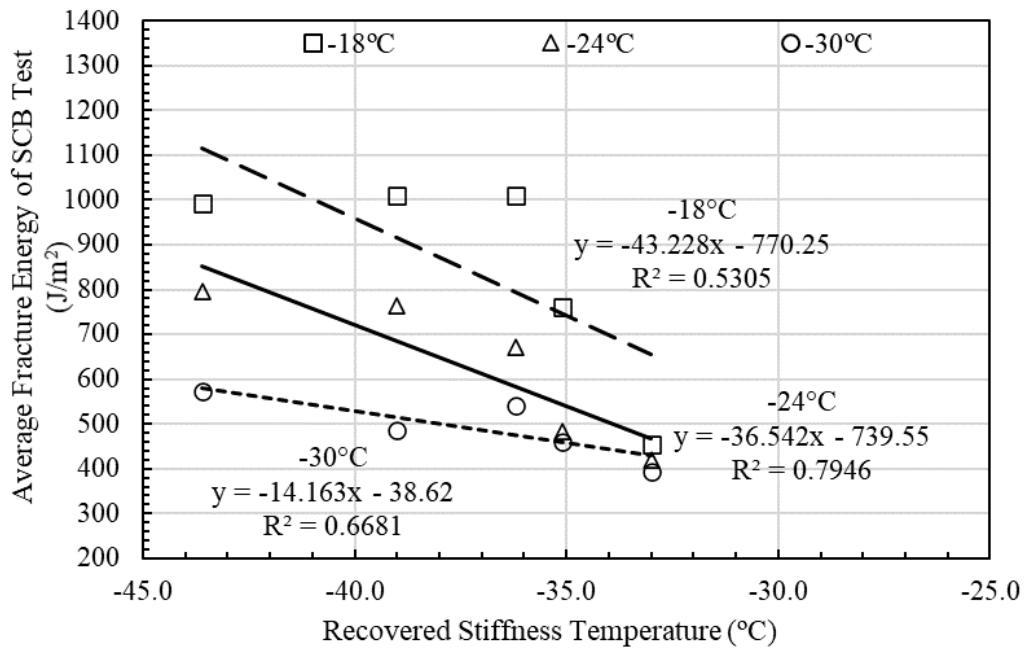
Figure 5.10 Relationship between the Fracture Energy of SCB Test and Recovered Stiffness Temperature.

100

Furthermore, Figure 5.11 and Figure 5.12 demonstrate the relationship between ΔT_c and fracture energy of DC(T) and SCB tests, respectively. As shown in Figure 5.11 and Figure 5.12, there are poor correlation between ΔT_c and the fracture energy of the DC(T) and SCB tests.
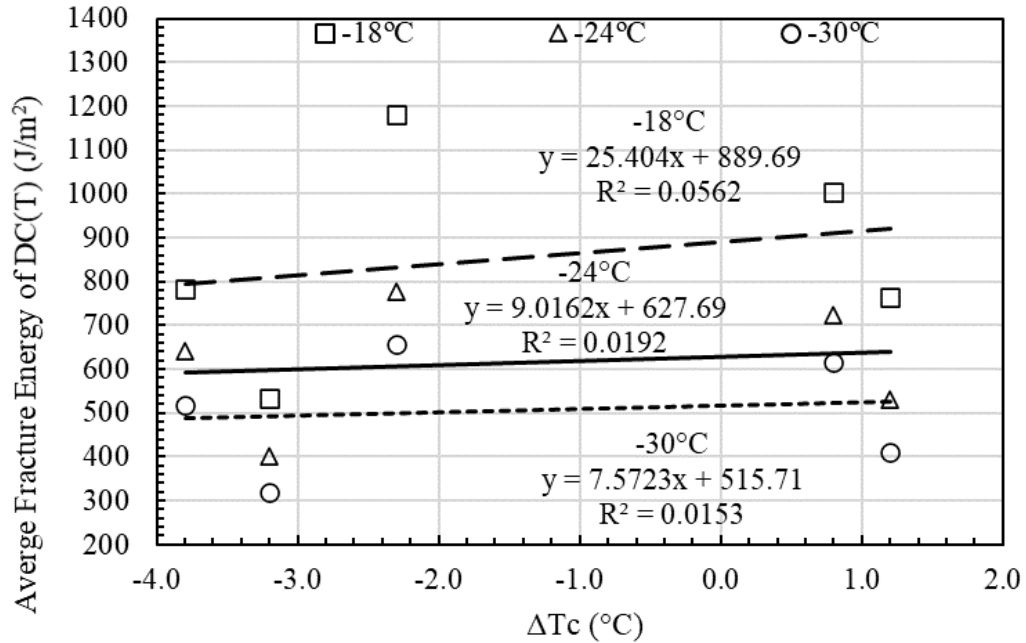
Figure 5.11 Relationship between the Fracture Energy of DC(T) Test and ΔT_c.
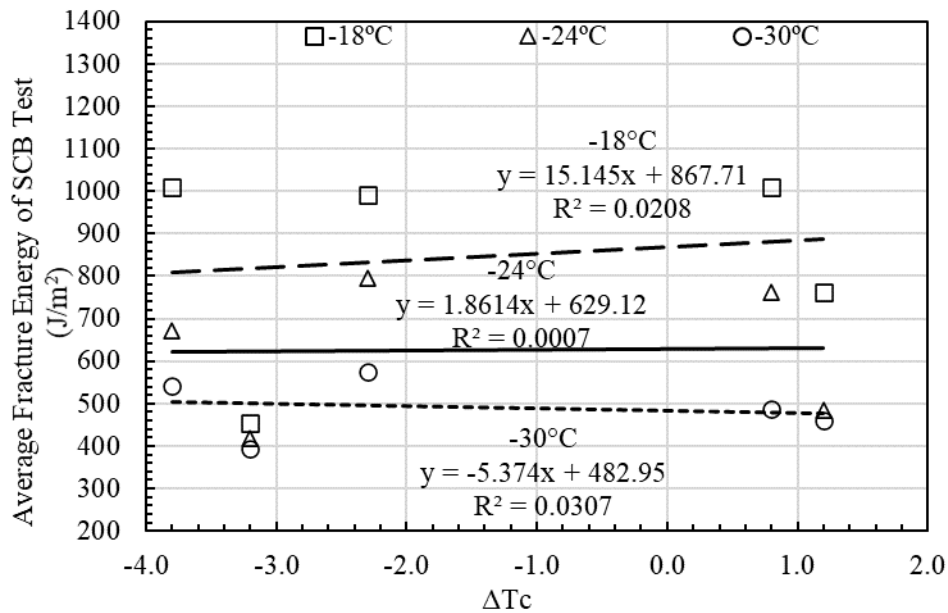
Figure 5.12 Relationship between the Fracture Energy of SCB Test and ΔTc.

5.4 Effect of Long-Term Aging on DC(T) Fracture Energy

Two laboratory aging techniques are currently being practiced according to AASHTO R30 standard: short-term oven aging on the loose mix before compaction (4 hours in the oven at compaction temperature) to simulate aging happening during asphalt mix production in the asphalt plant, hauling to the site, placing and compaction activities, and long-term oven aging on the compacted asphalt specimen to simulate long-term aging happening to asphalt pavement during service time (forced-draft oven aging at 85 °C for 120 hours). Generally, forced-draft oven aging has been of interest for industry because of its availability, practicability, and feasibility; however, reducing the time of long-term aging to enhance its degree of practicability for industry is important. Therefore, in this research the results of two methods of long-term aging, forced-draft oven aging at 85 °C for 120 hours and forced-draft oven aging at 95 °C for 72 hours were compared.

As seen in Figure 5.13, DC(T) fracture energy was not sensitive to two methods of long-term aging in that only in Mix5 there existed a slight reduction in the value of fracture

energy. Statistical t-test showed that there was not a statistically significant difference between the fracture energy results obtained from short-term aged and long-term aged specimens (p-value>0.05).

S.T.A	5.5	16.7	10.1	8.2	18.1
L.T.A (85°C/120hours)	7.4	7.7	1.0	4.2	6.0
L.T.A (95°C/72 hours)	4.8	6.4	2.0	12.7	9.1

Figure 5.13 Effect of Long-Term Aging on DC(T) Fracture Energy.

5.5 Conclusions

The following conclusions can be drawn based on the experimental results and discussions provided in this chapter:

- DC(T) and SCB tests, two fracture mechanics-based tests, were able to distinguish the low temperature cracking resistance of asphalt mixtures, especially the mixes containing RAP, at 10°C warmer than the low PG grade.

- There was not statistically difference between fracture energies of DC(T) and SCB tests at three testing temperatures, including -18°C, -24°C and -30°C for asphalt mixtures investigated.

- SCB test was not able to distinguish and rank low temperature cracking resistance of asphalt mixtures at -18 °C and -30 °C. This can be attributed to the behaviour of asphalt mixtures when they are too ductile and too brittle, respectively, and the

discrepancies existing with the geometry of DC(T) and SCB specimens, and CMOD rate.

- There was a good correlation between fracture energies of DC(T) and SCB tests.
- DC(T) fracture energy had a good correlation with Recovered low temperature properties of asphalt binders.
- DC(T) fracture energy was not sensitive to long-term aging.

Chapter 6

The Evaluation of I-FIT Test Using Five Plant-Produced Asphalt Mixtures

Parts of this chapter have been presented in the Canadian Society of Civil Engineering (CSCE) 2021 conference (Salehi-Ashani, 2021) I-FIT test Was investigated in detail by conducting laboratory research on five plant-produced asphalt mixtures. The objective of this research was to evaluate the sensitivity of I-FIT test results to four main factors: 1) PG asphalt binder of asphalt mixtures, 2) testing temperature, 3) testing equipment setup (i.e., hydraulic or screw-driven devices, and 4) aging conditioning of the asphalt mixtures. The latter was studied by following two aging procedures for compacted asphalt mixtures specimens: 1) the currently used AASHTO R30 standard practice for 120 hours at 85 ℃, and 2) oven aging for 72 hours at 95 ℃. On the other hand, given that the default testing temperature for I-FIT test is specified to be 25 ℃, it was deemed necessary to investigate the sensitivity of flexibility indices to changes in testing temperature, where considering the effect of intermediate PG asphalt binder on the FI results becomes important. Furthermore, the temperature sensitivity of FI was investigated by conducting the tests at 25 ℃, 24 ℃ and 23 ℃ and at the intermediate temperature based on PG asphalt binder of the asphalt mixtures.

6.1 Effect of Temperature Sensitivity on I-FIT Results

Figure 6.1, Figure 6.2, and Figure 6.3 show the bar charts of average fracture energy, post-peak slope, and flexibility index, respectively, obtained from I-FIT test at 23°C, 24°C and 25°C on triplicate of asphalt mixtures by using DTS-30 testing device. The error bars shown on the bar charts represent one standard deviation from the average. In addition, Table 6.1 summarizes the general factorial regression for fracture energy, post-peak slope, and flexibility index obtained from ANOVA. Figure 6.1 demonstrates that as the testing temperature decreases from 25°C to 23°C, fracture energy values increase for asphalt mixtures. In general, the average of fracture energy values obtained at 23°C and 24°C are equal. As seen in Figure 6.2, as the temperature decreases from 25°C to 23°C, the value of post-peak slope increases. In general, asphalt mixtures containing hard PG asphalt binder, i.e., Mix4 and Mix5, were more prone to

have a drastic increase in their post-peak slope values. Overall, considering all asphalt mixtures, the average of post-peak slope values at 24°C is greater and less than that at 25°C and 23°C, respectively. Figure 6.3 shows that for Mix1, Mix2 and Mix3, flexibility index values are comparable at the three testing temperatures. However, dropping the testing temperature from 25°C to 23°C causes the flexibility index to decrease for Mix4 and Mix5. The effect of testing temperature on the flexibility index values were investigated, in detail, by using a paired t-test between the Flexibility Index values at three testing temperatures. T-test results showed that for Mix1, Mix2 and Mix3, testing temperature was statistically non-significant (p-value>0.05). However, for Mix4, the difference between flexibility index values at 25°C and 23°C is statistically significant (p-value<0.05). Moreover, t-test results indicated that for Mix5, the difference between flexibility index values at 25°C and 23°C as well as the difference between flexibility index values at 24°C and 23°C were statistically significant (p-value<0.05). Therefore, based on the results, it could be concluded that asphalt mixtures containing hard PG asphalt binder (Mix4 and Mix5) were more sensitive to testing temperature compared to asphalt mixtures having softer PG asphalt binders (Mix1, Mix2 and Mix3).
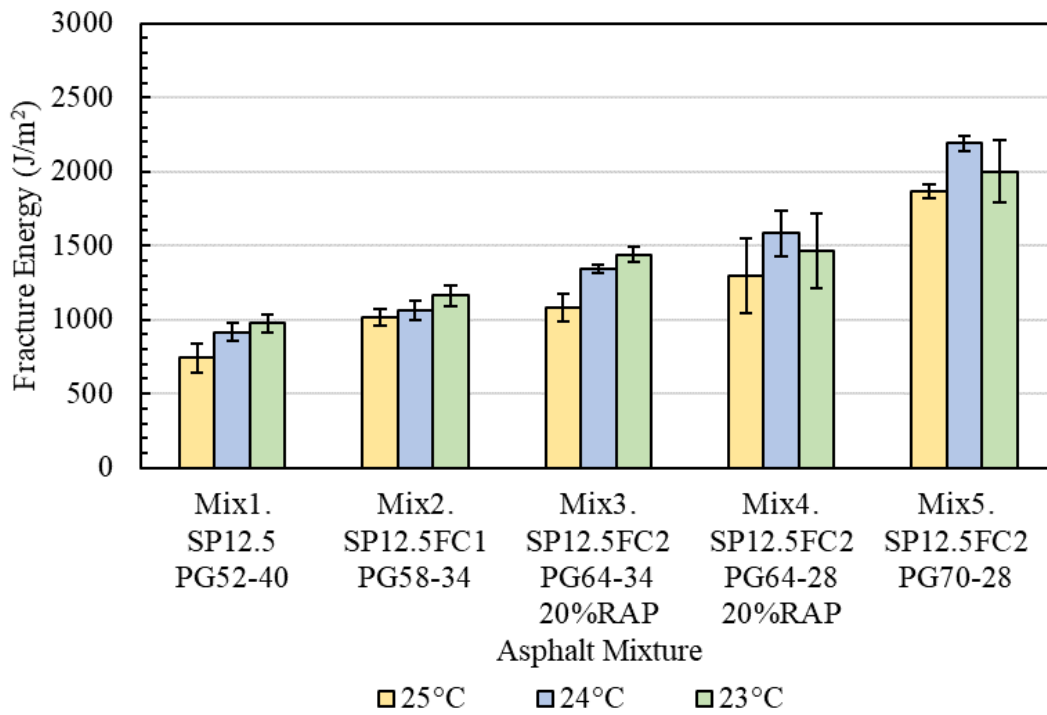
Figure 6.1 Effect of Temperature Sensitivity on Fracture Energy Results.
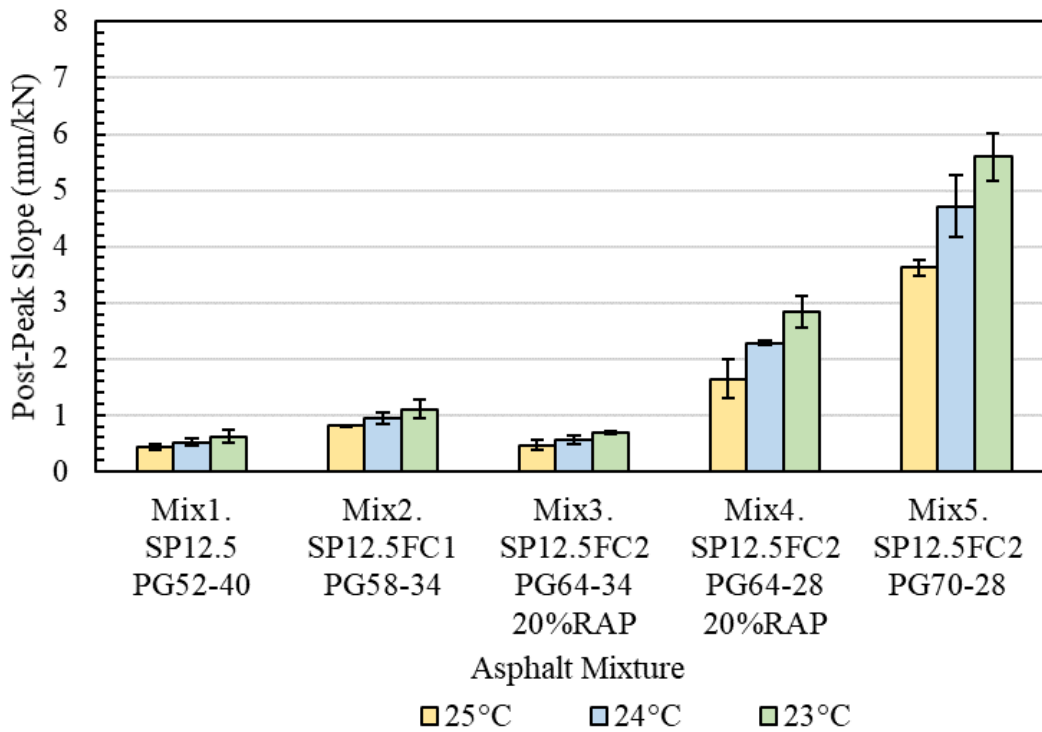
Figure 6.2 Effect of Temperature Sensitivity on Post-Peak Slope Results.
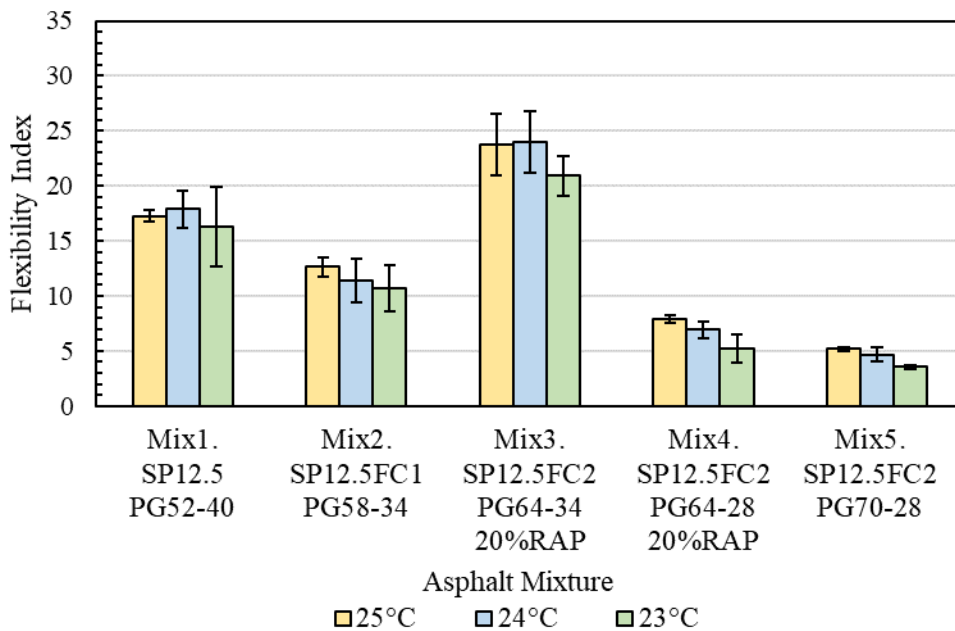
Figure 6.3 Effect of Temperature Sensitivity on Flexibility Index Results.

Table 6.1 Summarized Analysis of Variance (ANOVA) for Temperature Sensitivity.

General Factorial Regression: Fracture Energy versus Asphalt Mix, Temperature					
Source	DF[1]	Adjusted SS[2]	Adjusted MS[3]	P-Value[4]	Statistically Significance
Asphalt Mix	4	6810081	1702520	0.000	Yes
Temperature	2	454100	227050	0.000	Yes
Asphalt Mix-Temperature	8	158830	19854	0.319	No
General Factorial Regression: Slope versus Asphalt Mix, Temperature					
Source	DF	Adjusted SS	Adjusted MS	P-Value	Statistically Significance
Asphalt Mix	4	109.55	27.39	0.000	Yes
Temperature	2	4.55	2.27	0.000	Yes
Asphalt Mix-Temperature	8	3.76	0.47	0.000	Yes
General Factorial Regression: Flexibility Index versus Asphalt Mix, Temperature					
Source	DF	Adjusted SS	Adjusted MS	P-Value	Statistically Significance
Asphalt Mix	4	2059.28	514.82	0.000	Yes
Temperature	2	34.24	17.12	0.01	Yes
Asphalt Mix-Temperature	8	7.73	0.96	0.31	No

6.2 Effect of Testing Device on I-FIT Test Results

Figure 6.4, Figure 6.5, and Figure 6.6 show the bar charts of average fracture energy, post-peak slope, and flexibility index, respectively, obtained from I-FIT test conducted by two testing devices, namely a servo- hydraulic device (DTS-30) having a chamber set up at 25°C and a screw-driven testing device (Auto_SCB) without having a chamber, on triplicate of asphalt mixtures. The error bars shown on the bar charts represent one standard deviation from the average. Table 6.2 summarizes the general factorial regression for fracture energy, post-peak slope, and flexibility index obtained from ANOVA. Figure 6.4 and Figure 6.5 show that the average fracture energy and post-peak slope of asphalt mixtures obtained from Auto_SCB testing device are slightly greater than those obtained from DTS-30 testing device. Although,

Table 6.2 confirmed that testing device was statistically significant for fracture energy and post-peak slope, a paired t-test between the results of fracture energy and post-peak slope of asphalt mixtures obtained from two testing devices was applied. T-test results indicated that testing device was only significant for fracture energy results of Mix2 and Mix3 (p-value of 0.05 and 0.01 for Mix2 and Mix3, respectively). As seen in Figure 6.6, DTS-30 and Auto_SCB testing devices produced similar values of flexibility index for all asphalt mixtures. Table 6.2 states that testing device is not statistically significant for flexibility index results. Also, a paired t-test between the flexibility index results of asphalt mixtures, produced by two testing devices, proved the statement (p-value>0.05).
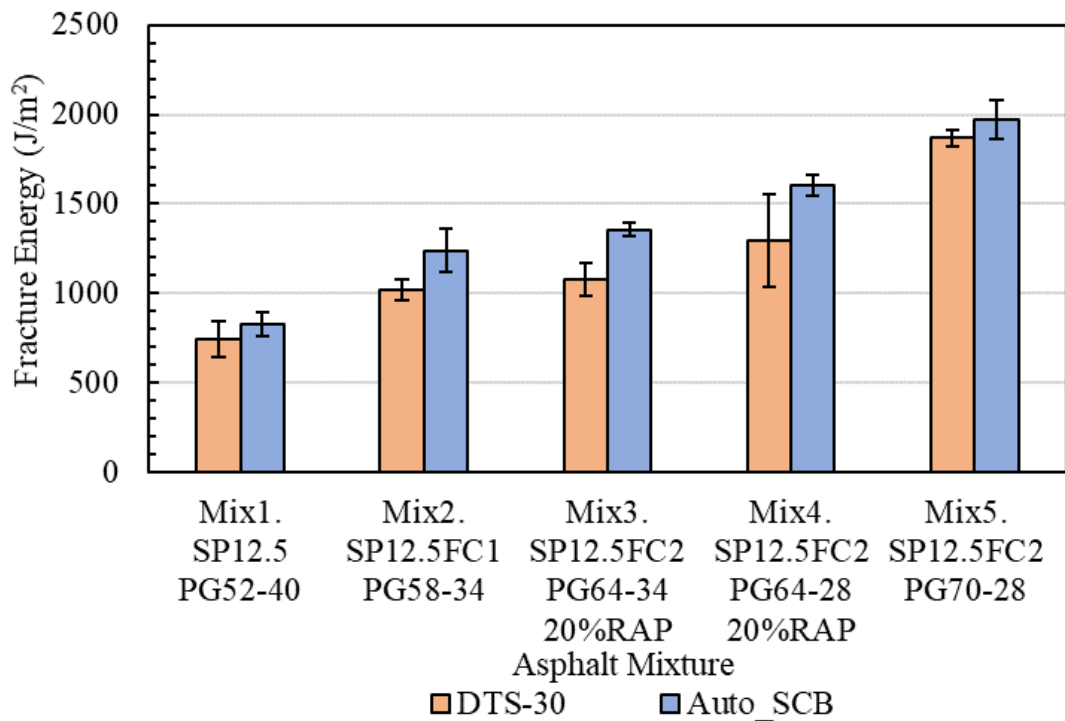
Figure 6.4 Effect of Testing Device on Fracture Energy Results.
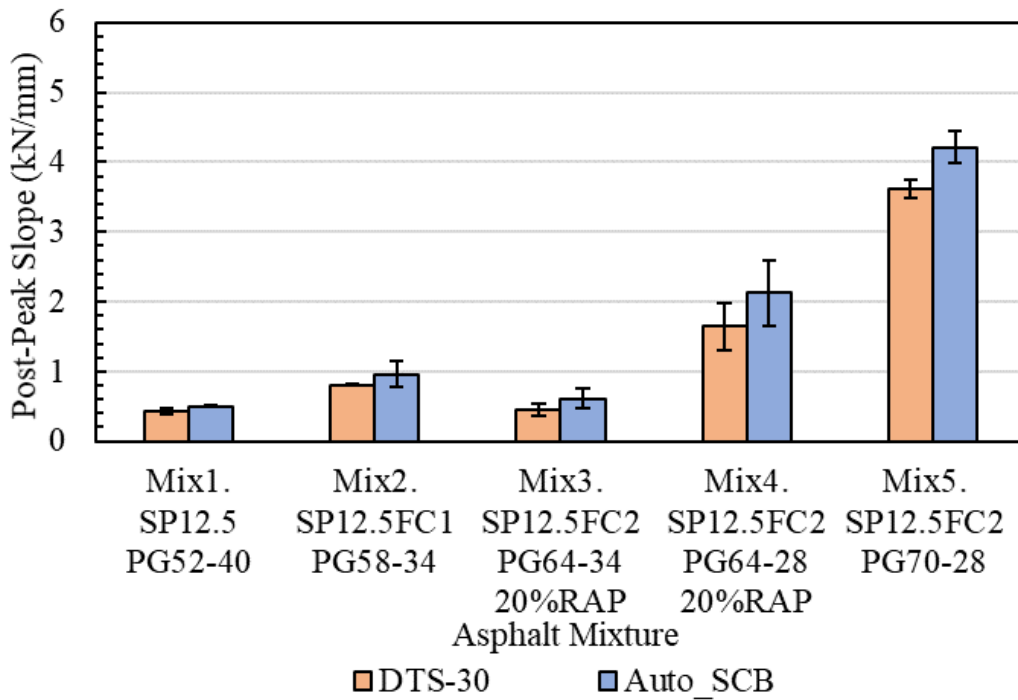
Figure 6.5 Effect of Testing Device on Post-Peak Slope Results.
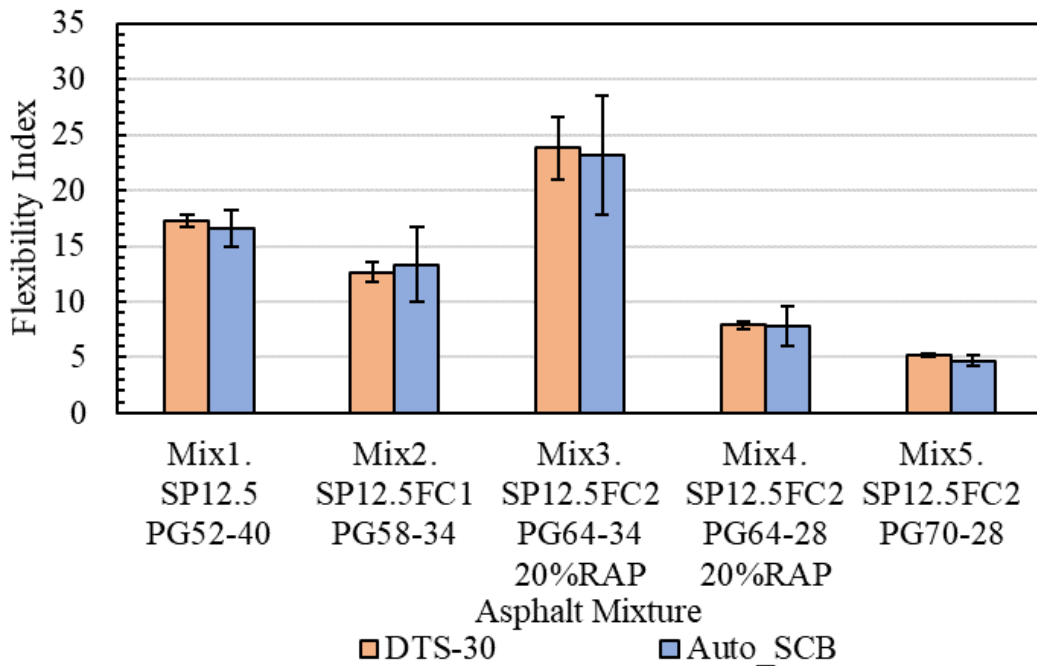
Figure 6.6 Effect of Testing Device on Flexibility Index Results.

111

Table 6.2 Summarized Analysis of Variance (ANOVA) for Testing Device.

General Factorial Regression: Fracture Energy versus Asphalt Mix, Testing Device					
Source	DF[1]	Adjusted SS[2]	Adjusted MS[3]	P-Value[4]	Statistically Significance
Asphalt Mix	4	4258920	1064730	0.000	Yes
Testing Device	1	294630	294630	0.000	Yes
Asphalt Mix- Testing Device	4	63356	15839	0.312	No
General Factorial Regression: Slope versus Asphalt Mix, Testing Device					
Source	DF	Adjusted SS	Adjusted MS	P-Value	Statistically Significance
Asphalt Mix	4	50.22	12.55	0.000	Yes
Testing Device	1	0.62	0.62	0.000	Yes
Asphalt Mix- Testing Device	4	0.32	0.08	0.185	No
General Factorial Regression: Flexibility Index versus Asphalt Mix, Testing Device					
Source	DF	Adjusted SS	Adjusted MS	P-Value	Statistically Significance
Asphalt Mix	4	1300.21	325.05	0.000	Yes
Testing Device	1	0.36	0.35	0.800	No
Asphalt Mix- Testing Device	4	1.81	0.45	0.987	No

6.3 Effect of Long-Term Aging on I-FIT Test Results

Two laboratory aging techniques are currently being practiced according to AASHTO R30 standard: short-term oven aging on the loose mix before compaction (4 hours in the oven at compaction temperature) to simulate aging happening during asphalt mix production in the asphalt plant, hauling to the site, placing and compaction activities, and long-term oven aging on the compacted asphalt specimen to simulate long-term aging happening to asphalt pavement during service time (forced-draft oven aging at 85 ℃ for 120 hours). Generally, forced-draft oven aging has been of interest for industry because of its availability, practicability, and feasibility; however, reducing the time of long-term aging to enhance its degree of practicability for industry is important. Therefore, in this research the results of two methods of long-term aging, forced-draft oven aging at 85 ℃ for 120 hours and forced-draft oven aging at 95 ℃ for 72 hours were compared.

I-FIT test was conducted on quadruplicate according to the AASHTO TP124 test method. In general, to decrease the variability of test results based on trim mean method, the test result having flexibility index value farther from the average was eliminated. Consequently, the average and standard deviation of fracture energy, slope, and flexibility index relevant to three testing replicates remained were reported. The analysis of variance (ANOVA) test using the Minitab software was utilized to statistically evaluate the results of I-FIT tests.

Figure 6.7, Figure 6.8, and Figure 6.9 show the bar charts of average fracture energy, post-peak slope, and flexibility index, respectively, obtained from I-FIT test conducted on short-term aged and long-term aged replicates of asphalt mixtures by using DTS-30 testing device. The error bars shown on the bar charts represent one standard deviation from the average. Moreover, Table 6.3 summarizes the general factorial regression for fracture energy, post-peak slope, and flexibility index obtained from ANOVA.

As seen in Figure 6.7, two methods of long-term aging resulted in a slight increase in the fracture energy values of asphalt mixtures. In general, the average of fracture energy values obtained from the method of long-term aging at 95°C for 72 hours was greater than that of the method of long-term aging at 85°C for 120 hours. The main reason for the increase in fracture energy values after aging can be attributed to age hardening and the increase in the peak loads of load-load line displacement curves obtained from I-FIT tests. Figure 6.10 to Figure 6.14 presents load-load lined displacement curves drawn from the average of three replicates tested. Even though Table 6.3 confirmed that the short-term aged/long-term aged condition was statistically significant for fracture energy, the effect of aging on the fracture energy values was investigated, in detail, by applying a paired t-test between the results of fracture energy of short-term aged and two long-term aged conditions (i.e., at 85°C for 120hours and 95°C for 72hours), and between two long-term aged conditions. T-test results indicated that aging was statistically non-significant (p-value>0.05) on the results of fracture energy for all asphalt mixtures except for Mix4 in which aging was statistically significant (p-value=0.05 between the short-term aged replicates and long-term aged replicates at 95°C for 72 hours, and p-value=0.03 between long-term aged replicates at 85°C for 120hours and long-term aged

replicates at 95°C for 72hours). This could stem from the existing RAP in Mix4 that combined with a hard asphalt binder contributes to a higher level of age hardening.
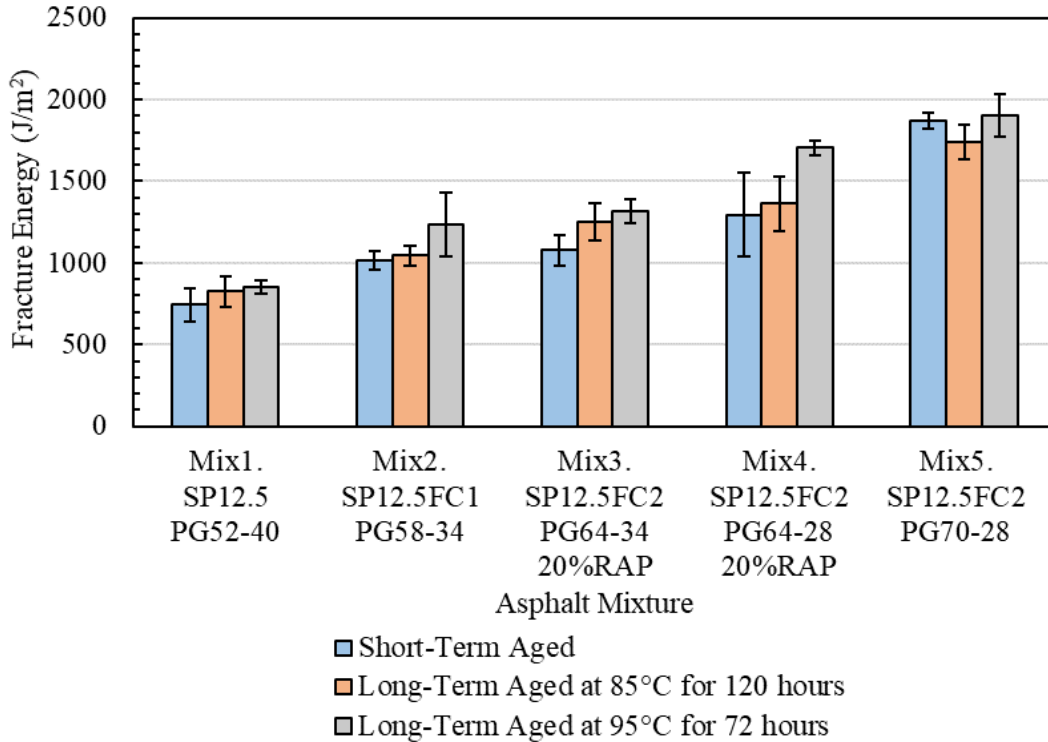
Figure 6.7 Effect of Long-Term Aging on Fracture Energy Results.

Figure 6.8 illustrates that long-term aging caused an increase in the post-peak slope values in comparison to short-term aged condition for all asphalt mixtures, thus accelerating the crack propagation. Brittleness in consequence of age hardening can be attributed to the increase in post-peak slope after aging. In general, the average of post-peak slope values obtained from the method of long-term aging at 95°C for 72 hours was greater than that of the method of long-term aging at 85°C for 120 hours. The results of a paired t-test between the results of post-peak slope values obtained from two methods of long-term aging and post-peak slope values obtained from short-term aged condition confirmed a statistically significant difference (p-values<0.05) for all asphalt mixtures.
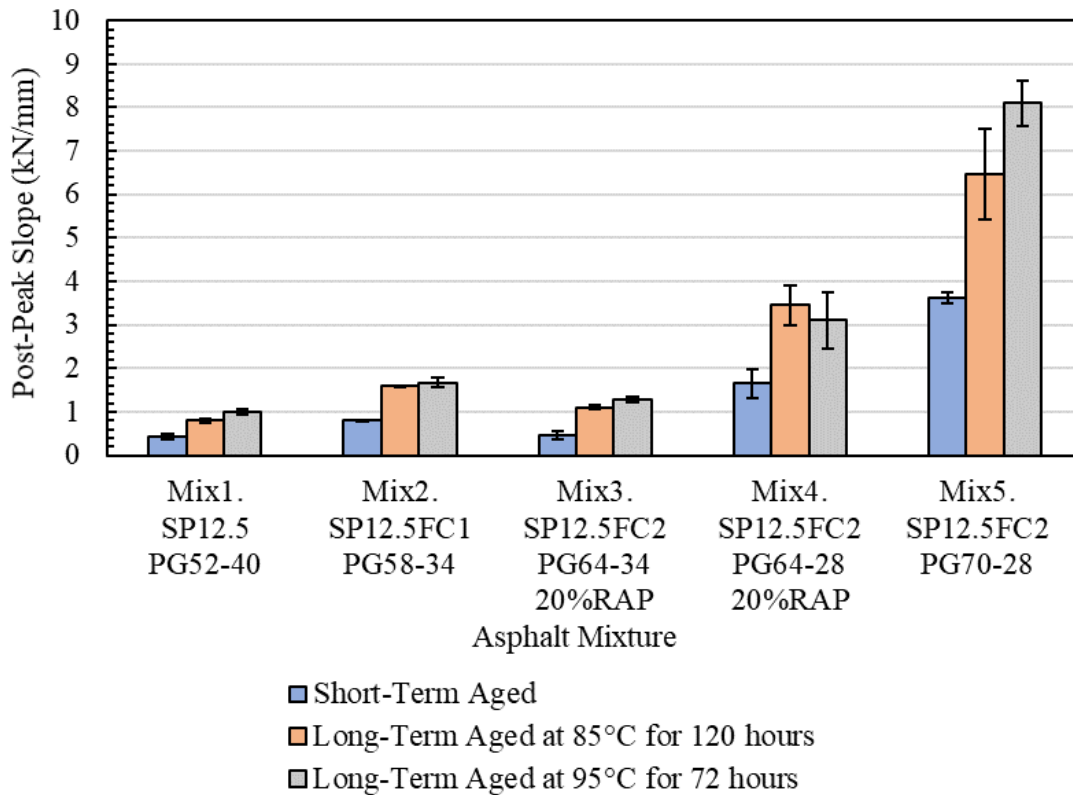
Figure 6.8 Effect of Long-Term Aging on Post-Peak Slope Results.

Figure 6.9 conspicuously displays that both methods of long-term aging caused the flexibility index values of all asphalt mixtures to decrease drastically. As mentioned earlier, age hardening and brittleness after aging are the main reasons for reduction in flexibility index. In general, the average of flexibility index values obtained from two methods of long-term aging are approximately equal. A paired t-test was applied between the results of flexibility index of short-term aged and two long-term aged methods, and between two long-term aged methods. T-test results for the former indicated that long-term aging was statistically significant (p-value<0.05) for all asphalt mixtures, while the t-test results for the latter showed that two different methods of long-term aging were statistically non-significant (p-value>0.05). Consequently, it can be concluded that two methods of long-term aging produced statistically equal flexibility index values. Furthermore, Table 6.4 shows that before long-term aging, Mix3

has the highest ranking among asphalt mixtures, however, after long-term aging, Mix1 and Mix3 has the same ranking followed by Mix2, Mix4 and Mix5.
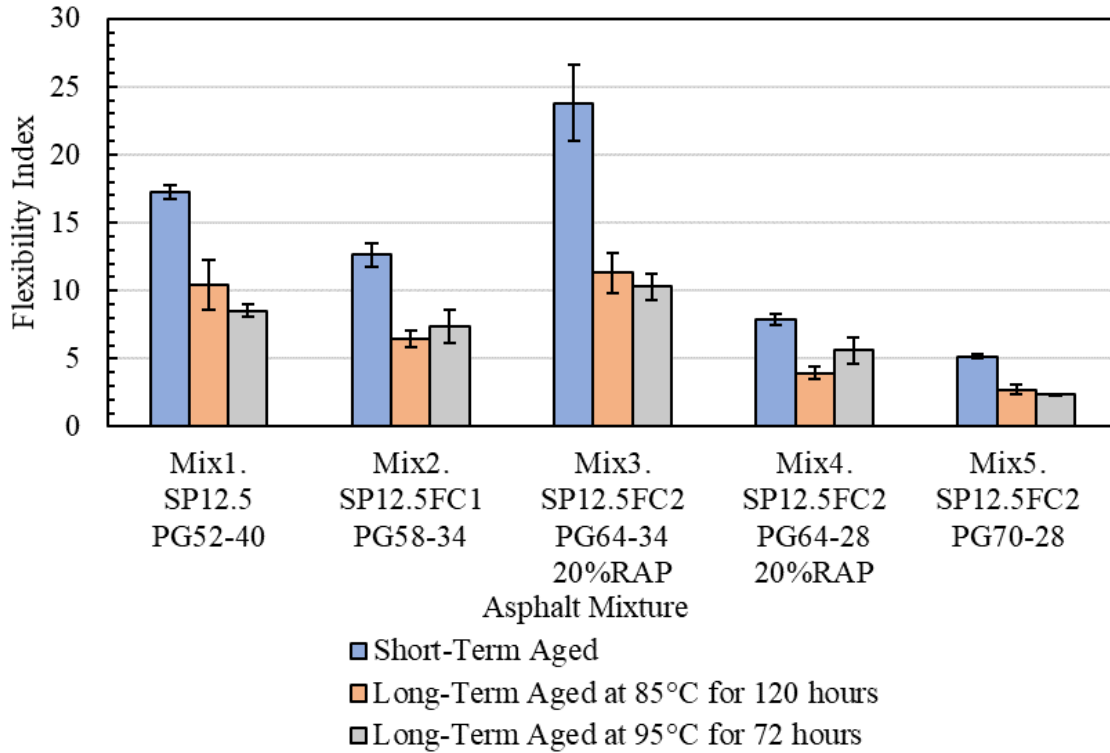
Figure 6.9 Effect of Long-Term Aging on Flexibility Index Results.
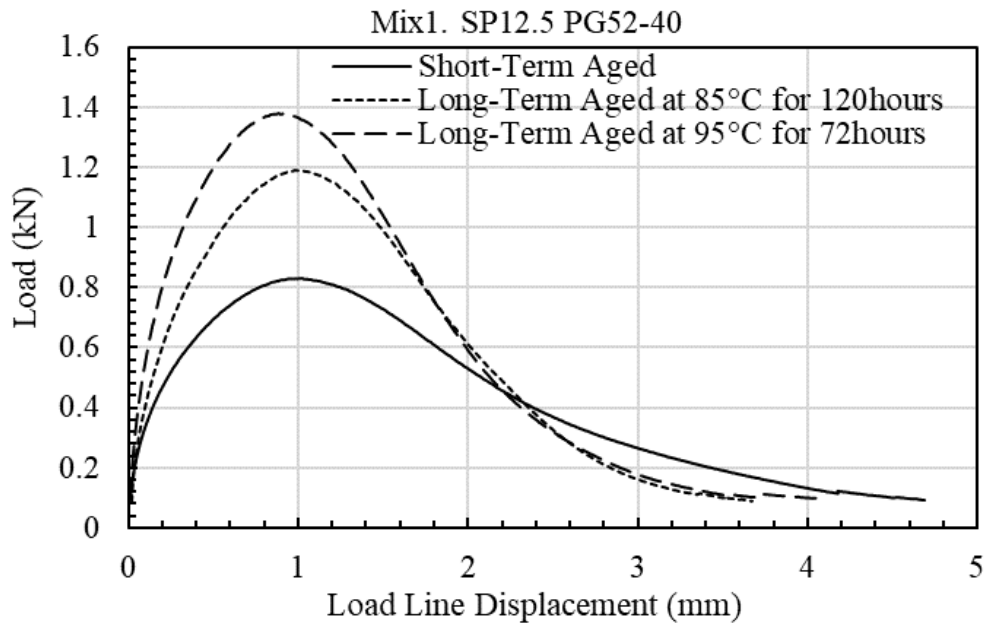
Figure 6.10 Load-Load Line Displacement Curve of Mix1 for Short-Term and Long-Term
Aged Conditions.
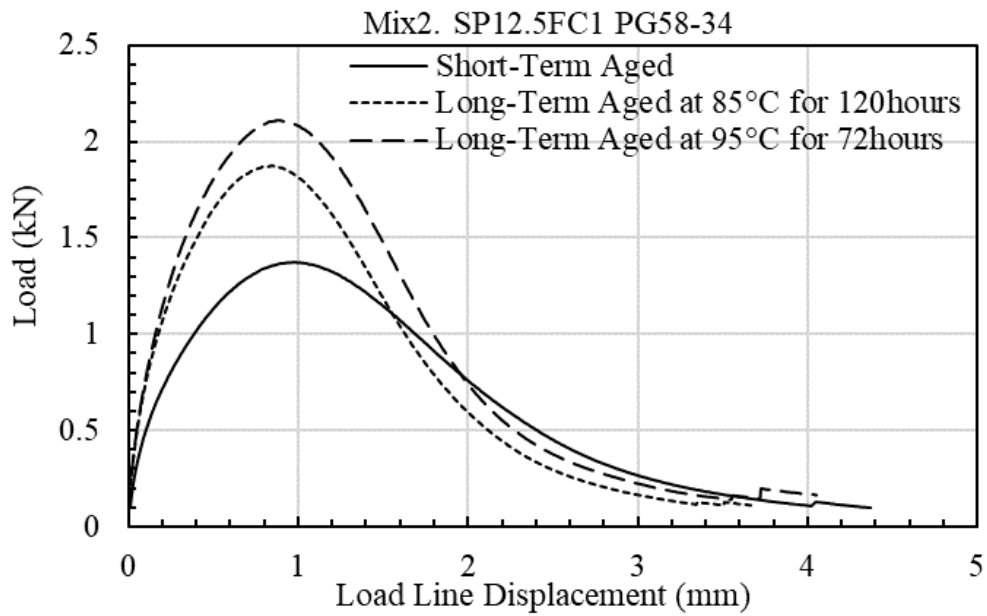
Figure 6.11 Load-Load Line Displacement Curve of Mix2 for Short-Term and Long-Term
Aged Conditions.

117
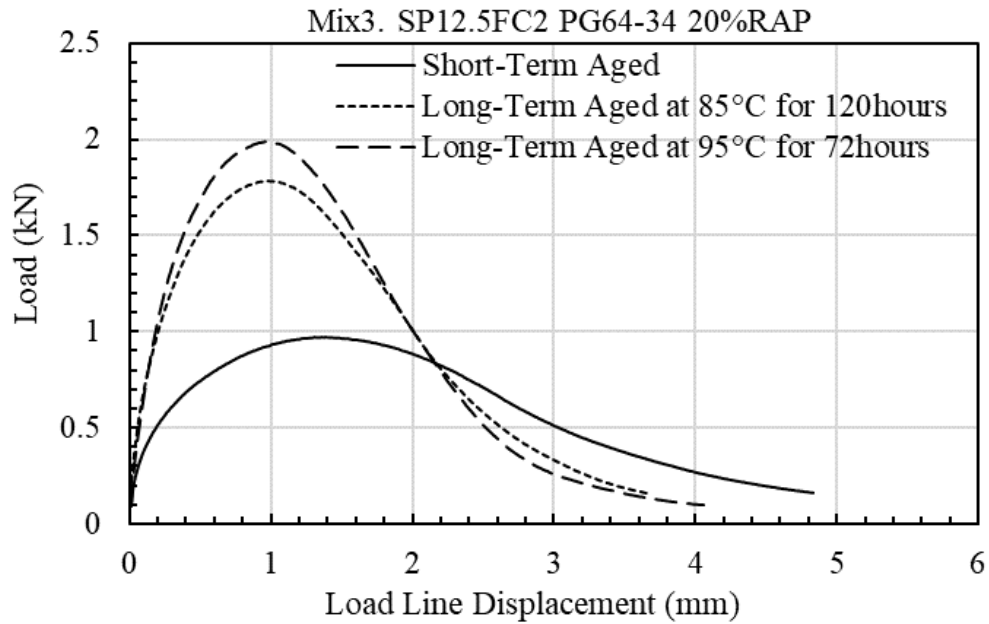
Figure 6.12 Load-Load Line Displacement Curve of Mix3 for Short-Term and Long-Term Aged Conditions.
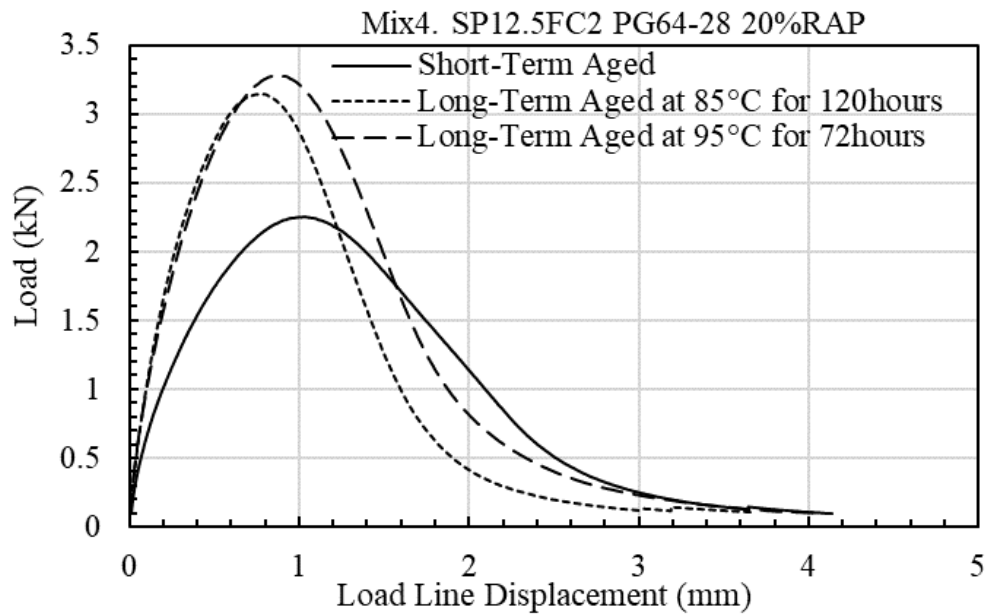
Figure 6.13 Load-Load Line Displacement Curve of Mix4 for Short-Term and Long-Term Aged Conditions.
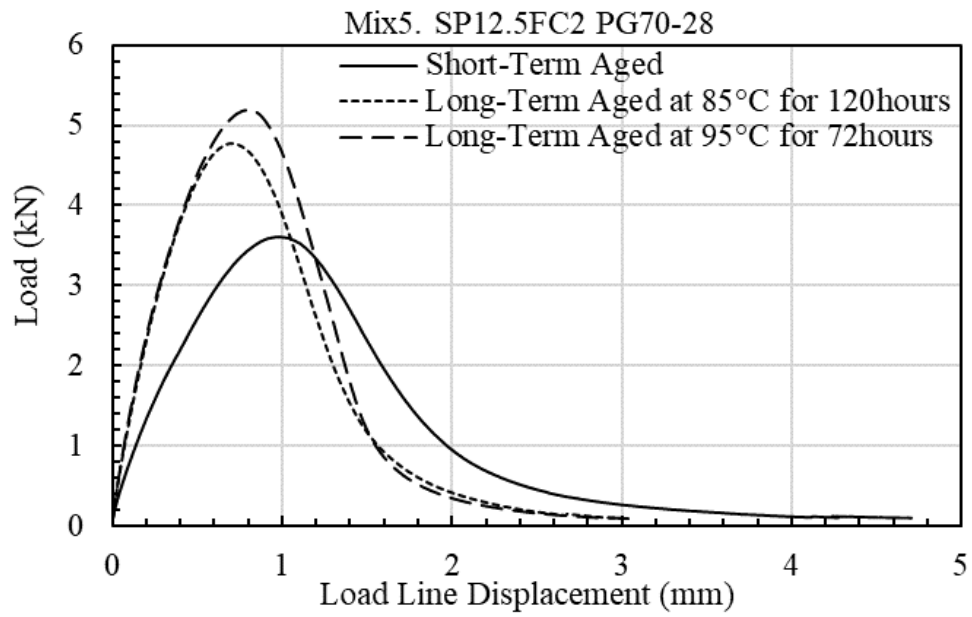
Figure 6.14 Load-Load Line Displacement Curve of Mix5 for Short-Term and Long-Term Aged Conditions.

Table 6.3 Summarized Analysis of Variance (ANOVA) for Long-Term Aging.

General Factorial Regression: Fracture Energy versus Asphalt Mix, Aging Condition					
Source	DF[1]	Adjusted SS[2]	Adjusted MS[3]	P-Value[4]	Statistically Significance
Asphalt Mix	4	5423489	1355872	0.000	Yes
Short/Long-Term Aged	2	331994	165997	0.000	Yes
Asphalt Mix-Aging Interaction	8	191471	23934	0.153	No
General Factorial Regression: Slope versus Asphalt Mix, Aging Condition					
Source	DF	Adjusted SS	Adjusted MS	P-Value	Statistically Significance
Asphalt Mix	4	174.94	43.73	0.000	Yes
Short/Long-Term Aged	2	22.35	11.17	0.000	Yes
Asphalt Mix-Aging Interaction	8	16.94	2.12	0.000	Yes
General Factorial Regression: Flexibility Index versus Asphalt Mix, Aging Condition					
Source	DF	Adjusted SS	Adjusted MS	P-Value	Statistically Significance
Asphalt Mix	4	795.7	198.93	0.000	Yes
Short/Long-Term Aged	2	414.0	207.0	0.000	Yes
Asphalt Mix-Aging Interaction	8	154.1	19.26	0.000	Yes

Table 6.4 Ranking After Long-Term Aging Based on Statistical Tukey's HSD.

Asphalt Mixture	Short-Term Aged	Long-Term Aged (85°C/120h)	Long-Term Aged (95°C/72h)
Mix1. SP12.5 PG52-40	B	A	AB
Mix2. SP12.5FC1 PG58-34	C	B	BC
Mix3. SP12.5FC2 PG64-34 20%RAP	A	A	A
Mix4. SP12.5FC2 PG64-28 20%RAP	D	BC	C
Mix5. SP12.5FC2 PG70-28	D	C	D

6.4 Effect of Intermediate Testing Temperature on I-FIT Results

Figure 6.15, Figure 6.16, and Figure 6.17 show the bar charts of average fracture energy, post-peak slope, and flexibility index, respectively, obtained from I-FIT test conducted by a servo-hydraulic device (DTS-30) at five intermediate testing temperatures, namely 10°C, 16°C,

19°C, 22°C and 25°C. The error bars shown on the bar charts represent one standard deviation from the average. As shown in Figure 6.15 and Figure 6.16, as the testing temperature increases from 10°C to 25°C, there is almost a similar trend whereby the fracture energy and the post-peak slope decrease, respectively. The reduction in fracture energy and post-peak slope can be attributed to the increase in ductility of asphalt mixtures as the testing temperature increases. The plots of load-load line displacement for all asphalt mixtures at conducted testing temperatures shown in Figure 6.18 to Figure 6.22 demonstrate a similar trend whereby as the temperature increases, the peak load and post-peak slope decreases. Moreover, Figure 6.23 to Figure 6.27 show the relationship between testing temperature and flexibility index for each asphalt mixture. Generally, power regression suggests a good relationship between intermediate testing temperature and FI values for all asphalt mixtures. As mentioned earlier (Chapter 4), the continuous intermediate temperature for the recovered asphalt binders were determined by using the continuous high and low temperatures of the recovered asphalt binders. Therefore, using the regression equations shown in Figures 6.28 to 6.32, and recovered continuous intermediate temperature, the flexibility index at the recovered continuous intermediate temperature for each asphalt mixture was determined. The relationship between the average of FI Values of the asphalt mixtures at testing temperatures, namely 10°C, 16°C, 19°C, 22°C, and 25°C with the values of FI of the asphalt mixtures at the continuous intermediate temperatures show that there is a good correlation at higher testing temperatures, especially at 25°C (power fits suggest an R^2=0.968).
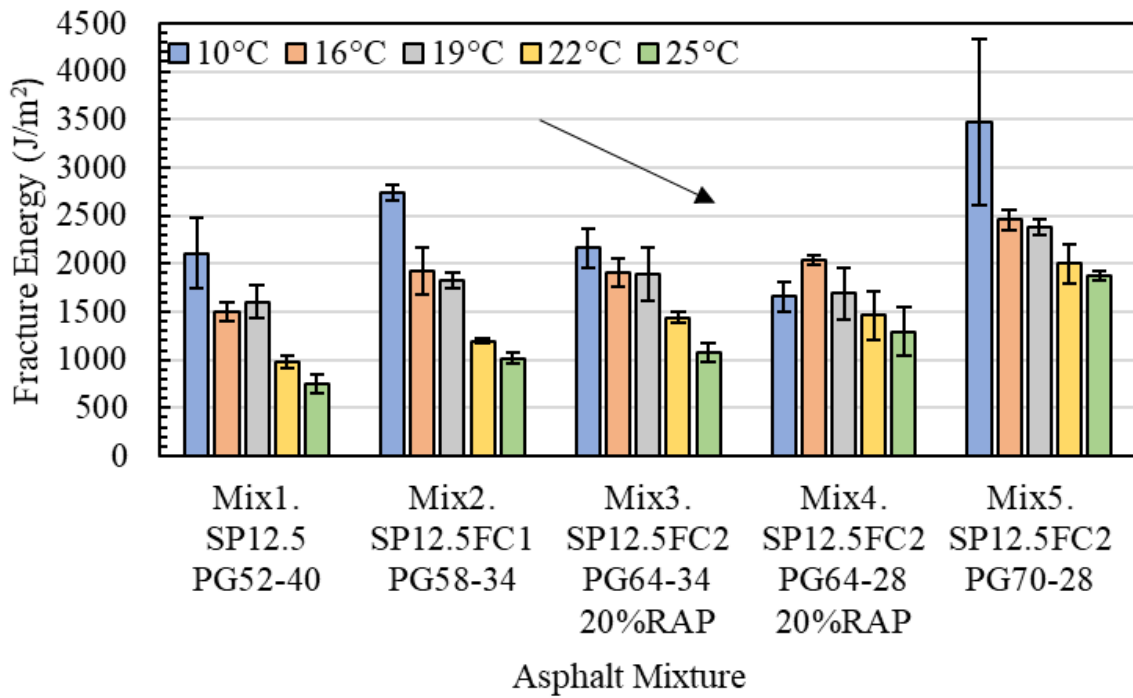
Figure 6.15 Effect of Intermediate Testing Temperature on Fracture Energy.
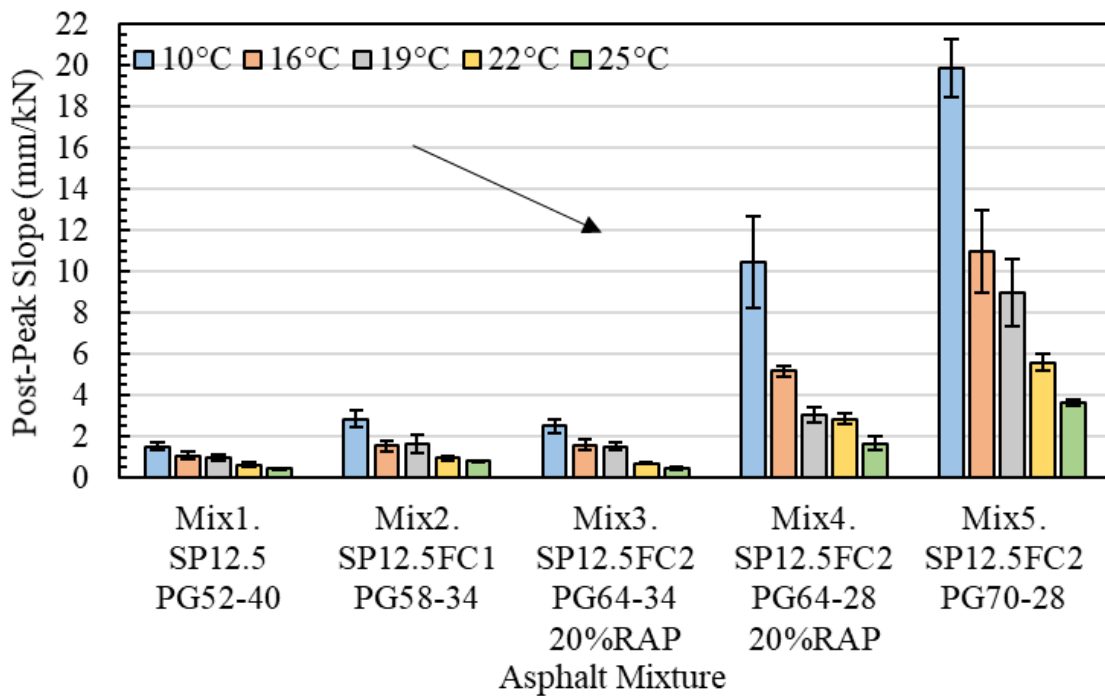
Figure 6.16 Effect of Intermediate Testing Temperature on Post-Peak Slope.
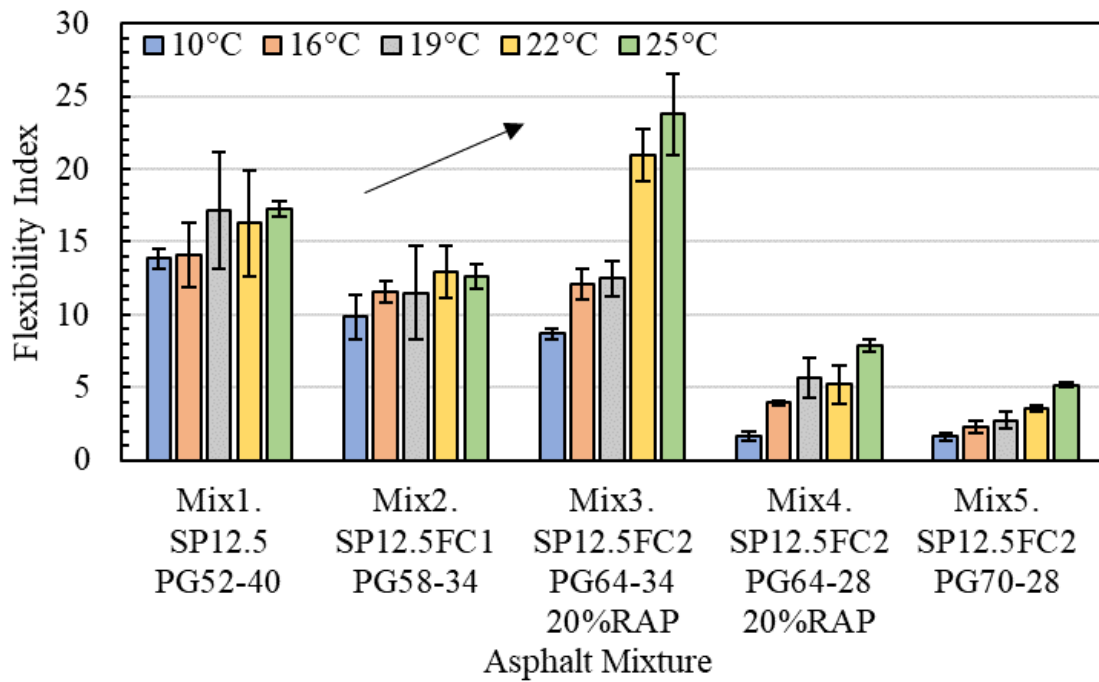
Figure 6.17 Effect of Intermediate Testing Temperature on Flexibility Index.
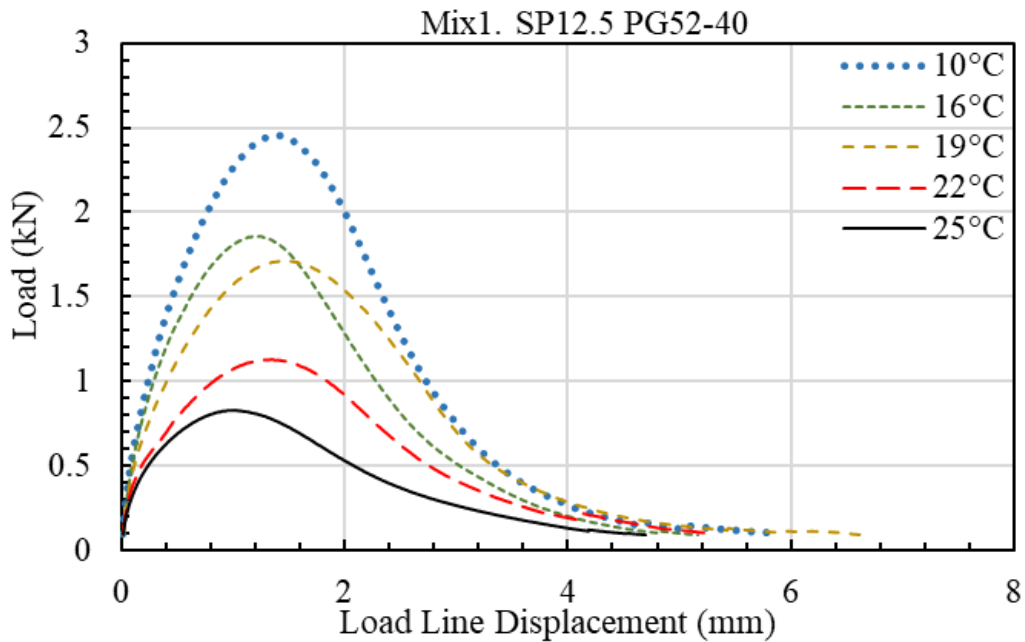
Figure 6.18 Load-Load Line Displacement Curve of Mix1 at Intermediate Testing
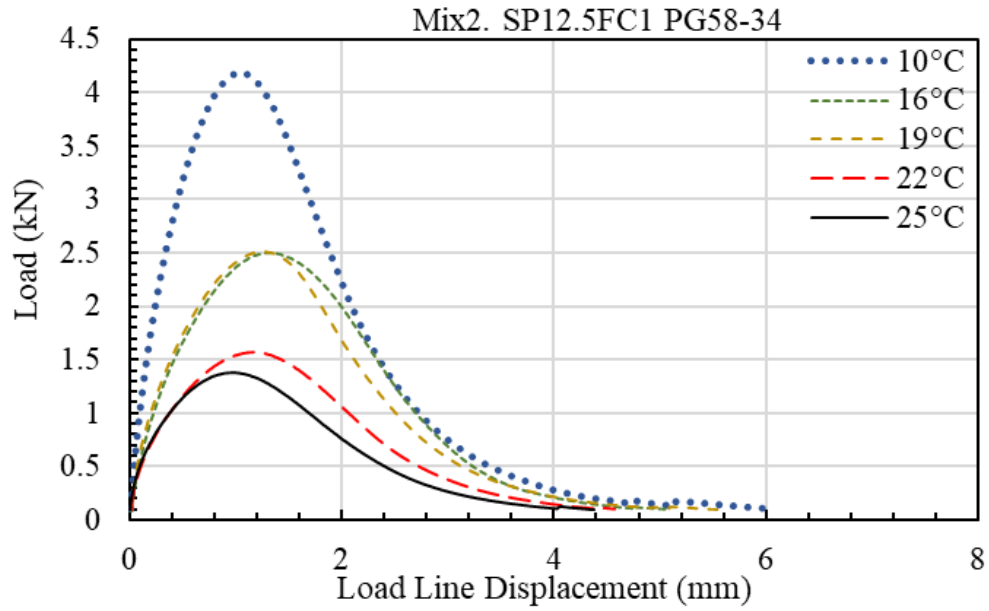
Temperatures.

Figure 6.19 Load-Load Line Displacement Curve of Mix2 at Intermediate Testing
Temperatures.
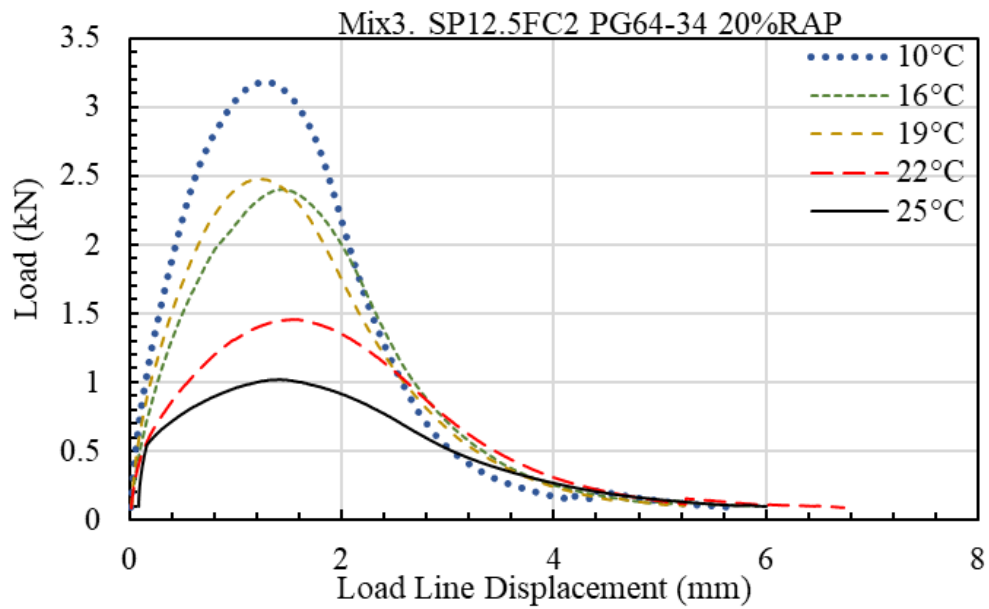
Figure 6.20 Load-Load Line Displacement Curve of Mix3 at Intermediate Testing
Temperatures.

124
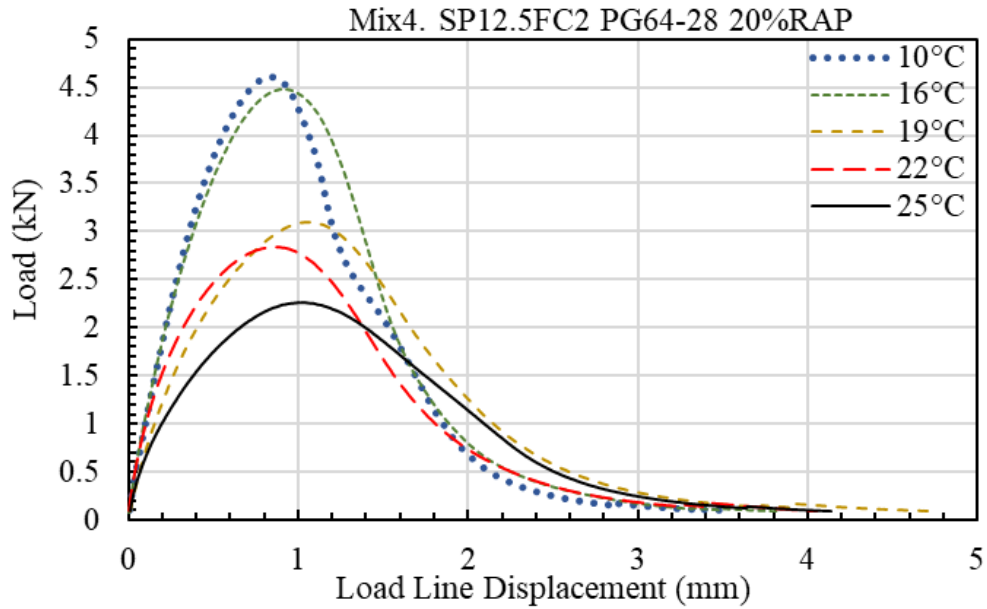
Figure 6.21 Load-Load Line Displacement Curve of Mix4 at Intermediate Testing
Temperatures.
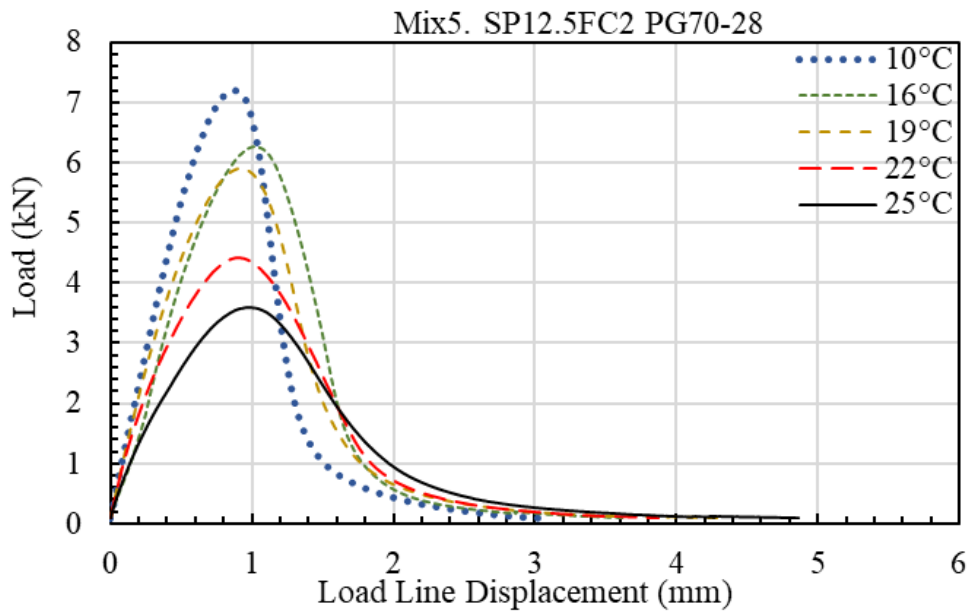
Figure 6.22 Load-Load Line Displacement Curve of Mix5 at Intermediate Testing
Temperatures.
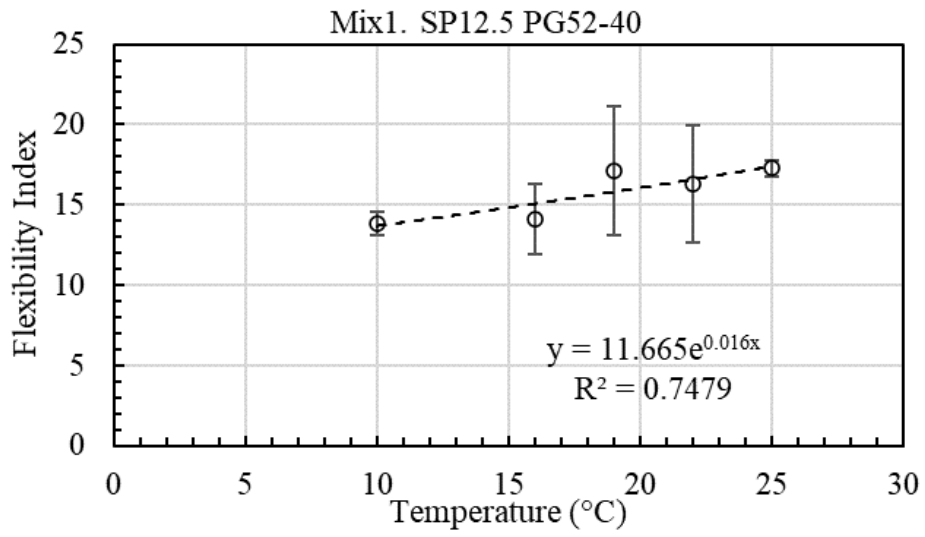
Figure 6.23 Relationship between Intermediate Testing Temperature and FI for Mix1.
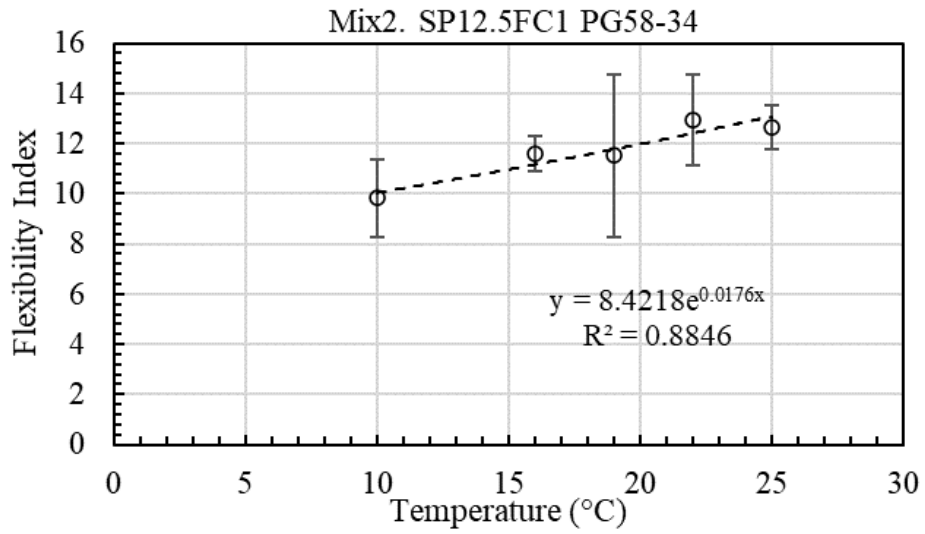
Figure 6.24 Relationship between Intermediate Testing Temperature and FI for Mix2.
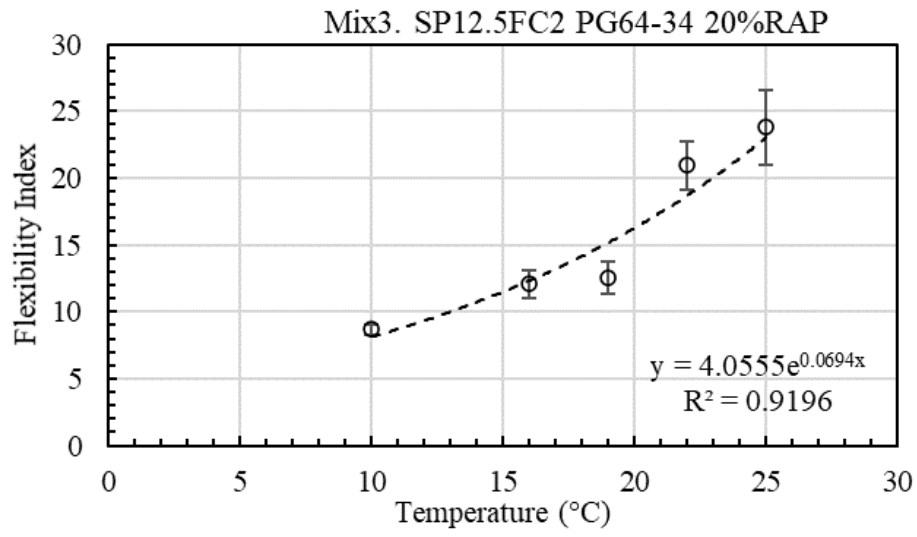
Figure 6.25 Relationship between Intermediate Testing Temperature and FI for Mix3.
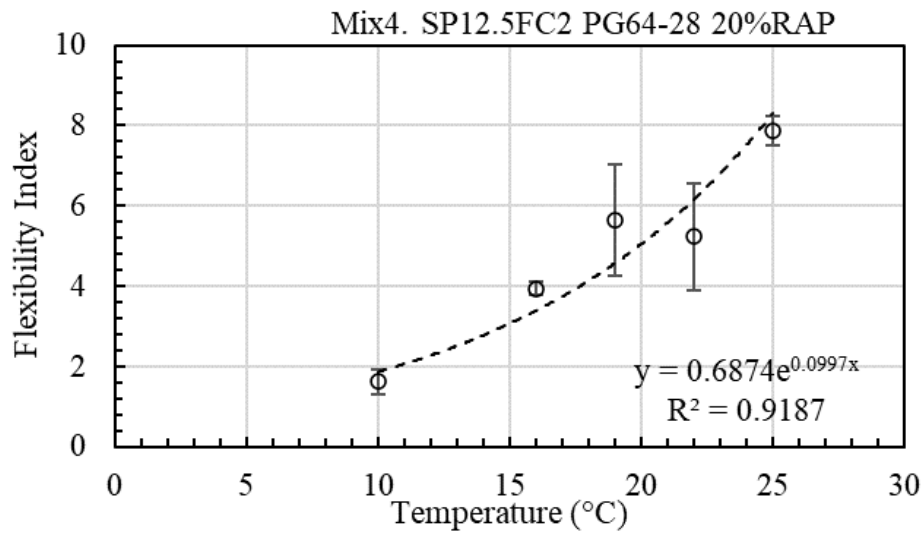
Figure 6.26 Relationship between Intermediate Testing Temperature and FI for Mix4.
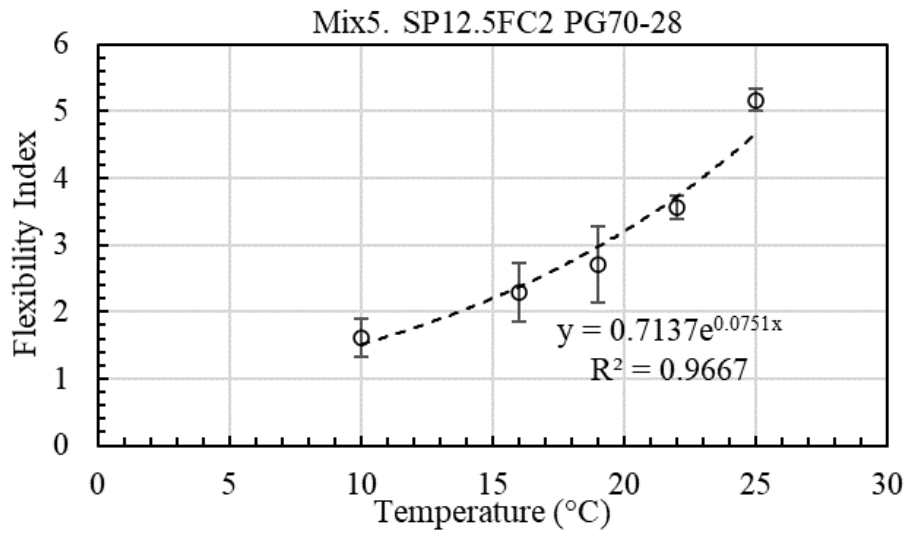
Figure 6.27 Relationship between Intermediate Testing Temperature and FI for Mix5.
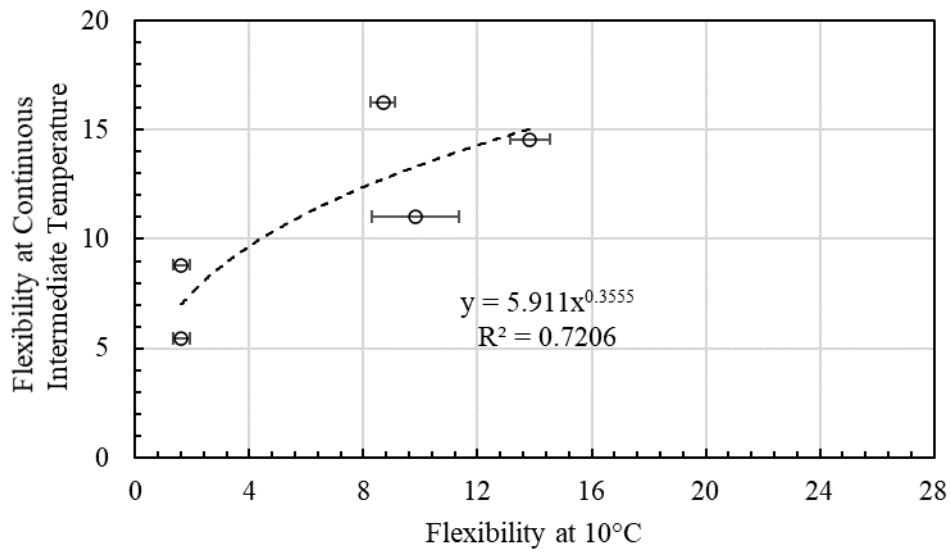
Figure 6.28 Relationship between Flexibility Index at 10°C and Continuous Intermediate
Temperature.

128
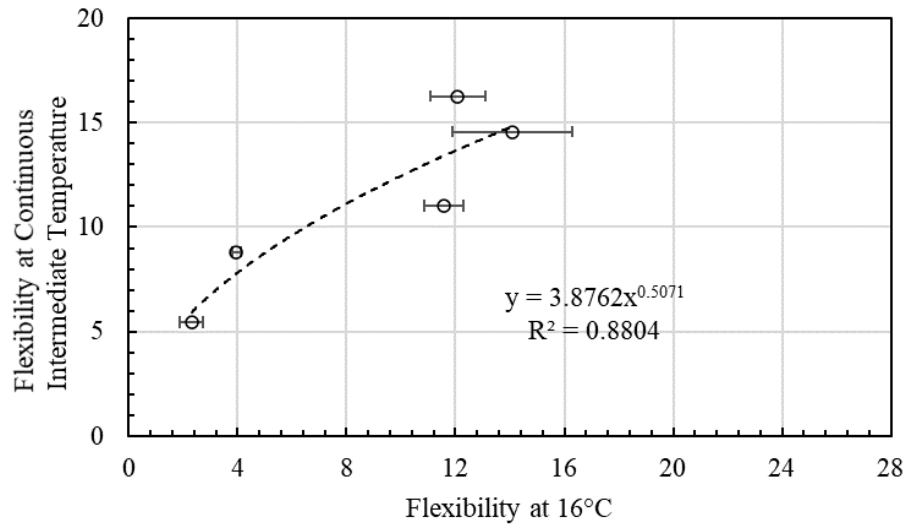
Figure 6.29 Relationship between Flexibility Index at 16°C and Continuous Intermediate Temperature.
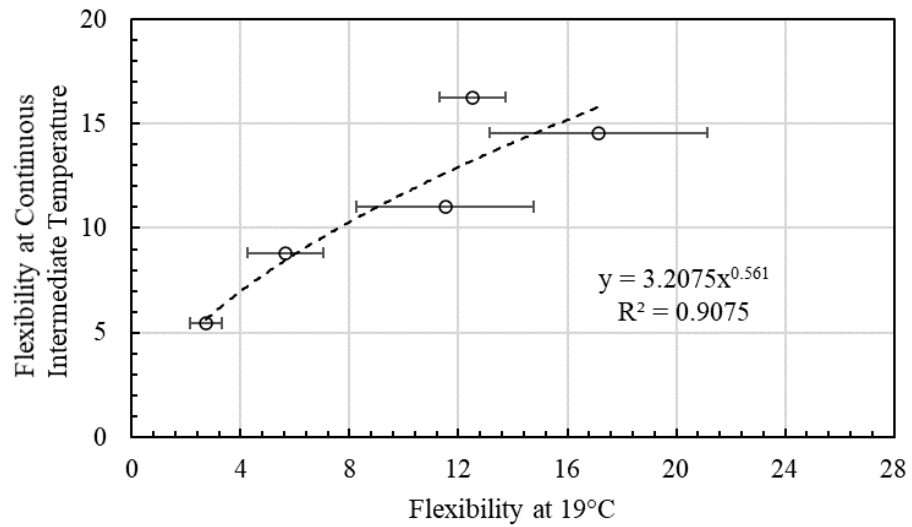
Figure 6.30 Relationship between Flexibility Index at 19°C and Continuous Intermediate Temperature.
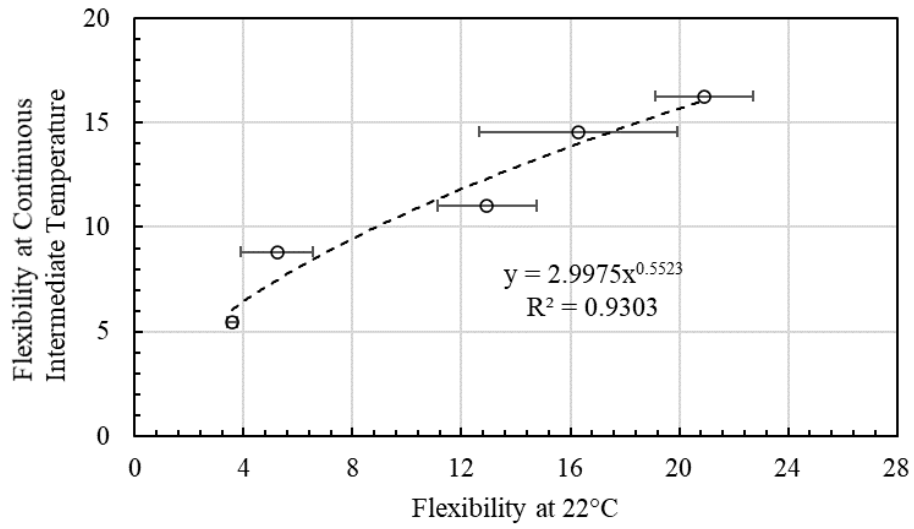
Figure 6.31 Relationship between Flexibility Index at 22°C and Continuous Intermediate Temperature.
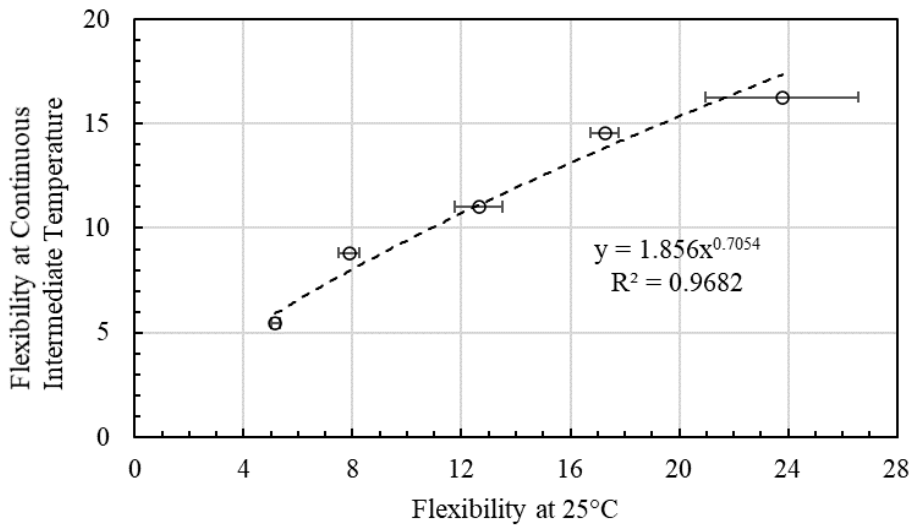
Figure 6.32 Relationship between Flexibility Index at 25°C and Continuous Intermediate Temperature.

6.5 Conclusions

The following conclusions can be drawn based on the experimental results and discussions provided in this chapter:

- Forced-draft oven aging of I-FIT specimens at 95°C for 72 hours produced statistically similar flexibility index values as the specimens aged at 85°C for 120 hours.

- Asphalt mixtures containing hard PG asphalt binder were more sensitive to testing temperature variability compared to asphalt mixtures having softer PG asphalt binder.

- DTS-30 (hydraulic testing device) and Auto_SCB (screw-driven testing device) produced statistically similar values of FI for the asphalt mixtures.

- There was a strong correlation between FI at 25°C and at continuous intermediate temperature for asphalt mixtures studied in this research.

Chapter 7

Investigation of Sixteen Asphalt Mixtures to Recommend Preliminary Specifications for I-FIT, DC(T) and HWT Tests

The research presented in this chapter has been published in a paper submitted to the Canadian Technical Asphalt Association (CTAA) conference in 2020 (Bashir, Salehi-Ashani, Ahmed, Tabib, & Vasiliu, 2020) Sixteen post-production surface course asphalt mixtures including fourteen Hot Mix Asphalt (HMA) and two Stone Mastic Asphalt (SMA), and their corresponding field cores were collected. The asphalt mixtures have been paved between 2017 to 2019 in Ontario and cover various PG asphalt binders and traffic levels. I-FIT, DC(T) and Hamburg Wheel Tracking tests were conducted on the Plant-Produced Laboratory Compacted (PPLC) specimens and their corresponding field cores in order to determine and provide recommendations for preliminary threshold values for the aforementioned performance tests that can lead to Quality Assurance (QA) acceptance criteria for post-production mix performance tests and new specifications validated through pavement performance.

7.1 Results of Recovered Asphalt Cement

The test results for asphalt binder content and recovered asphalt binder continuous performance grade for plant produced surface course asphalt mixtures studies are summarized in Table 7.1.

Table 7.1 Test Results of Recovered Asphalt Binder.

Mix No.	Asphalt Mixture	Asphalt Binder Content (%)	Continuous PG Grade (°C)	
			High	Low
Mix 1	SMA12.5 PG70-28	5.75	72.3	-33.1
Mix 2	SMA12.5 PG70-28	6.01	73.9	-34.0
Mix 3	SP12.5 FC2 PG70-28	5.26	78.5	-29.4
Mix 4	SP12.5 FC2 PG70-28 20% RAP	5.20	85.2	28.5
Mix 5	SP12.5 FC2 PG70-28 20% RAP	5.06	76.1	-30.1
Mix 6	SP12.5 FC2 PG64-28 20% RAP	5.07	73.0	-28.9
Mix 7	SP12.5 FC2 PG64-34 20% RAP	5.20	67.7	-36.9
Mix 8	SP12.5 FC2 PG64-34	5.23	81.0	39.3
Mix 9	SP12.5 FC2 PG58-28	5.17	57.7	-34.0
Mix 10	SP12.5 FC2 PG58-28	5.18	56.1	-33.1
Mix 11	SP12.5 FC1 PG58-34	5.17	61.6	-40.0
Mix 12	SP12.5 FC1 PG58-34	5.12	64.8	-37.1
Mix 13	SP12.5 PG58-34	5.00	64.2	-40.2
Mix 14	SP12.5 PG52-40	4.45	55.0	-44.2
Mix 15	SP12.5 PG52-40	4.70	56.3	-41.5
Mix 16	SP12.5 PG52-40	4.86	61.0	-43.4

7.2 Results of Recovered Asphalt Cement

I-FIT testing was conducted according to AASHTO TP124 test method at 25^0C on four replicates both for plant produced laboratory compacted (PPLC) specimens and pavement field cores for each test. The test result that was farther from the average was eliminated in order to reduce the testing variability.

Figure 7.1 to Figure 7.3 illustrate the average fracture energy, slope, and Flexibility Index (FI) of PPLC specimens and their corresponding pavement field cores corrected by

thickness, respectively, for each mix. The error bars show the standard deviation of the results. Furthermore, other I-FIT test data, including air void range of PPLC specimens and field cores, thickness range of field cores and coefficient of variance (C.V) of FI for both PPLC specimens and their corresponding pavement field cores for each mix are summarized in Table 7.2. It should be noted that pavement field core results have not been shown for Mix16 in Figure 7.1 to Figure 7.3 since field cores were not collected.
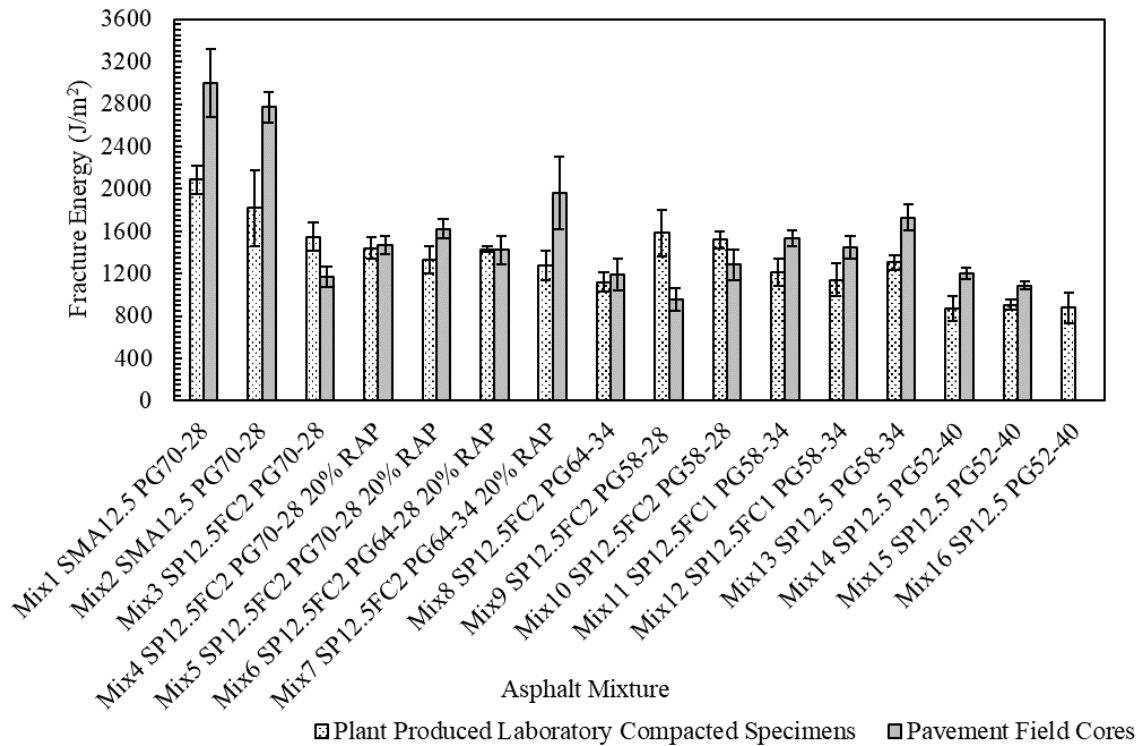
Figure 7.1 Fracture Energy of I-FIT Results.

134
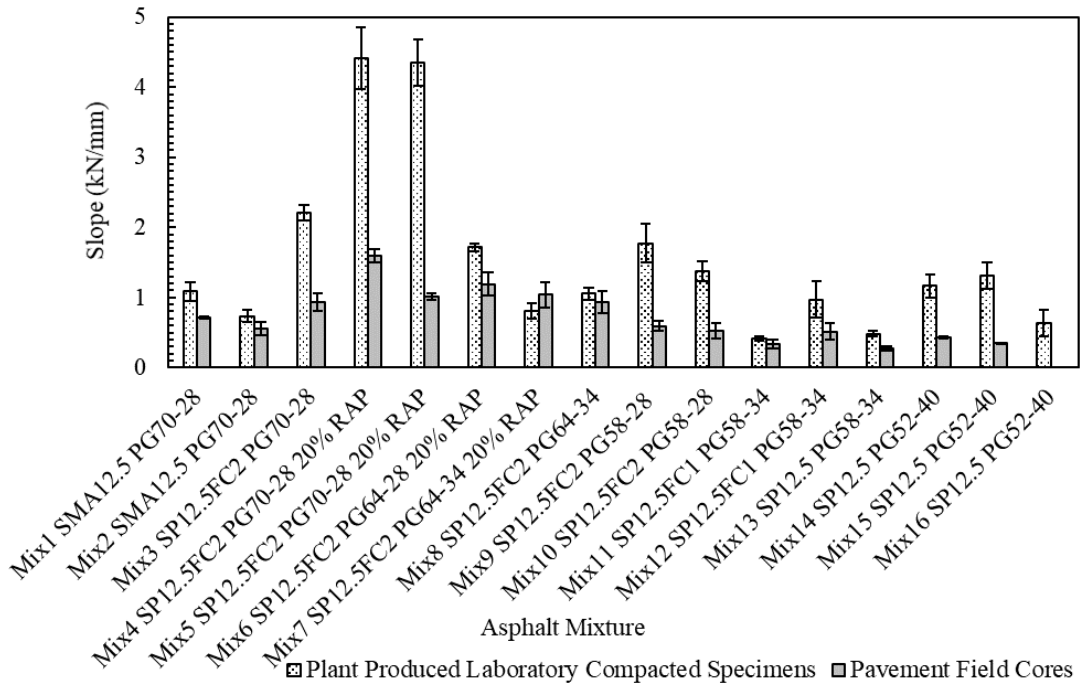
Figure 7.2 Post-Peak Slope of I-FIT Results.
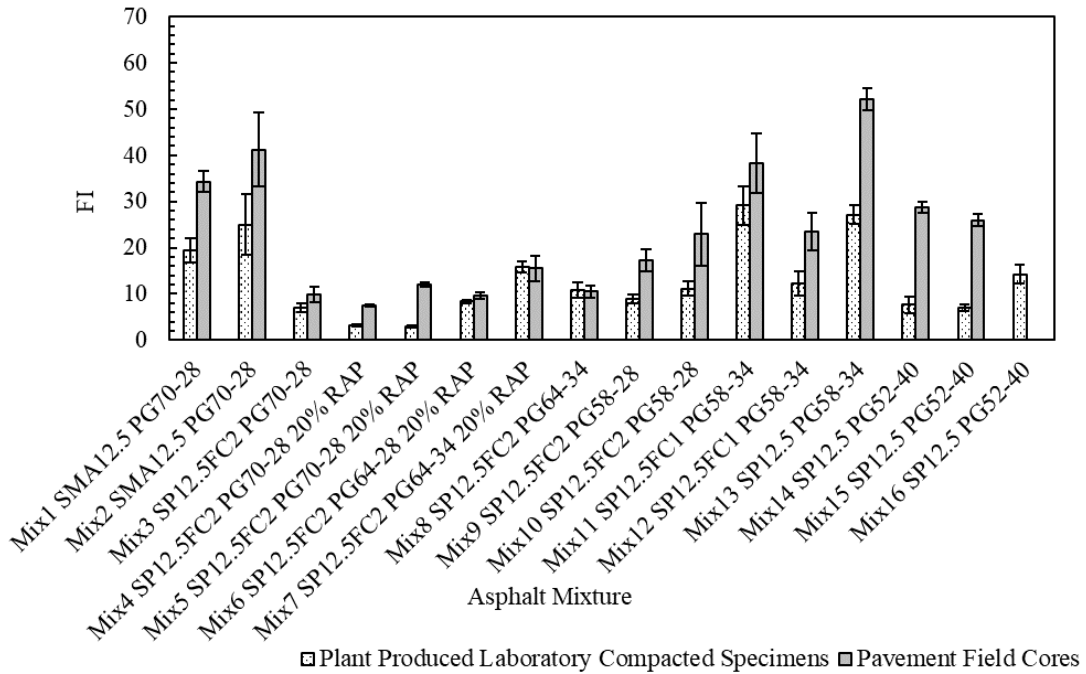
Figure 7.3 Flexibility Index (FI) of I-FIT Results.

135

Table 7.2 I-FIT Test Data.

Asphalt Mixture	PPLC Specimens				Pavement Field Core Specimens				
	Air Void Range %	FI	FI SD[1]	FI CV[2] %	Thickness Range (mm)	Air Void Range %	FI[3]	FI[3] SD	FI[3] CV %
Mix1	7.4-7.5	19.4	2.6	13.6	39.7-41.4	2.9-3.4	34.3	2.3	6.8
Mix2	6.7-7.1	25.0	6.5	25.8	40.4-41.0	4.9-5.6	41.2	8.0	19.3
Mix3	7.0-7.3	7.0	1.0	13.6	36.6-38.9	7.0-7.8	9.9	1.7	16.8
Mix4	6.7-7.0	3.3	0.2	6.9	40.6-40.9	6.9-7.5	7.4	0.3	3.9
Mix5	6.7-7.1	3.1	0.2	7.7	35.5-39.5	5.0-6.1	12.1	0.5	4.3
Mix6	8.3	8.4	0.4	4.7	40.1-40.4	5.8-6.4	9.6	0.6	6.4
Mix7	7.1-8.1	15.8	1.1	7.1	40.6-40.7	0.6-0.8	15.6	2.8	17.7
Mix8	6.3-8.4	10.7	1.7	15.5	40.7-41.0	4.8-6.2	10.5	1.4	13.4
Mix9	7.1-7.5	9.0	0.9	10.6	53.0-53.7	6.7-7.0	17.3	2.3	13.5
Mix10	7.3-7.6	11.2	1.5	13.4	44.1-45.9	3.5-4.2	22.9	6.7	29.3
Mix11	7.2-7.7	29.2	4.2	14.3	40.7-40.8	4.2-5.6	38.3	6.4	16.6
Mix12	7.6-8.6	12.2	2.6	21.7	40.4-40.7	5.9-7.1	23.5	4.0	16.9
Mix13	7.3-7.6	27.1	2.0	7.3	40.2-40.8	6.0-6.6	52.2	2.4	4.5
Mix14	6.7-6.9	7.6	1.9	24.3	50.8-51.2	5.1-5.8	28.8	1.2	4.3
Mix15	6.5-6.6	7.0	0.8	11.7	40.8-41.2	4.4-5.0	26.0	1.2	4.8
Mix16	7.5-7.6	14.2	2.0	14.2	-	-	-	-	-

The following observations can be made regarding I-FIT test results from Figure 7.1 to Figure 7.3 and Table 7.2:

- Figure 7.1 depicts that in general, the average fracture energy values of field core specimens are larger than their corresponding PPLC specimens. However, some

136

mixes such as Mix3, Mix9 and Mix10; PPLC specimens have greater values of fracture energy than those of field core specimens.

- Figure 7.2 demonstrates that mixes containing RAP such as Mix4 and Mix5, have greater values of slope than other mixes. The slope of the post peak portion of the curve is sensitive to changes to material properties. Generally, a high slope value will indicate a faster crack propagation and signify a more brittle mix, therefore, more susceptible to cracking. Figure 7.2 illustrates that the value of average slope of PPLC specimens is greater than that of field cores except for Mix7 in which field cores have higher value of average slope than that of PPLC specimens.

- Figure 7.3 indicates that in general, field cores have greater values of FI than those of PPLC specimens. However, the values of average FI in Mix6, Mix7 and Mix8 for PPLC specimens and field cores are comparable. As listed in Table 7.2, the air void values, and thickness of field core specimens are different from those of PPLC specimens. As a result, the discrepancy in the results of average FI between PPLC and field core specimens could be attributed to the thickness and air void differences between PPLC and field core specimens. In addition, there could be additional factors causing the discrepancy; reheating process to compact PPLC specimens and differences between modes of compaction for the two sample types, i.e., gyratory, and in-situ field compaction for the laboratory compacted PPLC and field core specimens, respectively.

It is evident from the figures above that fracture energy alone cannot indicate the cracking resistance of mixes at intermediate temperature. For example, Mix4 and Mix6 have comparable values of fracture energy, however, Mix6 has lower value of slope than that of Mix4 indicating Mix6 is more flexible than Mix4. Therefore, Mix6 has greater value of FI than that of Mix4.

As shown in Table 7.2, the C.V of the FI values for PPLC specimens has the range of 4.7-25.8% with the average of 13.2% while the C.V of field cores has the range of 3.9-29.3% with the average of 11.9%. Therefore, the variability of FI results from PPLC specimens and field cores are relatively comparable. Overall, the C.V of FI values of all PPLC specimens are

less than 20% except for three mixes, including Mix2, Mix12 and Mix14 (25.8, 21.7 and 24.3, respectively) while the C.V of the FI values of all field cores are less than 20% except for Mix10 (29.3%).

A t-test was performed for the purpose of statistical analysis to compare the results of average FI of PPLC and field core specimens. The t-test results showed that there is a statistically significant difference between the average FI of PPLC specimens and field core specimens for asphalt mixtures except for Mix3, Mix6, Mix7, Mix8 and Mix11. Furthermore, the t-test between the two sets of the FI results, including the FI obtained from PPLC specimens in one set and the FI obtained from field core specimens in the other set, results in the p-value of 0.003 indicating that, overall, there is a statistically significant discrepancy between the FI values of PPLC specimens and those of field cores.

Given various contributing factors such as thickness, air voids, mode of compaction (field vs laboratory) on the FI values in this study, only the results of FI from PPLC specimens were analyzed in order to determine preliminary thresholds for Quality Acceptance (QA) criteria according to PG asphalt binder/asphalt mix type and traffic category. As a result, sixteen surface asphalt mixtures studied in this study were categorized into seven and four individual groups according to PG asphalt binder/mix type and traffic category, respectively. Figure 7.4 and Figure 7.5 show the FI results with error bars representative of the standard deviations vs. PG asphalt binder/asphalt mix type and traffic category, respectively.

The following observations can be made from these figures:

- SMA mixes (Mix1 and Mix2) show higher values of FI due to having a noticeably high amount of asphalt binder content (5.75 and 6.01%, respectively), unique aggregate gradation producing stone on stone contact as well as a ductile mastic phase.

- I-FIT test can discriminate asphalt mixtures containing RAP from mixtures that do not have RAP in them as well as differentiate asphalt mixtures with softer or harder PG grades. For example, Mix4 and Mix5 (with PG70-28) which contain 20% RAP have the lowest values of FI among the mixes, FI values of 3.3 and 3.1 respectively. On the other hand, Mix6 (PG64-28) and Mix7 (with PG64-34) containing 20%

138

RAP have higher values of FI (8.4 and 15.8) and are more resistant to intermediate temperature cracking than Mix4 and Mix5 which contain the same amount of RAP.

- Figure 7.5 clearly shows that regardless of designed traffic category, using soft PG asphalt binder and higher amount of asphalt binder can increase intermediate temperature cracking resistance of asphalt mixtures. For instance, Mix11 and Mix13 which are SP12.5 with PG58-34 and were designed for traffic category D and C, respectively, have considerably higher FI value than rest of the asphalt mixtures which were designed for traffic category E.
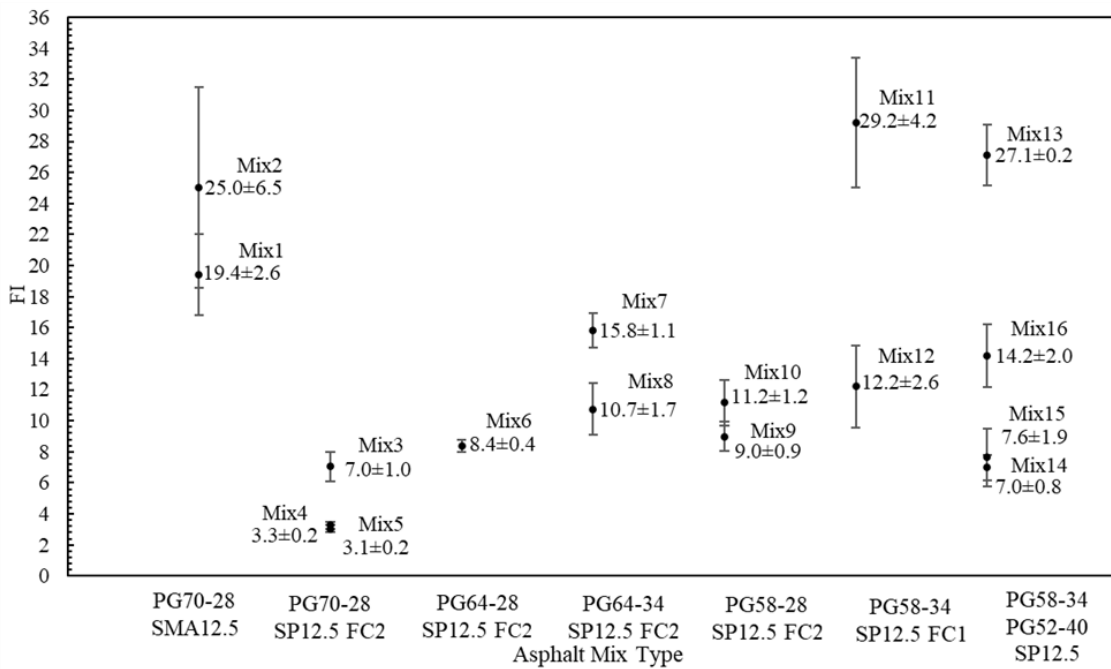
Figure 7.4 FI of PPLC Specimens vs. Asphalt Mix Type.
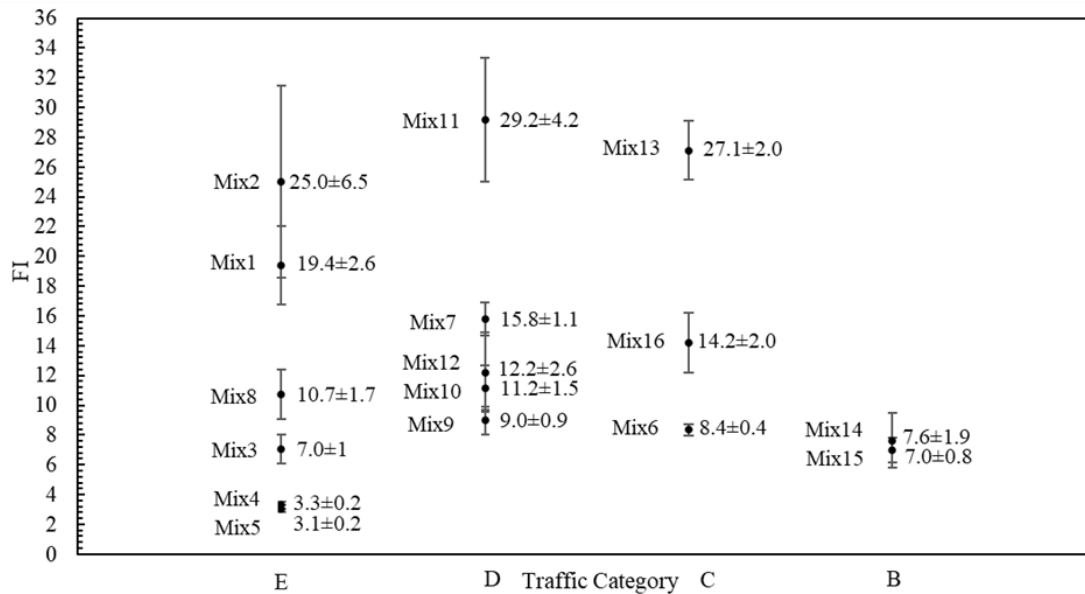
Figure 7.5 FI of PPLC Specimens vs. Traffic Category.

Based on current test data, to set forth a minimum FI as a pass/fail criterion for the post-production asphalt mixtures evaluated in this study, the field performance of asphalt pavements needs to be monitored. Also, more post-production asphalt mixture samples will need to be collected and tested to assist in developing the acceptance criteria using unaged and aged samples for different asphalt mixtures. As Figures 14 and 15 suggest, based on available data, a minimum FI value of 10 can be used as a preliminary threshold for all PG asphalt binder/mix type, and traffic categories, except for SMA mixes for which a minimum threshold FI value of 15 is recommended as noted in Table 7.3 below.

Table 7.3 Recommended Preliminary Threshold Flexibility Index (FI) Criteria for Post-Production Mixes.

Mix Type	Test Temperature (°C)	Preliminary Minimum Average Flexibility Index (FI) Threshold
All Surface Course Mixes	25	10.0
SMA Surface Course Mixes	25	15.0

7.3 (DC(T)) Test Results

DC(T) test was carried out according to ASTM D7313 at 10 °C higher than the low temperature grade of the PGAC used in the mix on minimum of three replicates of PPLC specimens and pavement field core specimens. Since most of field cores did not have the thickness of 50 ± 1 mm specified in the testing standard, their value of fracture energy was corrected for thickness using the formula provided in the methodology section of this thesis. Figure 16 illustrates the DC(T) average fracture energy values of PPLC specimens and their corresponding pavement field core specimens for each mix coupled with the results of recovered asphalt binder continuous low temperature grade. The error bars show one standard deviation from the average of the DC(T) fracture energy values. It should be noted that pavement field core results have not shown for Mix10 and Mix16 in Figure 7.6 since there were not enough field cores to be tested for Mix 10 and no field cores were collected for Mix16. Furthermore, other DC(T) test data, including testing temperature, air void range of specimens, thickness range of field core specimens, average fracture energy and the coefficient of variation (CV) of the DCT fracture energy are summarized in Table 7.4. The following observations can be made regarding DC(T) test results from Figure 7.6 and Table 7.4:

- Figure 7.6 illustrates that, generally, the average fracture energy values of field core specimens are larger than their corresponding PPLC specimens. However, in a few mixes, e.g., Mix3, Mix6, Mix9, Mix11 and Mix13 PPLC specimens have greater values of the average fracture energy than those of field core specimens. As listed

in Table 7.4, the air void values, and thickness of field core specimens are different from those of PPLC specimens. As a result, the discrepancy in the results of average fracture energy between PPLC and field core specimens could be attributed to the differences between thickness and air void of PPLC and field core specimens. In addition, there could be additional factors causing the discrepancy; reheating process to compact PPLC specimens and differences between modes of compaction for the two sample types, i.e., gyratory and in-situ field compaction used for the laboratory compacted PPLC and field core specimens, respectively.

- Figure 7.6 shows a nearly dominant trend between DC(T) fracture energy and recovered asphalt binder low temperature grade for PPLC and field core specimens such that among the asphalt mixtures containing the same PG grade, the lower the recovered asphalt binder low temperature grade, the higher the value of fracture energy.

- As shown in Table 7.4, the CV of the fracture energy values for PPLC specimens has a range of 2.4-23.9% with an average of 11.1% while the CV of field core specimens has a range of 6.2-29.9% with an average of 14.9%. Therefore, fracture energy results from PPLC specimens are less variable than those of field cores. Overall, the CV of the fracture energy values of all mixes in both PPLC specimens and field cores are less than 20% except in Mix7 and Mix16 with the CV of 23.9 and 23.7, respectively, in PPLC test data, and Mix12 with the CV of 29.9% for the field cores test data.
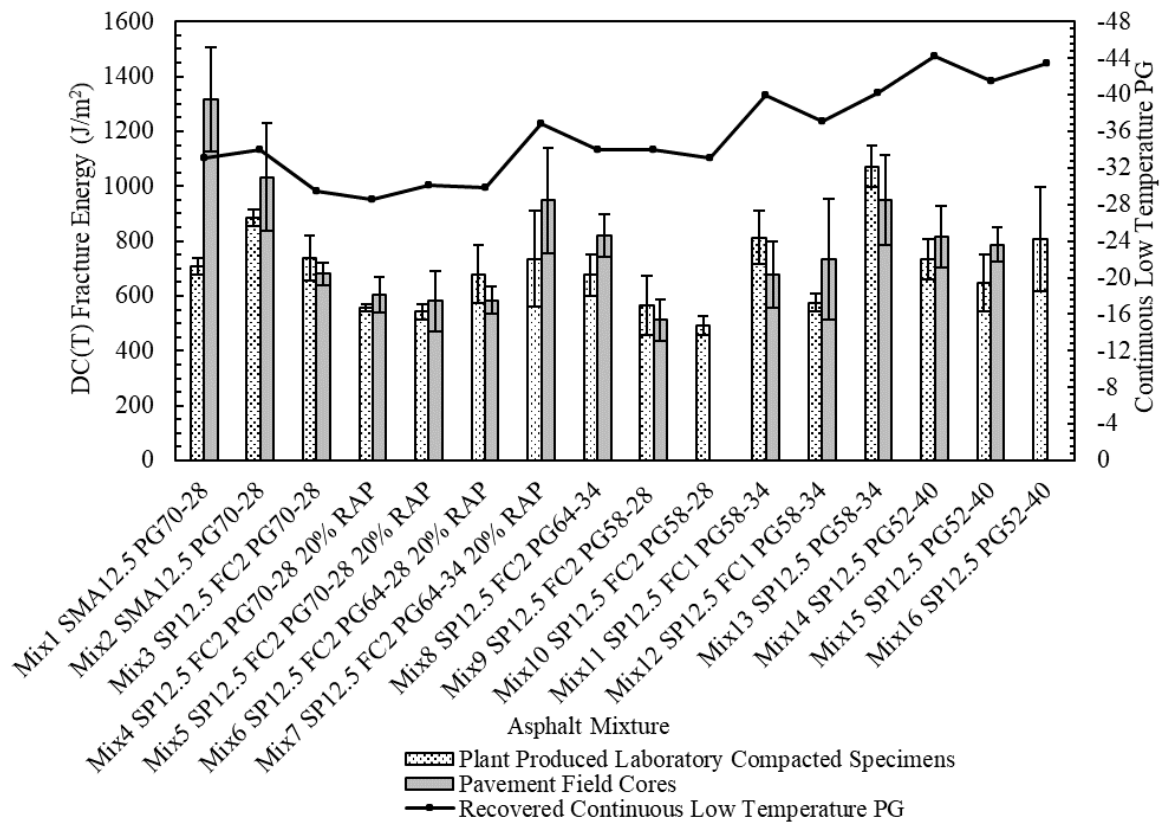
Figure 7.6 DC(T) Fracture Energy and Continuous Low Temperature Grade.

Table 7.4 DC(T) Test Data.

Asphalt Mix	DC(T) Testing Temperature (^{0}C)	PPLC Specimens				Pavement Field Core Specimens				
		Air Void Range %	FE[1]	FE SD[2]	FE CV[3] %	Air Void Range %	Thickness Range (mm)	FE[4]	FE[4] SD	FE[4] CV %
Mix1	-18	7.2-7.5	706	31	4.3	3.5-3.6	42-45.2	1317	188	14.3
Mix2	-18	6.7-6.9	886	30	3.4	5.5-7.6	40.8-49.2	1033	195	18.9
Mix3	-18	6.9-7.3	738	82	11.1	6.7-7.3	40.3-40.7	680	42	6.2
Mix4	-18	6.7-7.0	558	13	2.4	7.6-7.7	50.8-53.3	604	63	10.4
Mix5	-18	6.7-6.8	543	28	5.2	5.3-5.9	43.6-43.9	581	111	19.1
Mix6	-18	7.8-8	678	106	15.6	5.5-7.1	40.0-40.2	585	50	8.5
Mix7	-24	6.5-7.9	735	176	23.9	1.3-1.8	40.4-40.5	949	191	20.2
Mix8	-24	6.2-6.8	676	75	11.0	4.3-5.0	49.1-50.7	821	78	9.5
Mix9	-18	7.3-7.8	566	109	19.3	6.0-6.3	50.7-52.2	512	74	14.4
Mix10	-18	6.9-7.8	490	34	7.0	-	-	-		-
Mix11	-24	7-7.3	813	98	12.0	5.9-6.3	45.7-49.6	678	120	17.6
Mix12	-24	7.5-7.8	576	31	5.4	6.8-7.5	40.1-40.3	733	219	29.9
Mix13	-24	6.7-6.9	1072	77	7.2	6.5-6.9	50.5-50.9	955	168	17.3
Mix14	-30	6.4-6.9	734	72	9.9	5.2-5.8	49.3-50.7	815	113	13.9
Mix15	-30	6.4-6.8	647	102	15.8	4.2-4.7	50.6-51.2	787	64	8.1
Mix16	-30	6.7-7.5	806	191	23.7	-	-	-	-	-

A t-test was performed for the purpose of statistical analysis to compare the results of average fracture energy of PPLC and field core specimens by assuming the null hypothesis of no difference between the average fracture energy of PPLC and field core specimens. The p-value result (greater than 0.05) indicates that the null hypothesis cannot be rejected, i.e., the average fracture energy obtained from PPLC and field core specimens are statistically equal. Only Mix1 that is a Stone Mastic Asphalt (SMA) failed the t-test, i.e., the null hypothesis is rejected and there is a significant difference between the average of fracture energy value of PPLC specimens and that of field cores (p-value=0.03). The difference between the average fracture energy of PPLC and pavement field core specimens for Mix1 could be due to the large differences between the air void range of PPLC specimens (7.2-7.5%) and field cores (3.5-3.6%). It should be noted that the p-value of 0.25 was obtained for Mix7 even though there is

a conspicuous difference between the air void range of PPLC specimens (6.5-7.9%) and field core specimens (1.3-1.8%). Furthermore, the t-test between the two sets of the fracture energy results, including the fracture energy obtained from PPLC specimens in one set and the fracture energy obtained from field cores in the other set, resulted in the p-value of 0.08 indicating that, overall, there is not a statistically significant discrepancy between the fracture energy values of PPLC specimens and those of field cores in this research.

Given the effect of various contributing factors such as thickness, air voids, mode of compaction (field vs laboratory) on the DC(T) fracture energy values, only the results of DC(T) fracture energy from PPLC specimens were further analyzed in this study. Also, for mix design process, the mode of compaction is similar to PPLC specimens and both follow a more controlled process, therefore preliminary thresholds developed based on post-production samples for quality acceptance (QA) acceptance criteria (based on PG grade, mix type and traffic category) will probably correlate more compared to field cores. As a result, sixteen surface asphalt mixtures studied in this research were categorized in seven and four individual groups according to PG grade/mix type and mix designed traffic category, respectively. Figure 7.7 and Figure 7.8 depict the fracture energy results with error bars representative of the standard deviations vs. asphalt mix type and traffic category, respectively. The following observations can be made from Figure 7.7 and Figure 7.8.

- Figure 7.7 illustrates that SMA mixes (Mix1 and Mix2) manifest higher values of fracture energy due to having a noticeably high amount of AC content (5.75 and 6.01%, respectively), unique aggregate gradation producing stone on stone contact as well as a ductile mastic phase.

- Figure 7.7 shows that DCT test can discriminate mixes containing RAP from mixes without RAP as well as differentiate mixes with softer or harder PGAC grade. For instance, Mixes4 and 5 containing 20% RAP (with PG70-28 and tested at -18^0C) have generally lower values of fracture energy (558 and 543J/m^2, respectively). On the other hand, Mix6 which contains the same amount of RAP (with PG64-28 and tested at -18^0C) has higher value of fracture energy (678 J/m^2) than that of Mix 4 and Mix5. Furthermore, Mix7 containing 20% RAP (with PG64-34 and tested at -

24^0C) with a fracture energy of 735 J/m^2 is more resistant to low temperature cracking than Mix4 and Mix5. These observations suggest that responsible use of RAP could produce durable asphalt mixtures.

- As depicted from Figure 7.7, the Mix9 and 10 have low DC(T) fracture energy due to the use of non-modified straight run PG 58-28 for traffic category E.

- As shown in Figure 7.7, Mix7 and Mix8 are SP12.5 FC2 64-34 between which Mix8 has greater fracture energy than Mix 7 due to higher AC content (5.23% of AC in Mix8 compared to 5.07% AC in Mix6) and not containing RAP.

- Figure 7.8 clearly shows that regardless of designed traffic category, using soft AC and high amount of AC can increase low temperature cracking resistance of asphalt mixes. For instance, Mix13 which is SP12.5 PG58-34 and was designed for traffic category C has considerably higher fracture energy value than that of SMA mixes, i.e., Mix1 and Mix2 which were designed for traffic category E, even though Mix13 was tested at -24^0C.
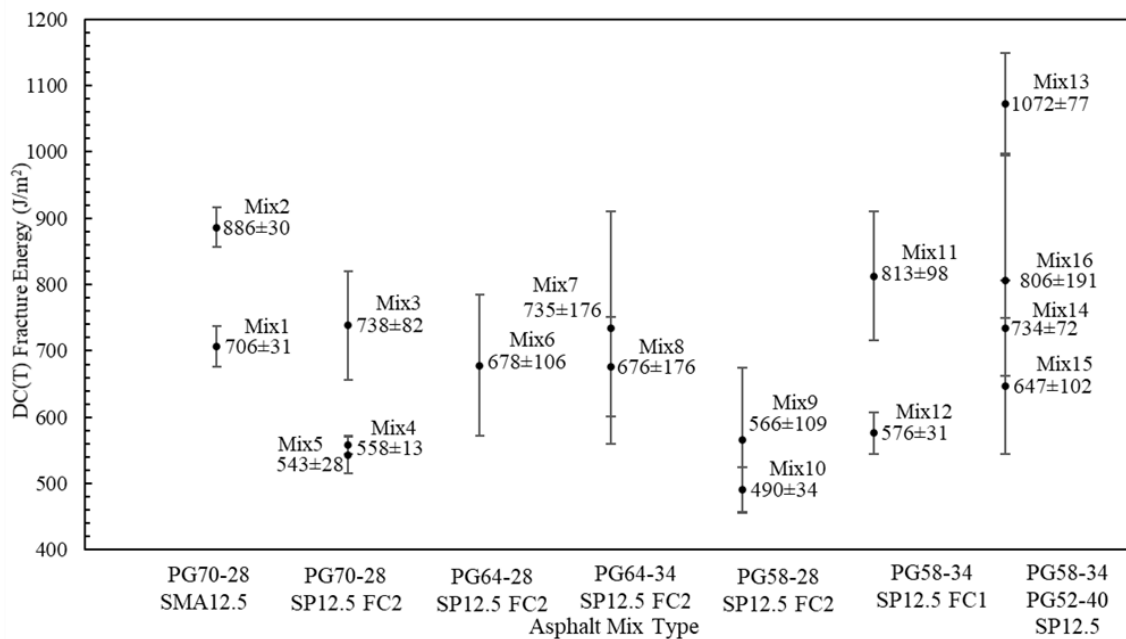
Figure 7.7 DCT Fracture Energy of PPLC Specimens vs. Asphalt Mix Type.
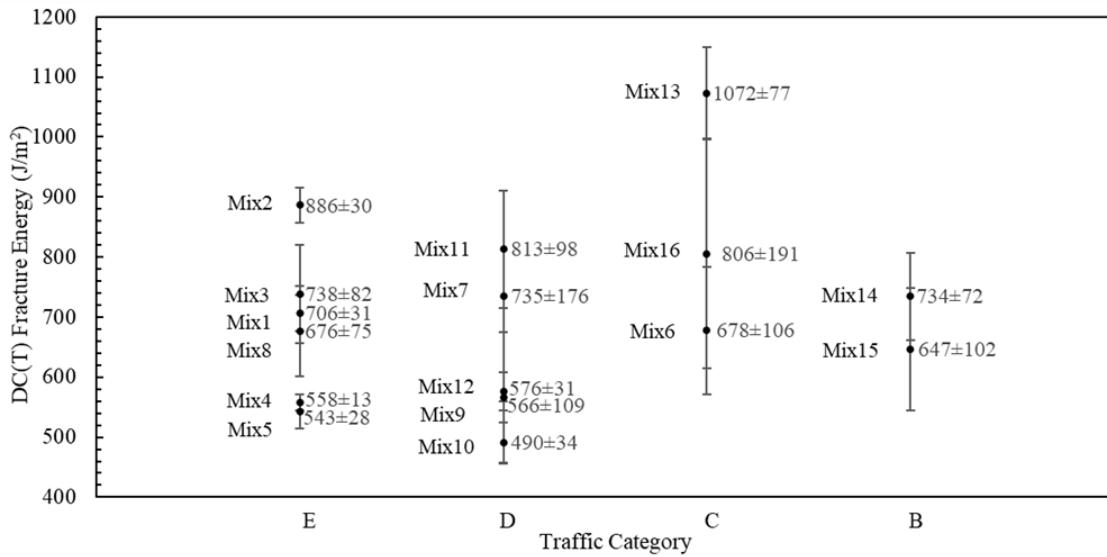
Figure 7.8 DCT Fracture Energy of PPLC Specimens vs. Traffic Category.

Based on current test data, to set forth a minimum DC(T) fracture energy as a pass/fail criterion for the post-production asphalt mixes evaluated in this study, the field performance of asphalt pavements needs to be monitored. Also, more post-production asphalt mixture samples will need to be collected and tested to assist in developing the acceptance criteria using unaged and aged samples for different asphalt mixtures. As Figure 7.7 and Figure 7.8 suggest, based on available data, a minimum DC(T) fracture energy value of 700 J/m^2 can be used as a preliminary threshold for traffic category E and a minimum fracture energy value of 600 J/m^2 can be used as a preliminary threshold for all other mixes with various PG grades/mix types (Table 7.5).

Table 7.5 Recommended Preliminary DC(T) Fracture Energy Threshold Criteria for Post-Production Mixes.

Mix Type	Test Temperature (°C)	Preliminary Minimum Average DC(T) Fracture Energy Threshold (J/m²)
All surface Course Mixes for Traffic Category E (>30 million ESALS)	Low PG Temperature+10 ℃	700
All other surface Course Mixes	Low PG Temperature+10 ℃	600

7.4 Hamburg Wheel Track (HWT) Test Results

The Hamburg Wheel Tracking (HWT) test procedure specified in the AASHTO T324 was used to investigate rutting and moisture susceptibility of PPLC specimens in this study. The specimens are loaded at test temperatures ranging from 46-50°C for a maximum number of passes or until reaching a certain rut depth as specified by various agencies. A maximum 20,000 passes and 12.5 mm rut depth are commonly used.

With respect to test criteria determined by various agencies, either a maximum rut depth at a specific number of wheel pass or a minimum wheel passe to reach a certain rut depth are required. Generally, the HWT test provides details on the total rut depth, the rut depth at specific wheel pass, post-compaction consolidation, creep slope (CS), stripping slope (SS) as well as the stripping inflection point (SIP). However, there is not a standardized method for determining SIP based on the creep and stripping slopes, and several methods used have not resulted in the same SIP. However, in this study, the HWT analysis is based on total rut depth, the rut depth at specific wheel passes and post-compaction consolidation.

For this study, the HWT test was conducted on PPLC specimens compacted at 7±0.5% air void submerged in water at 50°C and 44°C, depending on the PG grade. The test specimens received 20,000 passes or when a total rut depth of 12.5 mm was reached over a wheel path distance of 200 mm. Figure 7.9 demonstrates rut depth vs. number of wheel passes, and Table 5 shows how the rut depth increases in the process of testing as the number of passes increase. The following observations can be made from data presented in Figure 7.9 and Table 7.6:

- As depicted in Figure 7.9, Mix1 and Mix2 which are SMA mixes containing PG70-28 performed well by completing the test and reaching a total rut depth of 4.12 and 3.63 mm, respectively, without having moisture susceptibility. Furthermore, Mix3, Mix4 and Mix5 which are SP12.5 FC2 containing PG70-28 completed the test by reaching total depths of 1.89, 1.76 and 1.86 mm, respectively, without showing moisture susceptibility. Generally, HWT results obtained from Mix1 to Mix5, containing PG70-28 used for category E traffic, show that test temperature set at 50°C and a preliminary criterion of maximum 6.0 mm rut depth at 20000 passes can be set forth for these mixes. It should also be noted that Mix4 and Mix5 each contained 20% RAP.

- Figure 7.9 shows that among Mix6, Mix7 and Mix8 containing PG64-XX, only Mix8 completed the test by reaching to the maximum rut depth of 2.75 mm, and without having moisture susceptibility. Mix6 completed the test by reaching the rut depth of 14.8 mm, which is greater than 12.5 mm, and showing moisture susceptibility. Mix7 was not able to complete the test and reached to 13.5 mm rut depth at 15,200 passes also showing moisture susceptibility. Even though Mix 8 was designed for traffic category E, Mix6 and Mix7 were designed for traffic category C and D, respectively. It should be noted that most of highway agencies have specified the HWT test at 50°C with the maximum total rut depth of 12.5 mm and 15000 passes for mixes containing PG64-XX. Considering the maximum total rut depth of 12.5 mm and 15000 passes, Mix6 was able to pass the test.

- As seen in Figure 7.9, asphalt binder stiffness predominantly influences HWT results for Mix9 to Mix16 containing softer PGAC grades (i.e., PG58-XX and PG52-XX) such that most of them reached to rut depth of 12.5 mm at low number of passes. Also, Table 7.6 clearly shows that post-compaction consolidation (rut depth at 1000 passes) for these mixes were high except for Mix6 and Mix10. None of these mixes were able to complete the test at 50°C except for Mix13 that completed the test at 20000 passes and reaching to 13.85 mm rut depth.
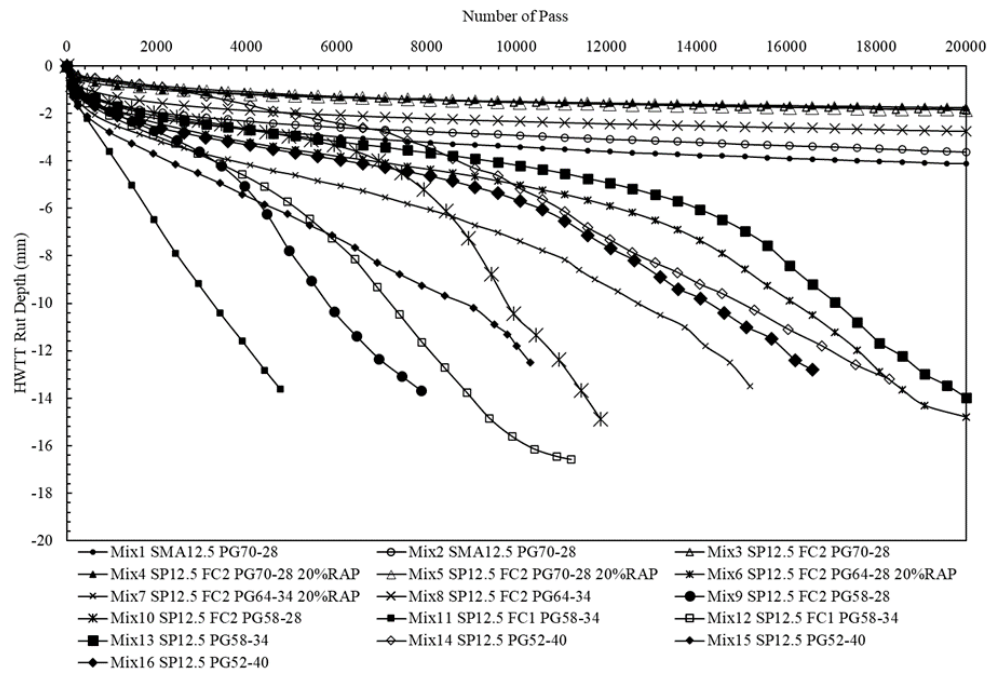
Figure 7.9 Rut Depth vs. Number of Passes at 50°C.

Table 7.6 Rutting Depth at Different Number of Wheel Passes.

Asphalt Mix	Traffic Category	Test Temperature (°C)	HWT Rut Depth (mm)				
			Number of Wheel Passes				
			1,000	5,000	10,000	15,000	20,000
Mix1. SMA12.5 PG70-28	E	50	1.86	2.82	3.42	3.84	4.12
Mix2. SMA12.5 PG70-28	E	50	1.62	2.47	2.92	3.29	3.63
Mix3. SP12.5 FC2 PG70-28	E	50	0.65	1.20	1.50	1.71	1.89
Mix4. SP12.5 FC2 PG70-28 20% RAP	E	50	0.83	1.27	1.49	1.66	1.76
Mix5. SP12.5 FC2 PG70-28 20% RAP	E	50	0.72	1.26	1.53	1.74	1.86
Mix6. SP12.5 FC2 PG64-28 20% RAP	C	50	1.58	2.96	4.09	6.35	10.74
Mix7. SP12.5 FC2 PG64-34 20% RAP	D	50	2.45	4.58	7.31	13.50	N/A
Mix8. SP12.5 FC2 PG64-34	E	50	1.26	1.98	2.33	2.55	2.75
Mix9. SP12.5 FC2 PG58-28	D	50	1.96	7.94	N/A	N/A	N/A

150

Mix10. SP12.5 FC2 PG58-28	D	50	1.55	2.97	10.50	N/A	N/A
Mix11. SP12.5 FC1 PG58-34	D	50	3.76	13.62	N/A	N/A	N/A
Mix12. SP12.5 FC1 PG58-34	D	50	2.15	5.86	15.86	N/A	N/A
Mix13. SP12.5 PG58-34	C	50	1.74	2.95	4.22	7.10	13.98
Mix14. SP12.5 PG52-40	B	50	0.62	2.08	5.25	11.84	N/A
Mix15. SP12.5 PG52-40	B	50	2.89	6.37	11.80	N/A	N/A
Mix16. SP12.5 PG52-40	C	50	1.97	3.63	5.64	10.86	N/A

Various highway agencies have specified HWT test temperature ranging from 40 to 46°C for asphalt mixtures containing PG58-XX and lower. For instance, Iowa, Montana, Colorado, and Utah are testing at 40°C, 44°C, 45°C and 46°C, respectively. Therefore, HWT tests were repeated on Mix12, Mix15 and Mix16 at 44°C to compare the results between 50°C and 44°C for these asphalt mixtures, and to determine whether 44°C is an appropriate testing temperature for asphalt mixtures containing softer binders (PG58-XX and PG52-XX). Figure 7.10 demonstrates rut depth vs. number of passes for these three mixes at 44°C and 50°C. Also, Table 7.7 shows how the rut depth increases during testing as the number of passes increases at 44°C and 50°C. The following observations can be made regarding HWT test results from Figure 7.10 and Table 7.7:

- As shown in Figure 7.10, Mix12, Mix15 and Mix16 withstood the HWT test at 44°C by reaching 20000 passes with total rut depths of 7.26, 2.32 and 3.60 mm, respectively, however, these asphalt mixtures were not able to complete the test at 50°C.

- Table 7.7 shows that Mix12, Mix15 and Mix16 have low value of post-compaction consolidation at 44°C compared to 50°C, i.e., asphalt binder stiffness predominantly did not impact HWT results at 44°C.

- There is a significant decrease in the rut depth as the testing temperature is decreased, which shows a high sensitivity of the mix to temperature due to lower asphalt binder stiffness.
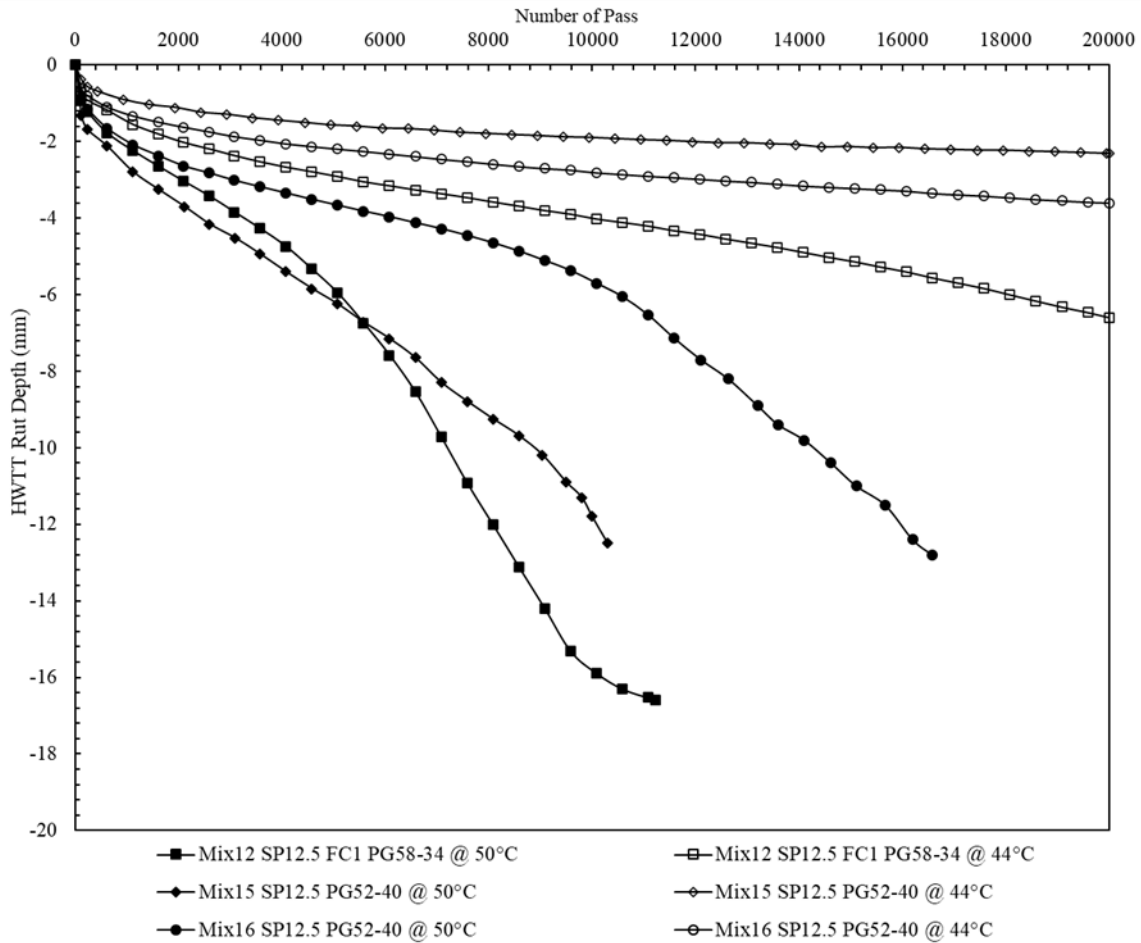
Figure 7.10 Rut Depth vs. Number of Passes at 50°C and 44°C.

Table 7.7 Rutting Depth at Different Number of Passes for Soft PG.

Asphalt Mix	Traffic Category	Test Temperature (°C)	HWTT Rut Depth (mm)				
			Number of Wheel Passes				
			1,000	5,000	10,000	15,000	20,000
Mix12. SP12.5 FC1 PG58-34	D	50	2.15	5.86	15.86	N/A	N/A
Mix12 SP12.5 FC1 PG58-34	D	44	1.59	2.94	4.02	5.17	7.26
Mix15 SP12.5 PG52-40	B	50	2.89	6.37	11.80	N/A	N/A
Mix15 SP12.5 PG52-40	B	44	0.9	1.57	1.91	2.14	2.32
Mix16 SP12.5 PG52-40	C	50	1.97	3.63	5.64	10.86	N/A
Mix16 SP12.5 PG52-40	C	44	1.29	2.19	2.79	3.21	3.60

Based on current test data, to set forth a maximum rut depth at a specific temperature and number of wheel passes as a pass/fail criterion for asphalt mixtures evaluated in this study, the performance of asphalt pavements in the field should be monitored for rutting. Also, more post-production asphalt mixture samples will need to be collected and tested to assist with developing the acceptance criteria for various asphalt mixtures. Based on our available test results, Table 7.8 shows the recommended preliminary thresholds values for the HWT test.

Table 7.8 Recommended preliminary HWT Threshold Criteria for Plant Produced Surface Course Mixes.

PGAC Grade	Test Temperature (°C)	Preliminary Average Threshold Values over 200 mm Path
70-XX	50	Max. 6.0 mm Rut Depth @20000 Passes
64-XX	50	Max. 12.5 mm Rut Depth @20000 Passes
58-XX and 52-XX	44	Max. 12.5 mm Rut Depth @20000 Passes

7.5 Interaction Plots Between FI, DC(T) Fracture Energy and HWT Rut Depth

Cracking resistance at intermediate and low temperatures and rutting resistance are the three main performance criteria utilized in this study to characterize sixteen surface course asphalt mixes. Generally, stiff mixes could withstand rutting while flexible or soft mixes could better

resist intermediate and low temperature cracking. This validates an existing trade-off between rutting and intermediate cracking resistance as well as rutting and low temperature cracking resistance of asphalt mixes. To characterize cracking and rutting resistance of asphalt mixtures investigated in this study, the FIT, DC(T) and HWT test results of PPLC specimens, summarized in Table 7.9, were used to develop two individual performance space diagrams: HWT rut depth vs. FI and HWT rut depth vs. DC(T) fracture energy. The recommended preliminary thresholds for each test are shown on the performance space diagrams. These preliminary thresholds formed four distinctive quadrants for each space diagram, three of which are failing (either rutting susceptible or crack susceptible, or both), and only the top right quadrant is passing (i.e., cracking, and rutting resistance). Figure 7.11 and Figure 7.12 illustrate the performance space diagrams for HWT rut depth vs. FI and HWT rut depth vs. DC(T) fracture energy, respectively.

Table 7.9 Summary of FI, DC(T) and HWT Results of PPLC Specimens.

Asphalt Mix	Traffic Category	FI	DC(T) FE (J/m^2)	HWT Rut Depth, mm (testing temperature)
Mix1 SMA12.5 PG70-28	E	19.4	706	4.12 (50°C)
Mix2 SMA12.5 PG70-28	E	25.0	886	3.63 (50°C)
Mix3 SP12.5 FC2 PG70-28	E	7.0	738	1.89 (50°C)
Mix4 SP12.5 FC2 PG70-28 20% RAP	E	3.3	558	1.76 (50°C)
Mix5 SP12.5 FC2 PG70-28 20% RAP	E	3.1	543	1.86 (50°C)
Mix6 SP12.5 FC2 PG64-28 20% RAP	C	8.4	678	10.74 (50°C)
Mix7 SP12.5 FC2 PG64-34 20% RAP	D	15.8	633	13.50 (50°C)
Mix8 SP12.5 FC2 PG64-34	E	10.7	676	2.75 (50°C)
Mix9 SP12.5 FC2 PG58-28	D	9.0	566	13.66 (50°C)
Mix10 SP12.5 FC2 PG58-28	D	11.2	490	14.88 (50°C)
Mix11 SP12.5 FC1 PG58-34	D	29.2	813	13.62 (50°C)
Mix12 SP12.5 FC1 PG58-34	D	12.2	576	7.26 (44°C)
Mix13 SP12.5 PG58-34	C	27.1	1072	13.98 (50°C)
Mix14 SP12.5 PG52-40	B	7.6	734	13.20 (50°C)
Mix15 SP12.5 PG52-40	B	7.0	647	2.32 (44°C)
Mix16 SP12.5 PG52-40	C	14.2	806	3.60 (44°C)
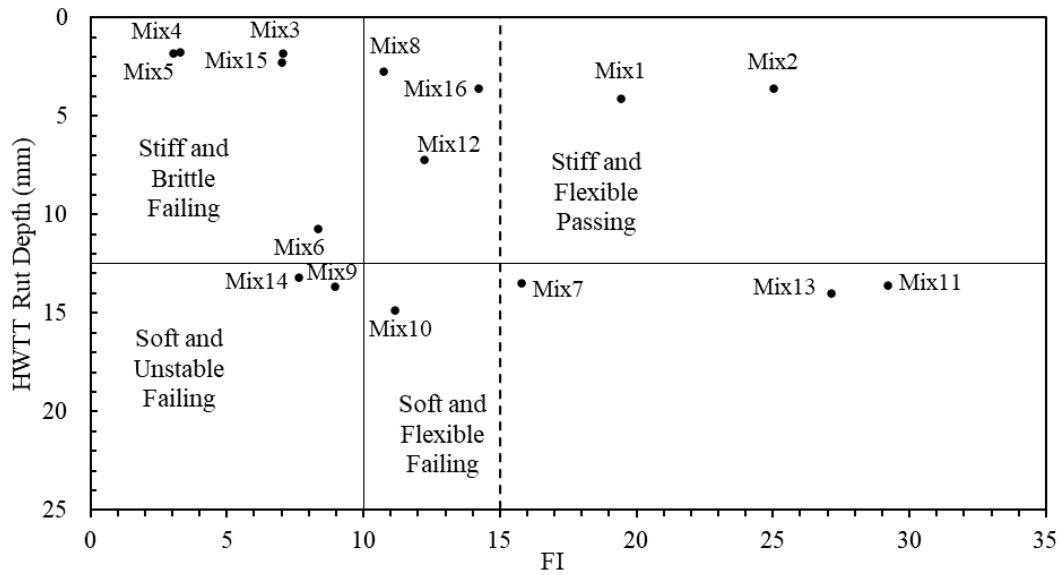
Figure 7.11 Performance Space Diagram of Rut Depth vs. FI with preliminary Threshold Criteria.
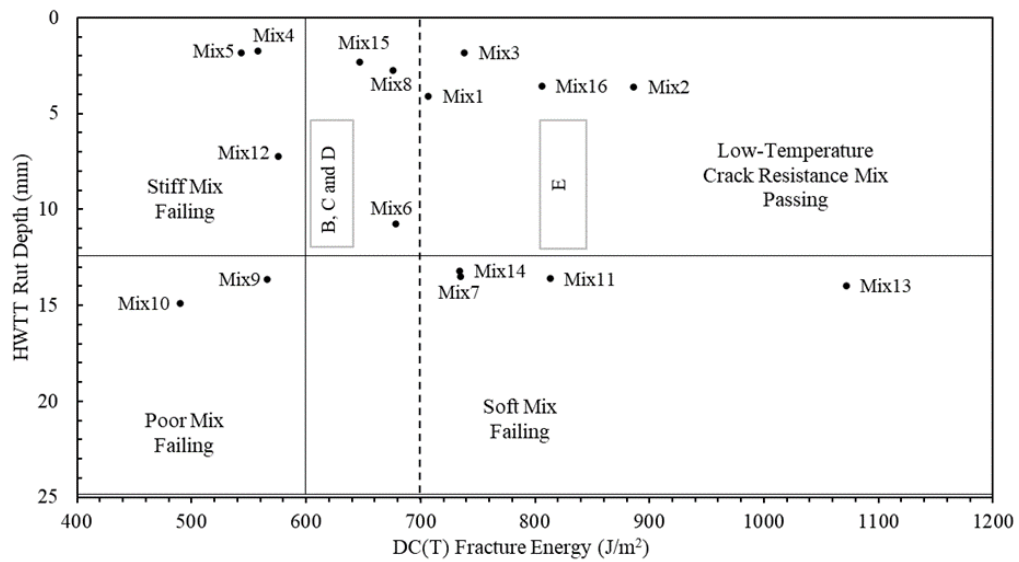
Figure 7.12 Performance Space Diagram of Rut Depth vs. DC(T) Fracture Energy with preliminary Threshold Criteria.

155

Generally, the following observations can be made from Figure 7.11 and Figure 7.12:

- Figure 7.11 demonstrates that four mixes, including Mix3, Mix4, Mix5 and Mix15 are stiff (rut resistant) and brittle (intermediate temperature cracking susceptible), among which Mix4 and Mix5 contain RAP. Although Mix15 has a soft asphalt binder (PG52-40), insufficient asphalt binder content (4.70% recovered asphalt binder content) which is one of the lowest contents of asphalt binder among the mixes investigated in this study could give a rise for its location in the space diagram.

- As seen in Figure 7.11, six mixes (Mix6, Mix7, Mix9, Mix10, Mix11, Mix13 and Mix14) are in the bottom of space diagram, either soft and unstable or soft and flexible quadrants (failing quadrants). It should be noted that Mix9, Mix10, Mix11, Mix13 and Mix14 were tested at 50°C in HWT test and resulted in the rut depths ranging from 13-15 mm in the space diagram. If these five mixes were tested at 44°C, the total rut depth could have been less than 12.5 mm, and they could have moved up to the top part of the space diagram. In that case, Mix14 would have located in stiff and brittle (failing) quadrant, whereas Mix9, Mix10, Mix11 and Mix13 would have located in the passing quadrant (stiff and flexible quadrant). Generally, Mix7 is in soft and flexible (failing) quadrant implying that PG64-34 and RAP did not interact well (RAP asphalt binder did not produce a certain level of stiffness) resulting in a soft asphalt mix.

- Figure 7.11 clearly shows that two SMA mixes (Mix1 and Mix2) performed very well and have a high value of flexibility index at intermediate temperature, while also having significant rutting resistance characteristics, which are desirable characteristic for a good performing mix.

- Figure 7.12 illustrates that Mix4, Mix5 and Mix12 are too stiff and failed the preliminary threshold values of DC(T) fracture energy even though performed well in HWT test.

- As it can be seen in Figure 7.12, similar to space diagram of HWT vs. FI, six mixes (Mix7, Mix9, Mix10, Mix11, Mix13 and Mix14) are in the bottom of space diagram

156

of HWT and DC(T) fracture energy; either poor or soft mixes (failing quadrants). Furthermore, the same as in HWT rut depth vs. FI space diagram, Mix7 is in the failing quadrant because of being a soft mix (susceptible to rutting).

- Figure 7.12 shows that considering the same scenario for Mix9, Mix10, Mix11 and Mix13 and Mix14 as in HWT rut depth vs. FI, Mix9 and Mix10 would have located in stiff quadrant failing the preliminary threshold criteria of DC(T) fracture energy. However, Mix11, Mix13 and Mix14 would have been in passing quadrant.

- As it can be seen in Figure 7.12, even though Mix8 is in the passing quadrant, it does not satisfy the preliminary threshold value of fracture energy value required for traffic category E (having the fracture energy value of 676 J/m^2 which is less than 700 J/m^2). Furthermore, SMA mixes (Mix1 and Mix2) show a good level of rutting and low temperature cracking resistance.

- Considering Figure 7.11 and Figure 7.12, Mix4 and Mix5 containing PG70-28 and 20% RAP are too stiff and do not have adequate intermediate and low temperature cracking resistance while having a high level of rutting resistance. The lack of cracking resistance can arise from existing RAP in aforementioned mixes and not being balanced. However, Mix6 containing PG64-28 and 20% RAP is enough stiff to be rutting resistance and enough flexible to be both intermediate and low temperature cracking resistance. Generally, comparing Mix4 and Mix5 with Mix6 proves that RAP can be used responsibly if it results into a balanced mix (both rutting and cracking resistance).

- Figure 7.11 and Figure 7.12 show that SMA mixes (Mix1 and Mix2) show a high level of resistance to rutting, and intermediate and low temperature cracking.

7.6 Conclusions

The following conclusions can be drawn based on the experimental results and discussions provided in this chapter:

- Volumetric mix design is not solely able to guarantee that an asphalt mix will perform well in the field. Therefore, performance tests to evaluate cracking and

157

rutting susceptibility of asphalt mixes can be used in addition to volumetric mix design.

- I-FIT and DC(T) tests, known as fracture mechanics-based tests, have drawn attention for acceptance of mix design post-production asphalt mix. This study confirmed that these fracture mechanics-based tests will produce reasonable results when conducted on the post-production asphalt mix.

- Generally, I-FIT and DC(T) tests were able to differentiate asphalt mixes based on PG grades (soft or stiff), asphalt mix type, and presence of RAP in asphalt mixes.

- The HWT test has been used by many highway agencies to evaluate rutting and moisture susceptibility of asphalt mixes. The laboratory test results on the post-production asphalt mixes of this study show HWT as a promising test that can distinguish based on asphalt mix type, existing RAP and different PG grades (soft or stiff) in asphalt mixes.

- In this study, there were four mixes containing 20% RAP content, among which two mixes containing PG70-28 (Mix4 and Mix5) performed poorly in I-FIT and DC(T) tests. Among the other two mixes containing 20%RAP, the mix containing PG64-34 (Mix7) performed poorly in HWT test, however, the mix containing PG64-28 (Mix6) performed well in HWT test and cracking resistance (I-FIT and DC(T)) tests. This proves that RAP needs to be used responsibly.

- The statistical analysis conducted by t-test on sixteen mixes determined that there is a significant difference between the average FI of PPLC specimens and their corresponding field cores with some exception. In addition, the CV of FI results for most of PPLC specimens and pavement field cores is less than 20% showing the low variability for I-FIT test for post-production mixes and field cores.

- The statistical analysis conducted by t-test on sixteen mixes determined that there is not a significant difference between the average fracture energy of PPLC specimens and their corresponding field cores except for one mix in DC(T) test. Furthermore, the CV of fracture energy results for most of PPLC specimens and pavement field cores is less than 20% showing the low variability of DC(T) test.

158

- SMA mixes performed very well in three laboratory performance tests conducted in this study, i.e., SMA mixes presented high resistance to rutting, and cracking at intermediate and low temperatures.

- Regardless of designed traffic category, using soft AC combined with higher AC content can increase resistance to low and intermediate temperature cracking of asphalt mixes.

- Based on the data presented in this study, a preliminary threshold FI value of 10 can be used for all mixes except for SMA mixes. A preliminary threshold FI value of 15 is suggested for SMA mixes.

- Based on the data presented in this study, a premilitary threshold DC(T) fracture energy value of 700 J/m^2 can be considered for traffic category E mixes. Moreover, a preliminary threshold DC(T) fracture energy value of 600 J/m^2 can be considered for all other traffic categories.

- As a preliminary threshold criterion, mixes containing PG70-XX being used for traffic category E, must not reach a rut depth of more than 6.0 mm at 50°C after 20000 passes. In addition, mixes containing PG64-XX must not exhibit a rut depth of more than 12.5 mm at 50°C after 20000 passes. For mixes containing PG58-XX and PG52-XX, the rut depth should not exceed 12.5 mm at 44°C after 20000 passes.

- The field performance of the studied asphalt pavements will need to be monitored in order to adjust the preliminary acceptance thresholds for the mix performance tests.

- Performance space diagrams formed by HWT test results between FIT and DCT test results are showing as promising methods in mix design process to achieve a mix design which is balanced, i.e., the asphalt mix produced is both resistant to cracking and rutting based on the mix performance laboratory tests.

- According to the findings of this study, it can be concluded that mix performance tests, which include FIT, DC(T) and HWT tests, can be added to the current volumetric mix attributes to evaluate mixture's resistance to both cracking (fatigue,

159

low temperature) and rutting to create a balance between these mix properties to ensure the long-term performance of asphalt pavements.

Chapter 8

Conclusions and Recommendations

8.1 General Summary

The present work was conducted with four research objectives: (1) To determine suitable and practical tests for crack and rutting resistance of asphalt mixtures in Ontario, (2) To validate asphalt mix design through analysis of various new tests on the crack and rutting resistance of asphalt mixtures, (3) To provide a basis for implementation of performance specifications for crack and rutting resistance of asphalt mixtures in Ontario in the future and (4) To complete End Results Specifications (ERS), used as Quality Acceptance (QA) criteria, with suitable performance tests. Therefore, to achieve the first objective, performance tests such as Disc-Shaped Compact Tension (DC(T)) test, Semi-Circular Bend (SCB) test, Illinois Flexibility Index Test (I-FIT), IDEAL-CT test, complex modulus and cyclic tests, and Hamburg Wheel Tracking (HWT) test, which have shown promising results, were investigated through laboratory work. In addition, a survey was conducted in order to assess the capability of asphalt mixture laboratories in Ontario to carry out the aforementioned performance tests.

Based on the analysis of the laboratory results and survey data, I-FIT, DC(T) and HWT tests were selected and considered for further research to achieve the other objectives. Hence, to achieve the second objective, asphalt mix design was validated through conducting I-FIT, DC(T) and HWT tests on sixteen plant-produced asphalt mixtures that have been paved in Ontario. To achieve the third and fourth objectives, based on the analysis of the laboratory results of I-FIT, DC(T) and HWT tests from sixteen asphalt mixtures, preliminary specifications for I-FIT, DC(T) and HWT tests were recommended that can be used as QA criteria.

8.2 Major Findings and Conclusions

The results of five plant-produced asphalt mixtures showed that the cyclic test was able to distinguish asphalt mixtures in terms of fatigue cracking resistance, while I-FIT and IDEAL-CT tests were able to distinguish crack propagation resistance of asphalt mixtures at

intermediate temperature. Moreover, DC(T) and SCB tests were able to distinguish low temperature cracking resistance of asphalt mixtures. Furthermore, HWT test was able to evaluate rutting resistance of asphalt mixtures.

In general, DC(T) and SCB tests statistically ranked the asphalt mixtures similarly at 10 °C higher than the low PG grade, however, at -18 °C and -30 °C where asphalt mixtures had a ductile and brittle behaviour, respectively, SCB test was not able to distinguish asphalt mixtures as well as DC(T) test. This could be attributed to the discrepancies between the geometry of DC(T) and SCB specimens and loading rates. Overall, there was a good correlation between DC(T) and SCB tests, and DC(T) fracture energy had a good correlation with low temperature properties of the recovered asphalt binders. DC(T) fracture energy was not sensitive to two methods of long-term aging (forced-draft oven aging at 85 °C for 120 hours and forced-draft oven aging at 95 °C for 72 hours) employed in this research.

Generally, I-FIT and IDEAL-CT tests statistically ranked the asphalt mixtures similarly at 25 °C and were not able to distinguish asphalt mixtures at the intermediate temperature based on the climate of location where they were paved, and there was a good linear correlation between I-FIT and IDEAL-CT at 25 °C. I-FIT test was sensitive to long-term aging and forced-draft oven aging of I-FIT specimens at 95 °C for 72 hours produced statistically similar Flexibility Index values as the specimens aged at 85 °C for 120 hours. The temperature sensitivity of FI was investigated by conducting the I-FIT test at 25 ℃, 24 ℃, 23 ℃ and the results showed that asphalt mixtures containing hard PG asphalt binder (PG64-28 and PG70-28) were more sensitive to testing temperature variability compared to asphalt mixtures having softer PG asphalt binders. Sensitivity of FI to testing device was investigated by conducting I-FIT test with DTS-30 (hydraulic testing device) and Auto SCB (screw-driven testing device) and the results showed that both testing devices produced statistically similar values of FI for the asphalt mixtures. I-FIT test at intermediate temperatures showed that there was a strong correlation between FI at 25°C and at continuous intermediate temperature for asphalt mixtures studied in this research.

The results of sixteen plant-produced asphalt mixtures showed that volumetric mix design solely is not able to guarantee an asphalt mixture is performing well in the field.

Therefore, performance tests to evaluate cracking and rutting susceptibility of asphalt mixtures can be used in addition to volumetric mix design.

Generally, based on the data presented in this study, a preliminary threshold FI value of 10 can be used for all mixtures except for SMA mixtures. A preliminary threshold FI value of 15 is suggested for SMA mixtures. Moreover, based on the data presented in this study, a premilitary threshold DC(T) fracture energy value of 700 J/m^2 can be considered for traffic category E mixtures, and a preliminary threshold DC(T) fracture energy value of 600 J/m^2 can be considered for all other traffic categories.

With regard to HWT test results, as a preliminary threshold criterion, mixes containing PG70-XX being used for traffic category E, must not reach a rut depth of more than 6.0 mm at 50°C after 20000 passes. In addition, mixes containing PG64-XX must not exhibit a rut depth of more than 12.5 mm at 50°C after 20000 passes. For mixes containing PG58-XX and PG52-XX, the rut depth should not exceed 12.5 mm at 44°C after 20000 passes.

Overall, performance space diagrams formed by HWT test results between FIT and DCT test results are showing as promising methods in mix design process to achieve a mix design which is balanced, i.e., the asphalt mix produced is both resistant to cracking and rutting based on the mix performance laboratory tests.

According to the findings of this study, it can be concluded that mix performance tests, which include FIT, DC(T) and HWT tests, can be added to the current volumetric mix attributes to evaluate mixture's resistance to both cracking (fatigue, low temperature) and rutting to create a balance between these mix properties to ensure the long-term performance of asphalt pavements.

8.3 Significant Contributions

As mentioned, the implementation of suitable and practical performance tests in the mix design procedure and QA/QC activities can help overcome the limitations of volumetric mix design to evaluate cracking and rutting resistance of asphalt mixtures. According to the laboratory work conducted in this research, applicable tests to evaluate crack and rutting resistance of asphalt mixtures were determined. Moreover, asphalt mix design in terms of asphalt mixture

performance was verified through analysis of new tests and criteria. Furthermore, a basis for implementation of performance specifications for I-FIT, DC(T) and HWT tests in Ontario was prepared.

8.4 Recommendations and Future Work

In this research, plant-produced asphalt mixtures were investigated to determine preliminary performance specifications. Therefore, it is recommended that laboratory-produced asphalt mixtures be investigated to determine the effect of asphalt binder content, aggregate gradation, and air void on the test results. Overall, data collected from testing on laboratory-produced asphalt mixtures can be beneficial for mix designers and can help determine the effect of production variability in asphalt mixture plants on the test results. Furthermore, pavement distress data in the field can be collected from in-service highways constructed by plant-produced asphalt mixtures investigated in this research. The test data obtained by asphalt mixture performance tests in conjunction with the in-service pavement distress data can be used to fine-tune preliminary acceptance criteria for I-FIT, DC(T) and HWT where post-production asphalt mixtures are accepted based on asphalt mixture performance testing. Moreover, laboratory testing can be continued for additional asphalt mixtures in order to verify the following correlations: CT Index and FI values from IDEAL CT and I-FIT tests, respectively; HWT rut depth and the recovered $R_{e3.2kPa}$ and $J_{nr3.2kPa}$; DC(T) and SCB fracture energies with the low temperature properties of recovered asphalt binder.

Bibliography

American Society of Civil Engineers. (2009). *Modeling of Asphalt Concrete* (1st ed.). (Y. R. Kim, Ed.) McGraw Hill.

Anderson, T. (2005). *Fracture Mechanics Fundamentals and Applications* (3rd ed.).

Aschenbrener, T. (1992). *Comparison of Results Obtained from the French Rutting Tester with Pavements of Known Field Performance.* Colorado Department of Transportation.

Asphalt Institute. (2001). *Construction of Hot Mix Asphalt Pavements* (2nd ed., Vols. MS-22).

Asphalt Institute. (2014). *Asphalt Mix Design Methods.* Asphalt Institut.

Baaj, H. e. (2005). Effect of Binder Characteristics on Fatigue of Asphalt Pavement Using an Intrinsic Damage Approach. *Road Materials and Pavement Design, 6*(2), 147-174.

Bashir, I., Salehi-Ashani, S., Ahmed, D., Tabib, S., & Vasiliu, G. (2020). MTO's Experience with Post-Production Asphalt Mixture Performance Testing. *Proceedings Canadian Technical Asphalt Association*, *60*, pp. 315-344.

Bennert, T. (2018). Innovations in Asphalt Mixture Design Procedure. *Transportation Research Circular E-C237.* Transportation Research Board (TRB).

Bhasin, A., Button, J. W., & Chowdhury, A. (2003). *Evaluation of Simple Performance Tests on HMA Mixtures from the South-Central United States.*

Bonaquist, R. (2014). Enhancing the Durability of Asphalt Pavements. *Transportation Research Circular E-C186.* TRB.

Braham, A. F., Buttlar, W., & Marasteanu, M. (2007). Effect of Binder Type, Aggregate, and Mixture Composition on Fracture Energy of Hot-Mix Asphalt in Cold Climates. *Transportation Research Record, 2001*, 102-109. doi:10.3141/2001-12

Braham, A., & Underwood, S. (2016). State of the Art and Practice in Fatigue Cracking Evaluation of Asphalt Concrete Pavements. Retrieved from http://www.andrewbraham.com/AAPT_Fatigue_2016.pdf

Brown, E., Kandhal, P., Roberts, F., Kim, Y., Lee, D., & Kennedy, T. (2009). *Hot Mix Asphalt Materials, Mixture Design and Construction.* NAPA Research and Education Foundation.

Chehab, G. R., Kim, Y., Schepary, R. A., Witczack, M., & Bonaquist, R. (2003). Characterization of Asphalt Concrete in Uniaxial Tension Using a Visco-elasto-plastic Model. *Journal of the Association of Asphalt Paving Technology, 72*, 315-355.

Christensen, D. W., & Bonaquist, R. F. (2006). *Volumetric Requirements for Superpave Mix Design.* National Highway Research Program.

Christensen, D., & Bonaquist, R. (2004). *Evaluation of Indirect Tensile Test (IDT) Procedures for Low-Temperature Performance of Hot Mix Asphalt.* Washington, DC.

Cooper, S. B., & Mohammad, L. N. (2018). Innovations in Asphalt Mixture Design Procedure. *Transportation Research Circular E-C237.* Transportation Research Board (TRB).

Daniel, J. S., & Y., K. (2002). Development of a Simplified Fatigue Test and Analysis Procedure Using a Viscoelastic Damage Model. *Journal of Association of Asphalt Paving Technologists, 71*, 619-650.

Dave, E., C. Hoplin, B., Helmer, J., Dailey, D., & Deusen, V. (2016). Effects of Mix Design and Fracture Energy on Transverse Cracking Performance of Asphalt Pavements in Minnesota. *Transportation Research Record*, *2576*, pp. 40-50. doi:10.3141/2576-05

Delorme, J. L., Roche, C., & Wendling, L. (2007). *LPC Bituminous Mixtures Design Guide.* Laboratoire Central des Ponts et Chaussées.

Faruk, A. (2015). Measurement of HMA shear resistance potential in the lab: the simple punching shear test. *Construction and Building Materials, 99*, 62-72.

Francken, L. (1998). *Bituminous Binders and Mixes, State of the Art and Interlaboratory Tests on Mechanical Behaviour and Mix Design.*

Grobler, J., Rebbechi, J., & Denneman, E. (2018). *National Performance-based Asphalt Specification Framework, Austroads.*

Hill, B., Oldham, D., Behnia, B., Fini, E., Buttlar, W., & Reis, H. (2013). Low-Temperature Performance Characterization of Biomodified Asphalt Mixtures That Contain Reclaimed Asphalt Pavement. *Transportation Research Record, 2371*, 49-57. doi:0.3141/2371-06

Huber, G. (2017). *History of Mix Design in North America.* (A. Institute, Ed.) Retrieved from http://asphaltmagazine.com/history-of-asphalt-mix-design-in-north-america-part-2/.

Izzo, R., & Tahmoressi, M. (1999). Use of Hamburg Wheel Tracking Device for Evaluating Moisture Susceptibility of Hot-Mix Asphalt. *Transportation Research Record*(1682), 76-85.

Jahangiri, B., Majidifard, H., Meister, J., & Buttlar, W. (2019). Performance Evaluation of Asphalt Mixtures with Reclaimed Asphalt Pavement and Recycled Asphalt Shingles in Missouri. *Transportation Research Record, 2371*, 49-57. doi:10.1177/0361198119825638

Kandhal, P. S., Foo, K. Y., & Mallick, R. B. (1998). *Critical Review of VMA Requirements in Superpave.* National Center for Asphalt Technology (NCAT).

Lee, H., & Y, K. (1998). A Uniaxial Viscoelastic Constitutive Model for Asphalt Concrete under Cyclic Loading. *Journal of Engineering Mechanics, 124*(1).

Li, X., & Marasteanu, M. (2009). Using Semi Circular Bending Test to Evaluate Low Temperature Fracture Resistance for Asphalt Concrete. *Experimental Mechanics, 50*, 867-876. doi:10.1007/s11340-009-9303-0

Marasteanu, M., Buttlar, W., Bahia, H., & Williams, C. (2007). *Investigation of Low Temperature Cracking in Asphalt Pavements.* National Pooled Fund. Retrieved from https://www.lrrb.org/pdf/200743.pdf

Marasteanu, M., Buttlar, W., Bahia, H., & Williams, C. (2012). *Investigation of Low Temperature Cracking in Asphalt Pavements.* National Pooled Fund. Retrieved from https://lrrb.org/pdf/201223.pdf

McCarthy, L. M., Callans, J., Quigley, R., & Scott, S. V. (2016). *Performance Specifications for Asphalt Mixtures.* National Highway Research Program.

Michael, L. (2008). *Ruggedness Testing of the Dynamic Modulus and Flow Number Tests with the Simple Performance Tester.* National Cooperative Highway Research Program (NCHRP).

MTO. (2021). *Ministry of Transportation Ontario.* Retrieved from https://www.raqs.merx.com/public/contract/contractsByRegionMap.jsf.

Newcomb, D., & Zhou, F. (2018). *Balanced Design of Asphalt Mixtures.* Research Project, Texas A&M Transportation Institute. Retrieved from https://www.dot.state.mn.us/research/reports/2018/201822.pdf

Newcomb, D., Karki, P., Epps, J., Fernando, E., Arabali, P., Al-Khayat, H., & King, G. (2018). *A Review of Ontario Asphalt Industry Practices.* Ontario's Road Builders' Association. Texas A&M Transportation Institute.

Ozer, H., & Al-Qadi, I. L. (2018). Innovations in Asphalt Mixture Design Procedure. *Transportation Research Circular E-C237.* Transportation Research Board (TRB).

Rahbar-Rastegar, R., Dave, E., & Sias, J. (2018). Fatigue and Thermal Cracking Analysis of Asphalt Mixtures Using Continuum-Damage and Cohesive-Zone Models. *Journal of Transportation Engineering, Part B: Pavements, 144*(4). doi:doi/10.1061/JPEODX.0000066

Salehi-Ashani, S. (2021). Investigation of the effect of long-term aging and testing temperature sensitivity on the Flexibility Index (FI) parameter obtained from the Illinois Flexibility Test (I-FIT). *Canadian Society of Civil Engineering (CSCE) Conference.*

Salehi-Ashani, S., & Tighe, S. (2020). The Evaluation of Low Temperature Cracking Resistance of Asphalt Mixes in Ontario by Conducting Disk-Shaped Compact Tension (DC(T)) and Semi-Circular Bend (SCB) Tests. *Proceedings Canadian Technical Asphalt Association*, *60*, pp. 365-377.

Schapery, R. (1984). Correspondence Principles and a Generalized J-integral for Large Deformation and Fracture Analysis of Viscoelastic Media. *International Journal of Fracture, 25*, 195-223.

Tighe, S. (2013). *Pavement Asset Design and Management Guide.* Transportation Association of Canada.

Underwood, B. S. (2011). *Multiscale Constitutive Modeling of Asphalt Concrete.* Raleigh, NC: North Carolina State University.

Underwood, B. S., Beak, C., & Kim, Y. (2012). Simplified Viscoelastic Continuum Damage Model as Platform for Asphalt Concrete Fatigue Analysis. *Transportation Research Record: Journal of the Transportation Research Board, 2296*, 35-45.

Underwood, B. S., Kim, Y., & Guddati, M. (2006). Characterization and Performance Prediction of ALF Mixtures Using a Viscoelastic Continuum Damage Model. *Journal of the Association of Asphalt Paving Technologists, 75*, 577-636.

Wang, Y. D., Keshavarzi, B., & Kim, Y. R. (2018). Fatigue Performance Prediction of Asphalt Pavement with FlexPave, the SVECD Model, and DR Failure Criterion. *Transportation Research Record: Journal of the Transportation Research Board, 2672*, 217-227.

Wang, Y. D., Underwood, B. S., & Kim, Y. R. (2020). Development of a fatigue index parameter, Sapp, for asphalt mixes using viscoelastic continuum damage theory. *International Journal of Pavement Engineering, ERING*. doi:10.1080/10298436.2020.1751844

West, R. R. (2018). *Development of a Framework for Balanced Mix Design.* National Cooperative Highway Research Program (NCHRP).

Witczak, M. W., Kaloush, K., Pellinen, T., & El-Basyouny, M. (2002). *Simple Performance Test for Superpave Mix Design.* National Cooperative Highway Research Program (NCHRP).

Zhou, F. (2017). Development of an IDEAL Cracking Test for Asphalt Mix Design and QC/QA. *The Association of Asphalt Pavement Technologists, 86*, 549-578.

Zhou, F. (2018). Innovations in Asphalt Mixture Design Procedure. *Transportation Research Circular E-C237.* Transportation Research Board (TRB).

Zhou, F. (2020). Retrieved from https://www.youtube.com/watch?v=u6l0ka6uf34

Zhou, F., Newcomb, D., Gurganus, C., Banihashemrad, S., Park, E. S., Sakhaeifar, M., & Lytton, R. L. (2016). National Cooperative Highway Research Program (NCHRP).

Zhou, F., Newcomb, D., Gurganus, C., Banihashemrad, S., Park, E. S., Sakhaeifar, M., & Lytton, R. L. (2016). National Cooperative Highway Research Program (NCHRP).

Appendices

Appendix A

Survey

A. Test Specimen Preparation
1. Does your laboratory have a suitable cutting saw and jig facilities to cut Superpave Gyratory Compacted (SGC) specimens into discs of 50 mm thickness for conducting SCB and DC(T) tests? Yes☐　　　　　　No☐ Comment: ………………………………………………………….
2. Does your laboratory have a suitable cutting saw and jig facilities to cut the discs of 50 mm thickness into half for conducting SCB test? Yes☐　　　　　　No☐ Comment: ………………………………………………………….
3. Does your laboratory have a suitable tile saw to cut a notch of 15±1 mm depth and of 1.5±0.5 mm width for a half-disc specimen for conducting SCB test? Yes☐　　　　　　No☐ Comment: ………………………………………………………….
4. Does your laboratory have a suitable coring machine to drill 25±1 mm diameter hole in a 50 mm thick disc for conducting DC(T) test? Yes☐　　　　　　No☐ Comment: ………………………………………………………….
5. Does your laboratory have a suitable tile saw to cut the edge of a disc of 50mm and also cut a notch depth of 62.5 mm for conducting DC(T) test? Yes☐　　　　　　No☐ Comment: ………………………………………………………….

B. Test Specimen Conditioning

6. Does your laboratory have a suitable environmental chamber to condition specimens in the range of -40°C to 25°C?

Yes☐   No☐

Comment: ……………………………………………………….

7. Does your laboratory have a controlled temperature water bath?

Yes☐   No☐

If so, what range of temperature can the water bath provide? (e.g. 12°C to 25°C)

Comment: ……………………………………………………….

C. Testing Machines

8. If your laboratory has either a Humboldt loading machine or a pneumatic or hydraulic controlled actuator machine, please list them and answer the following questions with regards to the devices:

Device 1:

Name and Model (e.g. HM-3000)

…………………………………………………………….

Load Capacity (e.g. 50kN) …………………………………………………………….

Frequency of Data Acquisition (e.g. 40 data points per second)

…………………………………

Does the loader of machine handle an SCB testing apparatus?

Yes☐　　　　　　No☐

Does the loader of machine handle a DC(T) testing apparatus?

Yes☐　　　　　　No☐

Can the machine apply tensile loading?

Yes☐　　　　　　No☐

Can the machine apply compressive loading?

Yes☐　　　　　　No☐

Does the machine have a chamber to maintain test temperature (-40ºC to 25ºC)?

Yes☐　　　　　　No☐

Comment: …………………………………………………………….

C. Testing Machines

Device 2:

Name   and   Model   (e.g.   HM-3000)

…………………………………………………………….

Load Capacity (e.g. 50kN) ……………………………………………………….

Frequency of Data Acquisition (e.g. 40 data points per second)

……………………………….

Does the loader of machine handle an SCB testing apparatus?

Yes☐   No☐

Does the loader of machine handle a DC(T) testing apparatus?

Yes☐   No☐

Can the machine apply tensile loading?

Yes☐   No☐

Can the machine apply compressive loading?

Yes☐   No☐

Does the machine have a chamber to maintain test temperature (-40⁰C to 25⁰C)?

Yes☐   No☐

Comment: ……………………………………………………………….

C. Testing Machines
Device 3:
Name and Model (e.g. HM-3000) …………………………………………………….
Load Capacity (e.g. 50kN) ……………………………………………………….
Frequency of Data Acquisition (e.g. 40 data points per second) ……………………………….
Does the loader of machine handle an SCB testing apparatus?
Yes☐ No☐
Does the loader of machine handle a DC(T) testing apparatus?
Yes☐ No☐
Can the machine apply tensile loading?
Yes☐ No☐
Can the machine apply compressive loading?
Yes☐ No☐
Does the machine have a chamber to maintain test temperature (-40°C to 25°C)?
Yes☐ No☐
Comment: ………………………………………………………….

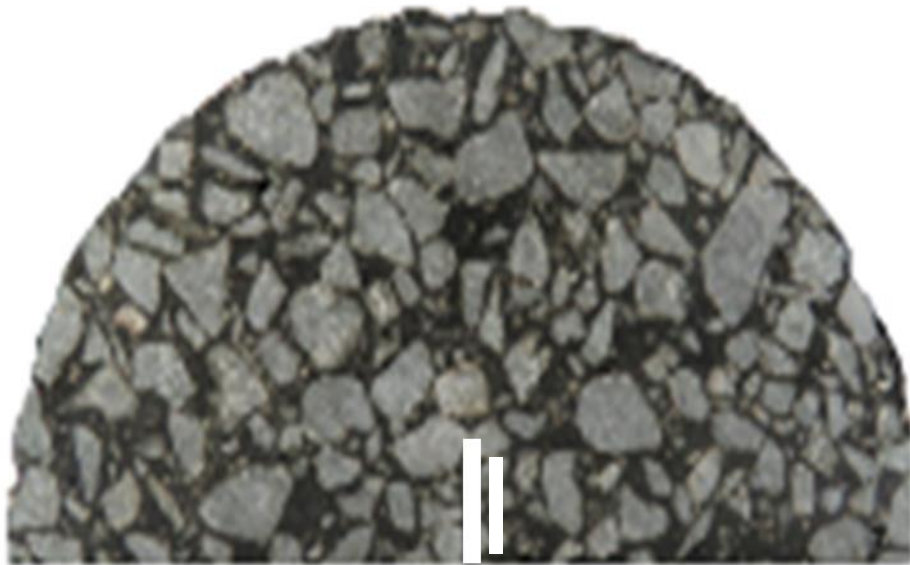Figure1. DC(T) specimen (A full disc including an edge cut, a notch and two loading holes

Figure 2. SCB specimen (A half disc with a notch)

Appendix B

Job Mix Formula (JMF) of Sixteen Asphalt Mixtures utilized in Chapter 7

	Sieve Size (mm)	Mix1 SMA12.5 PG70-28	Mix2 SMA12.5 PG70-28	Mix3 SP12.5FC2 PG70-28	Mix4 SP12.5FC2 PG70-28	Mix5 SP12.5FC2 PG70-28	Mix6 SP12.5FC2 PG64-28	Mix7 SP12.5FC2 PG64-34	Mix8 SP12.5FC2 PG64-34
	25.0	100	100	100	100	100	100	100	100
	19.0	100	100	100	100	100	100	100	100
	12.5	97.3	94.5	96.3	95.5	98.3	98.3	97.8	97.8
	9.5	73.6	72.4	84.7	81.9	83.6	88.0	82.1	88.4
Gradation (Passing%)	4.75	31.7	29.8	58.1	54.9	54.3	58.4	54.4	64.7
	2.36	23.2	19.6	40.1	40.0	40.9	42.8	48.9	50.2
	1.18	19.2	15.9	30.5	33.4	31.9	32.2	33.8	33.7
	0.6	16.0	13.8	23.3	28.3	26.8	23.5	22.0	21.6
	0.3	14.1	12.1	15.0	12.0	17.6	13.2	12.7	12.0
	0.15	12.6	10.1	7.5	6.1	8.8	6.5	7.1	7.2
	0.075	9.7	8.2	3.9	3.7	3.5	3.9	3.8	5.1
	RAP (%)	-	-	-	20	20	20	20	-
Asphalt Binder Content (%)		5.7	5.7	5.2	5.2	5.0	4.9	5.0	5.0
Voids in the Mineral Aggregate, VMA (%)		17.5	17.3	15.3	15.4	15.3	15.6	15.9	15.1
Voids Filled with Asphalt, VFA (%)		77.2	76.6	74.7	74.3	73.9	74.4	74.9	73.7
Asphalt Binder Performance Grade		70-28	70-28	70-28	70-28	70-28	64-28	64-34	64-34
Traffic Category		E	E	E	E	E	C	D	E

Gradation (Passing%)	Sieve Size (mm)	Mix9 SP12.5FC2 PG58-28	Mix10 SP12.5FC2 PG58-28	Mix11 SP12.5FC1 PG58-34	Mix12 SP12.5FC1 PG58-34	Mix13 SP12.5 PG58-34	Mix14 SP12.5 PG52-40	Mix15 SP12.5 PG52-40	Mix16 SP12.5 PG52-40
	25.0	100	100	100	100	100	100	100	100
	19.0	100	100	100	100	100	100	100	100
	12.5	98.3	98.2	97.4	97.5	97.5	96.2	96.6	99.4
	9.5	90.0	87.0	86.4	87.0	86.5	83.1	82.4	80.8
	4.75	62.6	61.9	57.0	59.2	59.6	56.0	55.0	53.4
	2.36	41.9	40.8	43.8	46.4	47.8	40.4	43.7	39.2
	1.18	31.4	22.1	34.5	35.8	35.9	27.8	32.0	25.8
	0.6	23.2	13.1	18.8	19.8	21.8	17.6	22.8	17.0
	0.3	13.8	8.4	8.2	9.1	10.8	9.5	13.8	11.1
	0.15	6.7	6.6	5.8	6.4	5.9	5.3	6.6	6.5
	0.075	3.5	4.3	4.2	4.7	3.9	3.7	4.4	3.7
	RAP (%)	-	-	-	-	-	-	-	-
Asphalt Binder Content (%)		5.0	5.6	5.2	5.2	5.1	4.3	5.0	4.8
Voids in the Mineral Aggregate, VMA (%)		15.6	15.1	14.8	15.0	15.0	14.5	14.9	14.2
Voids Filled with Asphalt, VFA (%)		76.4	73.5	73.0	73.3	73.3	72.4	72.0	71.8
Asphalt Binder Performance Grade		58-28	58-28	58-34	58-34	58-34	52-40	52-40	52-40
Traffic Category		D	D	D	D	C	B	B	B

179